REDOX ACTIVE LIPOPHILIC RUTHENIUM COMPLEXES AS POTENTIAL ANTI-CANCER DRUGS

by

NAGHAM ALATRASH

Presented to the Faculty of the Graduate School of

The University of Texas at Arlington in Partial Fulfillment

of the Requirements

for the Degree of

DOCTOR OF PHILOSOPHY

THE UNIVERSITY OF TEXAS AT ARLINGTON

MAY 2015

Acknowledgements

I would like to take this opportunity to deeply thank my advisor, Frederick M. MacDonnell, for his endless guidance and support during the course of my graduate work. He taught me how to manage my time wisely and provided me with the knowledge that helped me succeed throughout my graduate school career. In his lab, I have learned to trust myself and have come to believe that through hard work and diligence, anything can be accomplished.

I would like to express my appreciation for my committee members, Professors Brad Pierce and Kayunta Johnson-Winters for all of their feedback and suggestions through my graduate program.

I would like to take the opportunity to thank our collaborator, Prof. Rolf Brekken at the University of Texas Southwestern Medical Center, for his help in obtaining our cytotoxicity data. Also, I would like to thank our UTA collaborators, Prof. Purnendu Dasgupta and Prof. Subhrangsu Mandal, for their valuable advice throughout progression of my PhD. coursework. Furthermore, I would like to thank Akinde Kadjo for her help with the ICP-MS analysis.

Special thanks goes to Dr. Liping Tang from the Biomedical Engineering who kindly donated the animals for the maximum tolerable dose study. I would also like to thank Mr. Alphas Wicker and Nathan Moore from the Animal Care Facility for their help with the animal experiment.

I would also like to thank the current and previous lab members, Dr. Norma Tacconi, Dr. Shreeyukta Singh, Dr. Joseph Aslan, Dr. David Boston, Dr. Maher Alrashdan, Pooja Ahuja, Cynthia Griffith, Adam Dayoub, Angela Dickens, Mohammad Islam, Matthew West, Jimmy Nguyen, Evette A. Odhiambo, Yanling Chen, Kai-ling Huang and Steven Poteet for their help and support in the lab; especially my best friend, Eugenia Narh.

In addition, I would like to thank the Chemistry and Biochemistry staff including Debbie Cooke, Natalie Croy, Nancy Dunning, James Garner, Jill Howard, Brian Edward and Charles Savage for their friendship and assistance during these last three years.

I would also like to thank my parents and my brothers for their support and encouragement. Especially to my mom Nabilla, I want to thank her deeply for her infinite love and care, and also the sacrifice she had to endure in order for me to pursue my education.

I am sincerely grateful for the financial support from the Louis Stokes Alliance for Minority Participation & Bridge to the Doctorate Program Fellowship that enabled me to pursue this endeavor. Also, I would like to thank Lisa Berry who assisted me in many ways and coordinated my progress within the program in accordance with aforementioned guidelines.

Last, but not least, I would like to thank the most important person in my life, my lovely husband, Kamil Hamzah. Without him and his endless support and love, I would never have come so far in my education. He is the powerful force in my life, and I dedicate this to him as a thank you for his encouragement, patience, and help through the past three years; and for being a great dad to our sons, Hassan and Kareem. I cannot thank you enough. To my babies, Hassan and Kareem who are my gems, thank you for lighting up my life and filling my world with abundant joy, hope and happiness.

March 31, 2015

Abstract

REDOX ACTIVE LIPOPHILICRUTHENIUM COMPLEXES AS POTENTIAL ANTI-CANCER DRUGS

Nagham Alatrash, PhD

The University of Texas at Arlington, 2015

Supervising Professor: Frederick M. MacDonnell

The dinuclear ruthenium(II) polypyridyl complexes (RPCs) $[(phen)_2Ru(tatpp)Ru(phen)_2][PF_6]_4$ (**P**$^{4+}$) and the monomeric $[(phen)_2Ru(tatpp)]Cl_2$ (**MP**$^{2+}$) are promising candidates for anti-cancer drug development in terms of the observed anti-tumor activity *in vivo* and *in vitro*. These complexes contain the redox-active tatpp (9,11,20,22-tetraazatetrapyrido[3,2-a:2'3'-c:3'',2''-1:2''',3''']-pentacene) ligand which seems to be the critical component for biological activity. These complexes cleave DNA when reduced in situ to a radical species. Both complexes exhibit selective cytotoxicity toward cultured malignant cell lines and showed inhibition of tumor growth *in vivo*. This work expands on this platform by preparing and examining more lipophilic analogues of **P**$^{4+}$ and **MP**$^{2+}$. Specifically, four lipophilic ruthenium(II) polypyridyl complexes, $[(Ph_2phen)_2Ru(tatpp)Ru(Ph_2phen)_2][PF_6]_4$ (**P$_{Ph}$**$^{4+}$), (Ph_2phen, 4,7-diphenyl-1,10-phenanthroline), $[(Me_4phen)_2Ru(tatpp)Ru(Me_4phen)_2][PF_6]_4$ (**P$_{Me}$**$^{4+}$), (Me_4phen, 3,4,7,8-tetramethyl-1,10phenanthroline), $[(Me_4phen)_2Ru(tatpp)][PF_6]_2$ (**MP$_{Me}$**$^{2+}$), and $[(Ph_2phen)_2Ru(tatpp)][PF_6]_2$ (**MP$_{Ph}$**$^{2+}$), have been synthesized and characterized in which 4,7-diphenyl-1,10-phenanthroline or 3,4,7,8-tetramethyl-1,10-phenanthroline ligands were used to replace the 1,10-phenanthroline ligands in **P**$^{4+}$ and **MP**$^{2+}$. A structure-activity examination of their partition coefficient (log *P*), DNA cleavage activity, cytotoxicity, and

animal acute toxicity followed. Log *P* data revealed lipophilicity decreased in the order: $\mathbf{MP_{Ph}}^{2+} > \mathbf{P_{Ph}}^{4+} > \mathbf{MP_{Me}}^{2+} > \mathbf{P_{Me}}^{4+} > \mathbf{MP}^{2+} > \mathbf{P}^{4+}$ as expected. We hypothesized that increasing the lipophilicity of the ruthenium complexes would increase cytotoxicity and decrease animal toxicity, yet have little effect on their DNA cleavage activity. This is because all four analogues retain the putative DNA cleaving unit (tatpp ligand) but being more lipophilic, they should more easily enter cells, increasing cytotoxicity, and on the same basis, be slower to build up in the bloodstream after IP injection in animal toxicity studies. IC_{50} values for all complexes were obtained for H358, CCL228, MCF-7, and against normal cell line MCF-10. The cytotoxicity of $\mathbf{P}^{4+}$, $\mathbf{MP}^{2+}$ and $[Ru(phen)_2dppz]^{2+}$ were also evaluated in NSCLC cell lines H358, HCC2450, H522, H1993, H2073, H322, H2122, H460 and the pancreatic cancer (PANC1) cell line using standard MTS and clonogenic assays. The lipophilic ruthenium complexes $\mathbf{MP_{Ph}}^{2+}$, $\mathbf{P_{Ph}}^{4+}$, $\mathbf{MP_{Me}}^{2+}$, and $\mathbf{P_{Me}}^{4+}$ showed no acute animal toxicity in a screen of the MTD in Balb/c mice with doses up to 160 mg drug/Kg mouse. Furthermore, the absorption and the distribution of drug after administration by intraperitoneal (IP) injection in male Wister Han rats were discussed. Lastly, we present the results from a NCI-60 panel prescreen of $\mathbf{MP_{Ph}}^{2+}$ complex that was submitted through the Developmental Therapeutics Program of the National Cancer Institute. In comparison with $\mathbf{P}^{4+}$ and $\mathbf{MP}^{2+}$, these analogues generally showed similar DNA cleavage activity, enhanced cytotoxic activity in cultured malignant human cells, and reduced animal toxicity in Balb/c mice.

Table of Contents

List of Illustrations

List of Tables

List of Abbreviations

AChE	Acetylcholinesterase
AcOH	Acetic acid
bp	Base-pair
bpy	2,2´-Bipyridine
CCL228	Colon cancer cell line
CD_3CN	Deuterated acetonitrile
Cisplatin	*cis*-Diamminedichloroplatinum(II)
Conc.	Concentration
DMF	Dimethylformamide
DMSO	Dimethylsulfoxide
DNA	Deoxyribonucleic Acid
dppz	Dipyrido[3,2-a: 2',3'-c]phenazine
ee%	Enantiomeric Excess
EI-MS	Electron Impact Ionization Mass Spectrometry
eq	Equivalent
EtOH	Ethanol
EDTA	Ethylenediaminetetraacetic Acid
Fig	Figure
GSH	Glutathione
H-358	Human non-small cell lung cancer cells
IC_{50}	Half maximal inhibitory concentration
ICP-MS	Inductively coupled plasma mass spectrometry

IP	Intraperitoneal
K_b	Affinity bindingconstant
log *P*	Partition coefficient
MCF-10	Breast epithelial cell line
MCF-7	Human breast cancer cell line
MeCN	Acetonitrile
MeOH	Methanol
MP^{2+}	$[(phen)_2Ru(tatpp)]^{2+}$
MP_{Ph}^{2+}	$[(Ph_2phen)_2Ru(tatpp)]^{2+}$
MP_{Me}^{2+}	$[(Me_4phen)_2Ru(tatpp)]^{2+}$
MTD	Maximum tolerated dose
MTT	3-(4,5-Dimethylthiazol-2-yl)-2,5-diphenyltetrazolium bromide
NAMI-A	[ImH][trans-$RuCl_4$(DMSO)(Im)]
NCI	National Cancer Institute
NHE	Normal hydrogen electrode
NMR	Nuclear Magnetic Resonance
PBS	Phosphate buffered saline
DPBS	Dulbecco`s Phosphate Buffered Saline
P^{4+}	$[(phen)_2Ru(tatpp)Ru(phen)_2]^{4+}$
P_{Ph}^{4+}	$[(Ph_2phen)_2Ru(tatpp)Ru(Ph_2phen)_2]^{4+}$
P_{Me}^{4+}	$[(Me_4phen)_2Ru(tatpp)Ru(Me_4phen)_2]^{4+}$
Ph_2Phen	4,7-Diphenyl-1,10-phenanthroline
Me_4Phen	3,4,7,8-tetramethylphen-1,10-phenanthroline

RT	Room temperature
RPCs	Ruthenium Polypyridyl complexes
s	Singlet
SHE	Standard hydrogen electrode
t	Triplet
tatpp	9,11,20,22-Tetraaza tetrapyrido[3,2-a:2'3'-c:3'',2''-1:2''',3''']-pentacene
tpphz	Tetrapyrido[3,2-a: 2′,3′-c: 3″,2″-h: 2″,3‴-j]phenazine
Vol.	Volume
UV	Ultraviolet

Chapter 1

RUTHENIUM POLYPYRIDYL COMPLEXES AS POTENTIAL ANTI-CANCER AGENTS

1.1 Biological Activity of Coordinately Saturated Ruthenium(II) Polypyridyl Complexes

Cisplatin (cis-$Pt(NH_3)_2Cl_2$) is one of the most successful and widely used anti-cancer drugs in clinical use today.[1,2] However, it is not effective against all cancers and many cancers can develop resistance to this agent.[3] Moreover, there are a number of undesirable and often severe side effects that can limit its use.[4,5] Besides cisplatin, a number of platinum complexes such as carpoplatin, nedaplatin and lobaplatin, shown in Figure 1.1, have been approved for cancer therapy.[6] Carboplatin was introduced clinically and used worldwide along with cisplatin. Nedaplatin is available only in Japan while oxaliplatin is available in a few countries, such as France.[6]

Over the past 50 years, there have been thousands of platinum complexes examined as potential drugs with the goal of either expanding the scope of anti-tumor activity or lessening the severity of the side effects or both. Success has been limited to some new platinum-based drugs being introduced clinically in that time and these mainly address the side-effect issues, and do not expand the scope of cancers treatable.[7] The success and limitations of platinum-based drugs have motivated scientists to look for alternative metal-based cancer drugs. In particular, ruthenium(II) and (III) complexes have enjoyed considerable attention[8,3] as they display similar ligand exchange kinetics to Pt(II) complexes[9] but as a d^6 or d^5 transition metal complexes, they favor six coordination and therefore have unique geometries relative to Pt(II).[10]

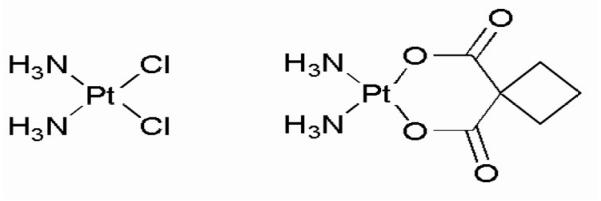

Cisplatin Carboplatin

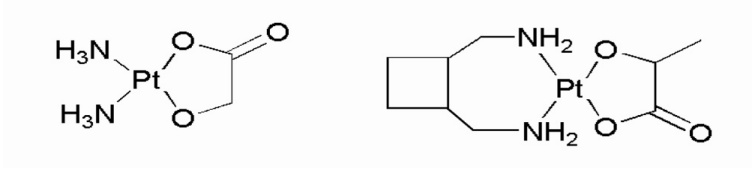

Nedaplatin Lobaplatin

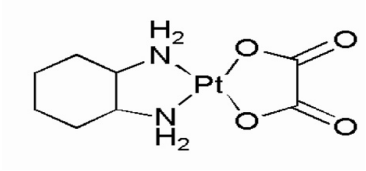

Oxaliplatin

Figure 1.1 The chemical structures of platinum complexes

Two octahedral ruthenium metal complexes, NAMI-A (ImH[trans-ImDMSORuCl$_4$]) and KP1019 (indazolium trans-[tetrachlorobis(1H-indazole)ruthenate(III)]), as seen in Figure 1.2, have shown considerable promise as anti-cancer agents both *in vitro* and *in vivo*.[11,12] The latter of these has progressed through Phase I clinical trials as IT-139, shown in Figure 1.2, with acceptable toxicity and observed activity in patients with NSCLC tumors.[13] The activity of these complexes is based on their labile chloride ligands which facilitate them to bind their biological target and behave in similar fashion to cisplatin. Some of the toxic side effects were discovered for NAMI-A during the first clinical study.[14,15]

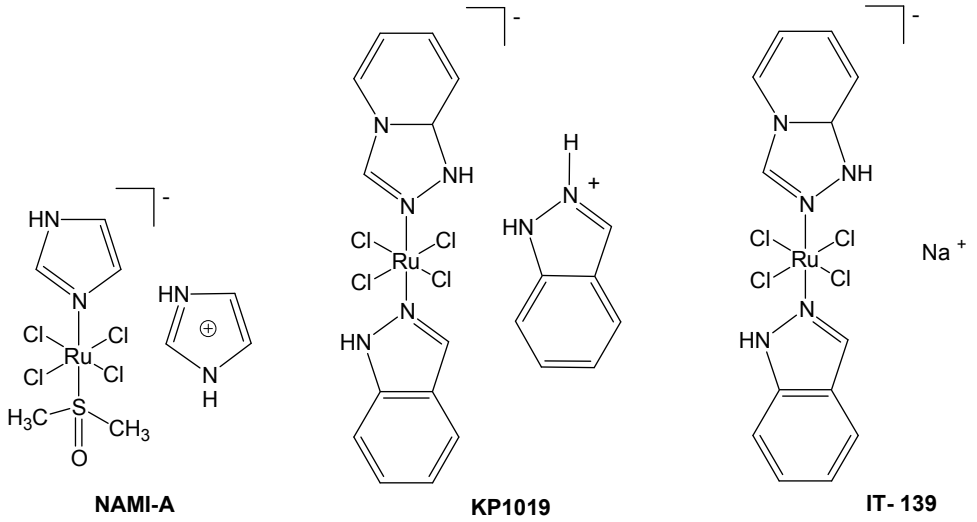

Figure 1.2 The chemical structures of NAMI-A, KP1019 and IT-139

Even before the discovery of NAMI_A and KP1019, scientists have examined a variety of ruthenium complexes such as chloro-ammino Ru(III) complexes, [fac-$Ru(Cl)_3(NH_3)_3$] and [cis-$Ru(Cl)_2(NH_3)_4$]Cl, depicted in Figure 1.3. It was found that these compounds exhibited anti-tumor activity against several cell lines, but the insolubility of these complexes prevent their use as drugs.[16]

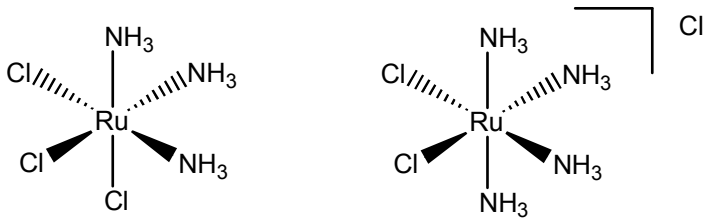

Figure 1.3 The chemical structures of [fac-$Ru(Cl)_3(NH_3)_3$] and [cis-$Ru(Cl)_2(NH_3)_4$]Cl

Furthermore, ruthenium(II) complexes cis-$[Ru(Cl)_2(DMSO)_4]$ and trans-$[Ru(Cl)_2(DMSO)_4]$ (DMSO = dimethylsulfoxi,de), shown in Figure 1.4, were investigated in 1975 and show low toxicity and similar antitumor activity to cisplatin.[17] More recently, there has been a wide interest in the redox properties of coordinately saturated Ru(II) polypyridyl complexes (RPCs), which are known for their advantages for cellular uptake *in vivo*,[18] stability,[19] and remarkable biological activity.[19] These complexes act in a different way than cisplatin, NAMI_A and KP1019 and that is due to the lack of the labile ligands.[20]

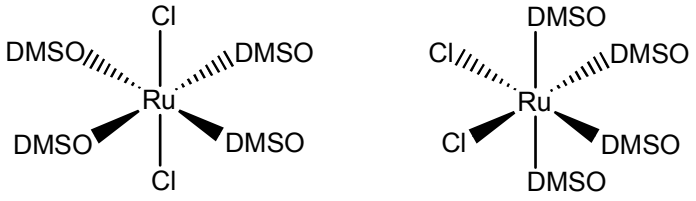

trans-$[RuCl_2(DMSO)_4]$ cis-$[RuCl_2(DMSO)_4]$

Figure 1.4 The chemical structures of cis-$[Ru(Cl)_2(DMSO)_4]$ and trans-$[Ru(Cl)_2(DMSO)_4]$

The early study by Dwyer *et al*. in 1950's investigated the biological activity of the parent complexes: $[Ru(2,2'\text{-bipyridine})_3]^{2+}$ and $[Ru(1,10\text{-phenanthroline})_3]^{2+}$, illustrated in Figure 1.5, where it was found that these cations are chemically stable, coordinatively saturated, substitutionally inert, and biologically active.[18]

.

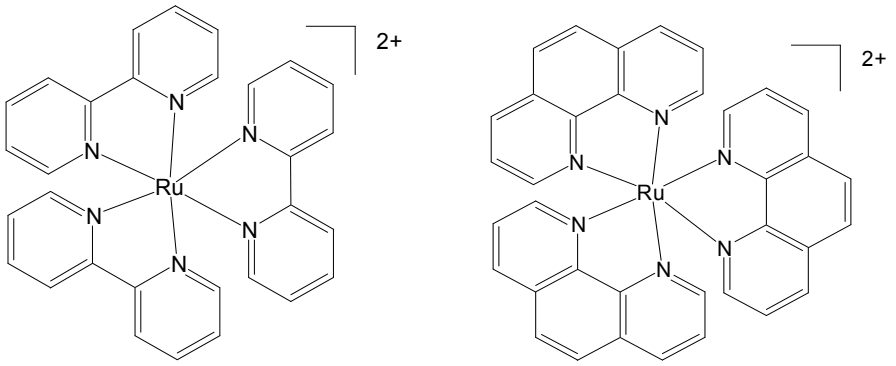

$[Ru(bpy)_3]^{2+}$ $[Ru(phen)_3]^{2+}$

Figure 1.5 The chemical structures of $[Ru(bpy)_3]^{2+}$ and $[Ru(1,10\text{-}phen)_3]^{2+}$ (where bpy=2,2'-bipyridine, phen = 1,10-phenanthroline)

The stability and the activity of these saturated RPCs were investigated via intraperitoneal (IP) injection of radiolabeled $[^{106}Ru(phen)_3]^{2+}$ into rats where it was found that this cation complex was not metabolized and excreted unchanged in urine.[21] These complexes exhibited enzyme inhibitory activities and toxicity in mice.[18,19 ,22]

Dwyer and coworkers also reported the neurotoxicity or curare-like behavior of these complexes *in vivo*. Ultimately, they showed that these complexes are competitive inhibitors of acetylcholinesterase (AChE).[18] Furthermore, they found that the capability of these compounds to inhibit AChE depends on many aspects such as the charge, size, enantiomeric forms and the properties of the ligands.[18] As it was found that the chirality of the homoleptic ruthenium complex has significant effect on their biological activity where Λ−$[Ru(phen)_3]^{2+}$ was less toxic in mice compared to Δ−$[Ru(phen)_3]^{2+}$ and that is due to the distribution rate of these complexes to the blood stream.[21] Δ−$[Ru(phen)_3]^{2+}$ complex (shown in Figure 1.6) reached the blood in smaller amount than Λ−$[Ru(phen)_3]^{2+}$ complex because of the lower rate of absorption.[21] The high toxicity or low toxicity of the ruthenium complexes

in mice is related to the capability of the complexes to penetrate the cells, which is dependent on the lipid/water partition (lipophilicity).[18] Ruthenium 3,4,7,8-tetramethyl-1,10-phenanthroline complex was the most cytotoxic compared to the parent compound Ruthenium 1,10-phenanthroline.[23]

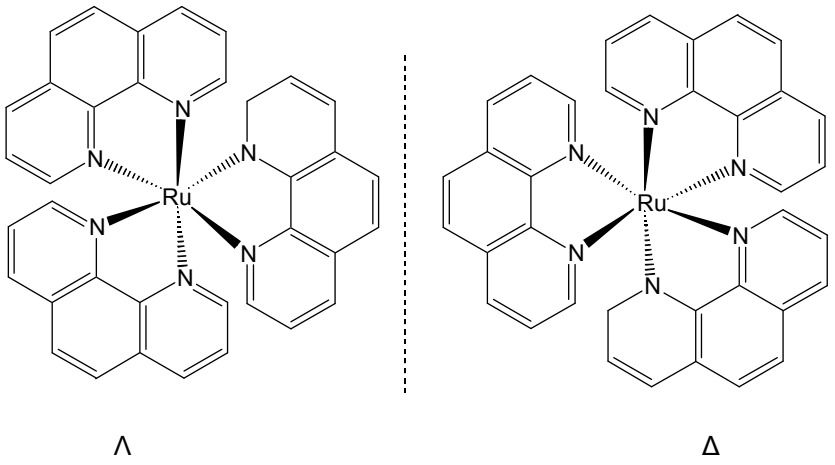

Figure 1.6 The chemical structures of Δ−$[Ru(phen)_3]^{2+}$ and Λ−$[Ru(phen)_3]^{2+}$

Following Dwyer's pioneering work on the biological activity of RPCs, Meggers and coworkers developed the inert octahedral organoruthenium compounds as kinase and acetylcholinesterase (AChE) inhibitors. [24] The shape of the trishetroleptic RPCs was used as structural scaffolds. The $[Ru(5,6\text{-}Me_2phen)(phen\text{-}4\text{-}CONH_2)Me_2dppz]^{2+}$ complex was found to inhibit acetylcholinesterase with an IC_{50} of 200 nM compared to other tris-ruthenium complexes.[24,25]

More recently the structure activity relationship (SAR) of the Ru(II) complexes was studied in Frederick MacDonnell's group. They have reported on the unusual DNA cleavage activity of the metallointercallator $[(phen)_2Ru(tatpp)Ru(phen)_2]^{4+}$ ($\mathbf{P}^{4+}$) which also

displays promising anti-tumor activity *in vivo*.[26] Both the dinuclear ruthenium(II) polypyridyl complexes, $[(phen)_2Ru(tatpp)Ru(phen)_2]^{4+}$ (**P**$^{4+}$), and it's mononuclear analogue, $[(phen)_2Ru(tatpp)]^{2+}$ (**MP**$^{2+}$), depicted in Figure 1.7, show promising anti-cancer activity *in vitro* and *in vivo* and much of this biological activity is attributed to the redox-active tatpp (where tatpp = 9,11,20,22-tetraazatetrapyrido[3,2-a:2',3'-c:3'',2''-l:2''',3'''-n]-pentacene) ligand present in these complexes. [27]

Yadav and Janaratne have shown that RPCs which containing tatpp ligand are potent chemotherapeutic agents as they exhibited potentiated DNA cleavage activity in the presence of the reducing agent, glutathione (γ-L-glutamyl-L-cysteinylglycine, GSH), under aerobic and anaerobic conditions.[27,28] Furthermore, it was found that the reduced form of **P**$^{4+}$ complex is capable to cleave DNA under low oxygen condition with the presence of GSH contrasting other ruthenium complexes and that is due to the redox-activity of **P**$^{4+}$ complex.[29] The maximum tolerable dose (MTD, mg complex/Kg mouse) for **P**$^{4+}$ and **MP**$^{2+}$ was examined in C57 BL/6 mice and it was found to be ~ 65 mg/Kg compared to 6.6 mg/Kg for the parent complex $[Ru(phen)_3]^{2+}$.[27] The cytotoxicity study against non-small cell lung cancer (NSCLC) H358 (Human Caucasian Bronchioalveolar Carcinoma) and H226 (Lung Squamous Carcinoma) cancer lines have revealed that the most promising activity was shown by **P**$^{4+}$ and **MP**$^{2+}$ compared to $[Ru(phen)_2(tpphz)]^{2+}$ (where tpphz is tetrapyrido[3,2-a:2',3'-c:3'',2''-h:2''',3'''-j]phenazine), $[Ru(bpy)_3]^{2+}$, and $[Ru(phen)_3]^{2+}$.[27]

Also, the previous study by Yadav *et al*. showed that the chirality of these Ru(II) complexes have significant effect on their biological activity against the non-small cell lung cancer cell lines.[27] In addition, cell cycle study on H358 cell line in our lab have shown that treatment the cells with Δ-**MP**$^{2+}$ caused a marked G2-M block.[26] Similar activity was shown before by antineoplastic agent paclitaxel. It is a microtubule stabilizing agent that induces apoptosis by arresting cells at the G2-M phase of the cell cycle.[30,31] It is also very important

to note that the types of ancillary ligands that surround the metal center play an important role in the biological activity of these RPCs.[27]

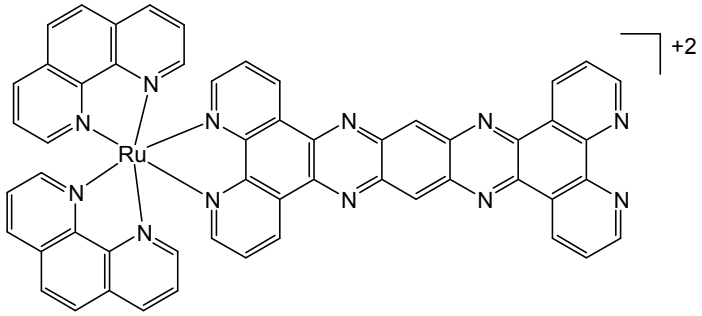

MP

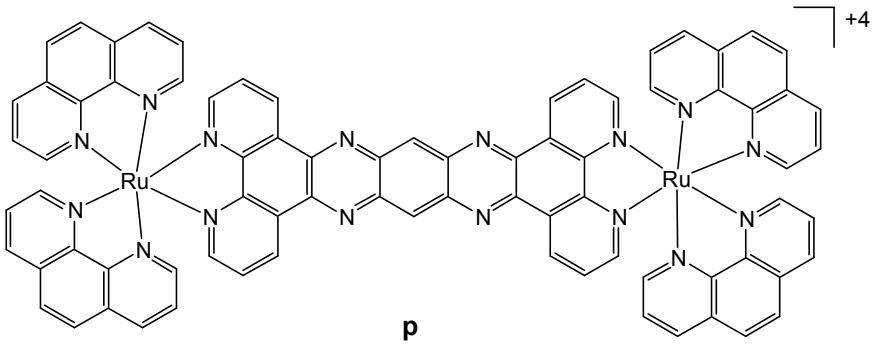

p

Figure 1.7 The chemical structures of $\mathbf{P}^{4+}$ = $[(phen)_2Ru(tatpp)Ru(phen)_2]^{4+}$ and $\mathbf{MP}^{2+}$ = $[(phen)_2Ru(tatpp)]^{2+}$

The terminal ligands seem to be one area in which changes can be made to the complex which is unlikely to alter the reactivity of the ruthenium complexes. Replacing the phen or the bpy ligands in $[Ru(bpy)_3]^{2+}$ and $[Ru(phen)_3]^{2+}$ complexes with larger aromatic ligand such as (dipyrido[3,2-a: 2',3'-c]phenazine) dppz ligand, illustrated in Figure 1.8, results in higher DNA binding affinity, which fully intercalate to the DNA.[27] Those tris-ruthenium(II) complexes have a binding constant (K_b) on the order of 10^3 M^{-1} compared to

the K_b of the dppz complex which is on the order of 10^6 M^{-1} where the K_b increased by three orders of magnitude.[32,26 ,27]

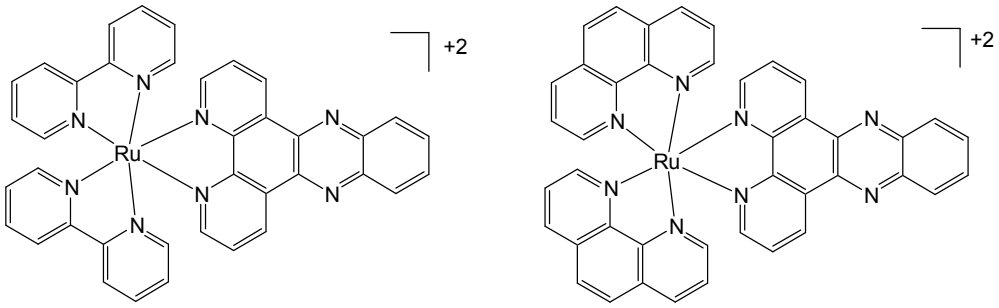

$[(bpy)_2Ru(dppz)]^2$ $[(phen)_2Ru(dppz)]^{2+}$

Figure 1.8 The chemical structures of $[(bpy)_2Ru(dppz)]^{2+}$ and $[(phen)_2Ru(dppz)]^{2+}$

There are many other factors that can affect the DNA binding affinity of ruthenium(II) complexes such as size, charge, stereochemistry and lipophilicity.[33] The chirality of the metal complexes has impact on the intercalation of the enantipore Ru(II) complexes with the DNA. For example, the binding constant of Δ− and Λ−[Ru $(phen)_2dppz]^{2+}$ into DNA are 3.2 X 10^6 M^{-1} and 1.7 X 10^6 M^{-1} where we can see that the Δ-complex has slightly stronger K_b compared to the Λ−complex.[34] The binding affinity increases by adding a second metal center to the monomeric complexes and that is due to their increase in size and higher charge.[27] For example, $[(phen)_2Ru(tatpp)Ru(phen)_2]^{4+}$ and $[(phen)_2Ru(bidppz)Ru(phen)_2]^{4+}$ have K_b on the order of 10^8 M^{-1} and 10^{12} M^{-1} respectively.[27]

P^{4+} and **MP**$^{2+}$ complexes are promising anti-tumor drugs, not only because they bind tightly to the DNA, but they also cleave DNA due to their low reduction potential

compared by other Ru(II) complexes such as $[Ru(phen)_3)]^{2+}$ and $[Ru(phen)_2dppz]^{2+}$ complexes as seen in Figure 1.9. The reduction potential of $\mathbf{P}^{4+}$ is -0.023 mV compared to tri-ruthenium complex which is -1.050 mV.

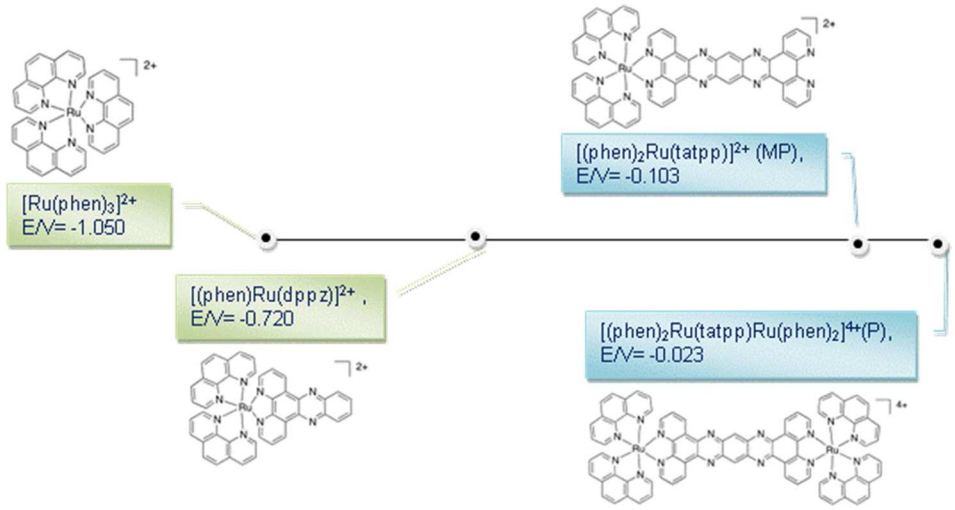

Figure 1.9 Reduction potential of ruthenium(II) polypyridyl complexes

The *in vitro* cytotoxicity of chloropolypyridyl ruthenium complexes against the murine L1210 leukemia cell line and human cervix carcinoma HeLa cell line was investigated by Novakova and coworkers in 1995.[35] The study was conducted on three different ruthenium complexes: [Ru(terpy)-bpy)Cl]Cl, cis-$[Ru(bpy)_2Cl_2]$, and mer-$[Ru(terpy)C1_3]$ where terpy = 2,2':6'2"-terpyridine and bpy = 2,2'-bipyridyl. It was found that *mer*-$[Ru(terpy)Cl_3]$ complex, depicted in Figure 1.10, has significantly higher cytotoxicity compared to the other ruthenium complexes and that was thought to be related to its ability to form interstrand crosslinks in the DNA.[35] The ID_{50} of mer-$[Ru(terpy)Cl_3]$ against L1210 and Hela cell lines was 7 μM and 8 μM respectively.[35] Also, mer-$[Ru(terpy)Cl_3]$ complex in the same study, has shown significant anti-tumor activity in standard murine screen.[35]

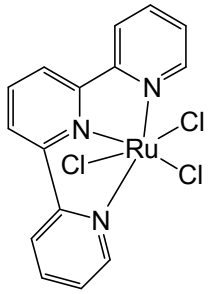

Figure 1.10 The chemical structure of *mer*-[Ru(terpy)Cl_3] (where terpy = 2,2':6'2"-terpyridine)

Early studies with three isomeric dichlororuthenium(II) complexes of the [Ru(azpy)$_2$$Cl_2$] complex where azpy = didentate ligand 2-phenylazopyridine showed that the activity of the isomers is related to the higher flexibility of the azpy ligand.[36] The dichlororuthenium(II) complexes: α-[Ru(azpy)$_2$$Cl_2$], β-[Ru(azpy)$_2$$Cl_2$], and γ-[Ru(azpy)$_2$$Cl_2$] were screened against a series of human tumor cell lines such as MCF-7, EVSA-T, WIDR, IGROV, M19, A498, and H266 where it was found that α-[Ru(azpy)$_2$$Cl_2$] complex has appreciably high cytotoxicity compared to the other isomers and cisplatin as seen in Table 1.1.[36] The structure of α-[Ru(azpy)$_2$$Cl_2$] plays a very important role in the biological activity of this complex where it has the capability to bind to the DNA in a very useful way.[36]

Table 1.1 ID_{50} values in mol/L of α-$[Ru(azpy)_2Cl_2]$, β-$[Ru(azpy)_2Cl_2]$, γ-$[Ru(azpy)_2Cl_2]$ and cisplatin complexes against different human cell lines[36]

	MCF-7 μmol/L	EVSA-T μmol/L	WIDR μmol/L	IGROV μmol/L	M19 μmol/L	A498 μmol/L	H266 μmol/L
α-$[Ru(azpy)_2Cl_2]$	0.6	0.1	1.9	0.8	0.2	1.2	1.5
β-$[Ru(azpy)_2Cl_2$	4.1	1.9	11.2	7.3	2.5	8.8	10.0
γ-$[Ru(azpy)_2Cl_2]$	5.9	5.4	16.6	11.8	4.5	15.3	14.8
Cisplatin	2.3	1.4	3.2	0.6	1.9	7.5	10.9

Previous research with analogues of $[Ru(phen)_3]^{2+}$ has revealed that use of lipophilic ancillary ligands in the synthesis of RPCs can increase their uptake by cells and potency.[37] Lipophilicity is an important factor that can affect the biological activity on most therapeutic compounds.[37] Another study with $[(phen)_2Ru(dppz)]^{2+}$ (where dppz is dipyrido[3,2-*a*:2′,3′-*c*]phenazine) has shown that cellular uptake is correlated to the structure and the lipophilicity of the compounds.[38] Substitution of the 1,10-phenanthroline with lipophilic 4,7-diphenyl-1,10-phenanthroline was shown to exhibit enhanced cellular uptake of the complex.[38]

In 2008, Barton *et al*. examined the mechanism of cellular entry of luminescent RPCs into HeLa cells where the cellular uptake was tracked and measured by confocal microscopy and flow cytometry. They reported that the more lipophilic ruthenium(II) complex , $[(Ph_2phen)_2Ru(dppz)]^{2+}$, as shown in Figure 1.11, was transported more rapidly inside the cell compared to $[(phen)_2Ru(dppz)]^{2+}$ and $[(bpy)_2Ru(dppz)]^{2+}$ complexes.[39]

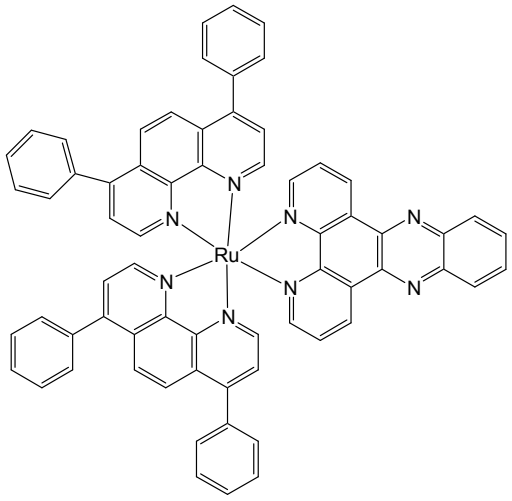

Figure 1.11 The chemical structure of $[(Ph_2phen)_2Ru(dppz)]^{2+}$

This transportation was more correlated to the lipophilicity of these compounds and not with the size or overall charge. This study's outcome was in agreement with reports on cisplatin analogues, where the complexes with the highest lipophilicity displayed the maximum cellular uptake. Hence, the poor uptake into the cell membrane is due to the hydrophilicity of the complexes.[38,40,41,42] The enhanced cytotoxicity of $[(Ph_2phen)_2Ru(dppz)]^{2+}$ towards HeLa cells over $[(phen)_2Ru(dppz)]^{2+}$ or $[(bpy)_2Ru(dppz)]^{2+}$ was postulated to be due to the increased lipophilic character.[43]

Zava and coworkers, in an earlier study, reported that the more lipophilic RPCs appeared to induce cell death by targeting the plasma membrane, not the nuclear DNA.[44] In their study, different concentrations of $[Ru(L)_3]^{2+}$ complexes (where L = bpy, [2,2'-Bipyridine]-4,4'-diamine, N^4,N^4,$N^{4'}$,$N^{4'}$-tetraethyl, [2,2'-Bipyridine]-4,4'-dicarboxylic acid, 4,4'-diethyl ester, [4,4′-dimethoxy-2,2′-bipyridine, 2,2'-Bipyridine, 4,4'-dimethyl) (illustrated in Figure 1.12) were evaluated for their effect on ovarian cancer cell growth using the MTT assay (MTT = 3-(4,5-Dimethylthiazol-2-yl)-2,5-diphenyltetrazolium bromide).[44]

One of the five different compounds was highly cytotoxic (less than 1 μm) toward A2780 cell line. The high cytotoxicity of this tris-(4,4′-dimethoxy-2,2′-bipyridine) ruthenium complex was explained by its high lipophilicity and its ability to bind to the plasma membrane of the cell. The lipophilicity of the five complexes was determined by using the partition coefficient (log $P_{o/w}$) experiment. The study showed that as the lipophilicity of the bipyridine ligand of the ruthenium(II) complexes increased, the cytotoxicity increased significantly.[44]

In general, the higher the lipophilicity of a drug, the stronger its binding to proteins and the better its volume of distribution.[45,46] In 1978, Watanabe *et al*. demonstrated that the volume of distribution is increased by increasing the lipophilicity of drugs, when administering fifteen basic drugs to animals, such as dogs.[47]

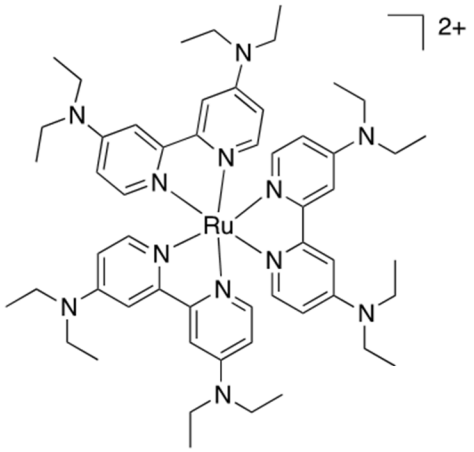

Ru([2,2'-bpy]-4,4'-diamine, N^4,N^4,$N^{4'}$,$N^{4'}$-tetraethyl)$_3$]$^{2+}$

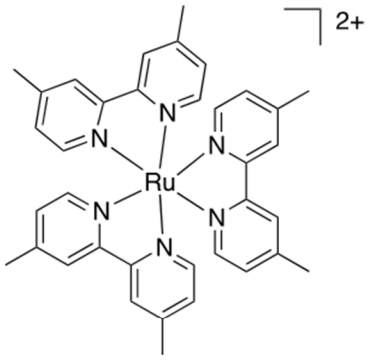

[Ru(4,4'-dimethyl-2,2′-bpy)$_3$]$^{2+}$

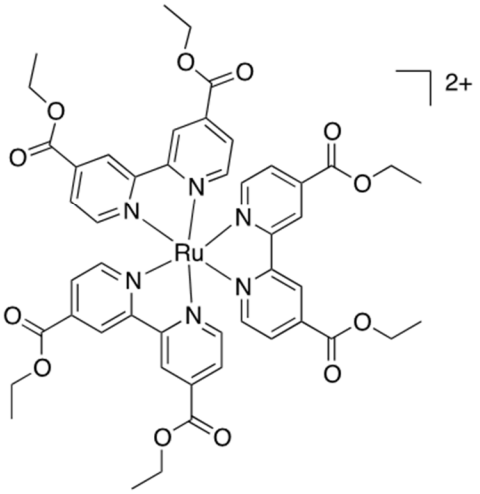

Ru([2,2'-bpy]-4,4'-dicarboxylic acid, 4,4'-diethyl ester)$_3$]$^{2+}$

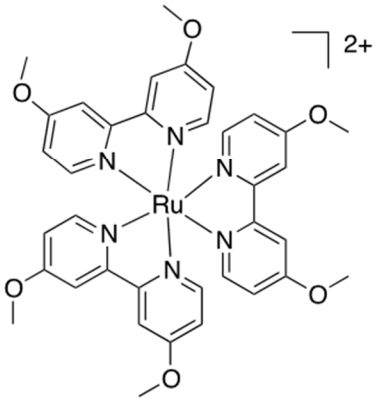

[Ru(4,4′-dimethoxy-2,2′-bpy)$_3$]$^{2+}$

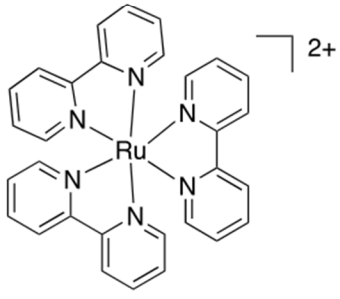

[Ru(2,2'-bpy)$_3$]$^{2+}$

Figure 1.12 The chemical structures of Ru(II) tris(bpy) complexes

In a previous study, Pisani and coworkers described the behavior of lipophilic Ru(II) polypyridyl cations as chemotherapeutic agents and their ability to target the mitochondria of L1210 murine leukemia cells and cause damage to these cells.[48] The dinuclear polypyridyl ruthenium(II) complexes $[\{Ru\text{-}(phen_2)_2\}\{\mu\text{-}bb_n\}]^{4+}$ where phen = 1,10-phenanthroline with flexible bridging ligands such as bb2 {1,2-bis[4(4'-methyl-2,2'-bipyridyl)]ethane}, bb5 {1,5-bis[4(4'-methyl-2,2'-bipyridyl)]pentane}, bb7 {1,7-bis[4(4'-methyl-2,2'-bipyridyl)]heptane}, and bb10 {1,10-bis4(4'-methyl-2,2'-bipyridyl)]decane} (Rubbn; where bbn=1,n-bis[4(4'-methyl-2,2'-bipyridyl)]-nane (n=2, 5, 7, 10, 12 or 16)) and their corresponding mononuclear complexes (shown in Figure 1.13) were synthesized and used in flow cytometry experiment to study the uptake mechanism and cellular localization.[48] The accumulation of the metal complexes in the mitochondria has a vast influence on their cytotoxicity, which is related to the nature of the ligand associated with the complex. The outcomes of this study demonstrated that lipophilic dinuclear ruthenium(II) complexes have a high cytotoxicity when they enter the cell by passive diffusion and poison the mitochondria, resulting in cell death by apoptosis.[48] Lipophilicity (hydrophobicity) is very important factor in drug delivery. This study shows a big correlation between the biological activity of a drug and its partition coefficient log *P*. [49]

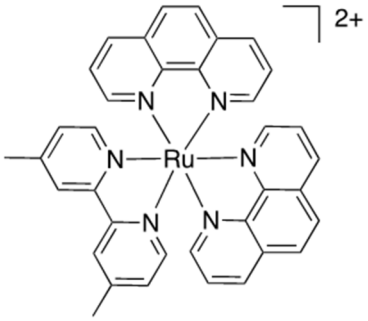

$[Ru(phen)_2(4,4'\text{-dimethyl-bipyridine})]^{2+}$

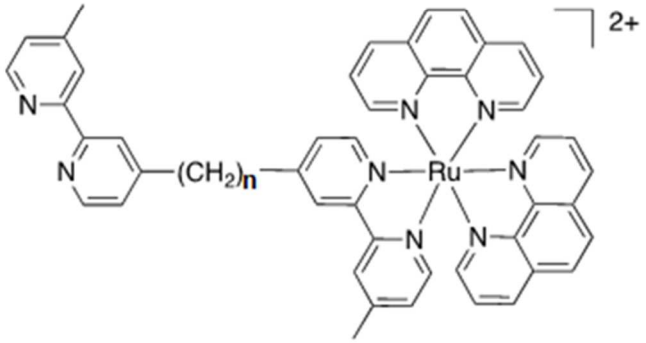

$[Ru(phen)_2\{bis\text{-}[4(4'\text{-methyl-}2,2'\text{-bipyridyl})\text{-}1,7\text{-heptane}\}]^{2+}$

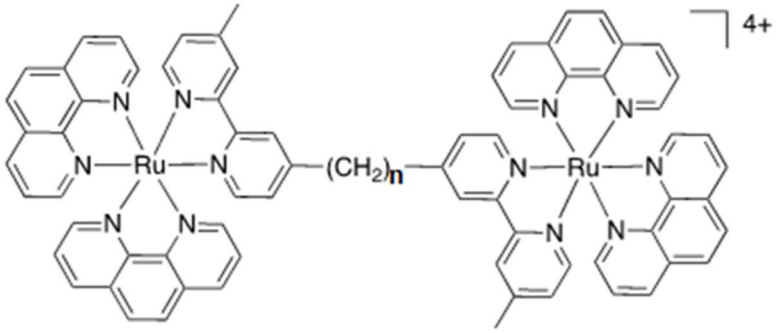

$[\{Ru\text{-}(phen_2)_2\}\{\mu\text{-}bb_n\}]^{4+}$

Figure 1.13 The chemical structures of dinuclear and mononuclear Ru(II) complexes (where bbn=1,n-bis[4(4'-methyl-2,2'-bipyridyl)]-nane (n=2, 5, 7, 10, 12 or 16))

1.3 Scope of Dissertation

The goal of our research is to investigate the structure-activity relationships of Ru(II) polypyridyl complexes and their biological activity. We postulated that by using lipophilic ancillary ligands, such as 4,7-diphenyl-1,10-phenanthroline (Ph_2phen) and 3,4,7,8-tetramethyl-1,10-phenanthroline (Me_4phen), as shown in Figure 1.14, to synthesize mononuclear and dinuclear analogues of $\mathbf{MP}^{2+}$ and $\mathbf{P}^{4+}$ we could alter their observed spectrum of cytotoxicity as well as their acute animal toxicity. We further postulated that an increase in the complexes lipophilicity would increase the observed cytotoxicity as these complexes would be better able to passively diffuse through the cell membrane and concentrate in cells.

The increased lipophilicity could also render them less acutely toxic according to Dwyer's hypothesis that the acute toxicity of RPCs is due to the peak blood concentration at which above some threshold, acetylcholinesterase inhibition causes neurotoxicity.[18] In principle, the more lipophilic complexes should be slower to partition into the blood after IP injection than the more hydrophilic complexes. As all of the complexes are cleared by excretion in urine, a complex slow to enter the bloodstream may never reach the threshold concentration required for toxic side effects, rendering it safer than the more hydrophilic analogues.

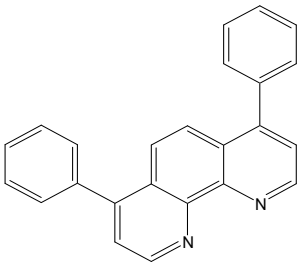

4,7-diphenyl-phen

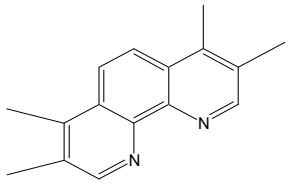

3,4,7,8-tetramethyl-phen

Figure 1.14 The chemical structures of lipophilic ancillary ligands (where phen = 1,10-phenanthroline)

Chapter 1 of this dissertation is a review of the relevant literature pertaining to the development of platinum and, in particular, ruthenium-based complexes for use as chemotherapeutic agents. From this perspective, we develop the thesis of this work. Chapter 2 presents the synthesis and characterization of the new RPCs: $[(Ph_2phen)_2Ru(tatpp)Ru(Ph_2phen)_2][PF6]_4$ ($[\mathbf{P_{Ph}}][PF_6]_4$), $[(Ph_2phen)_2Ru(tatpp)][PF_6]_2$ ($[\mathbf{MP_{Ph}}][PF_6]_2$), $[(Me4phen)_2Ru(tatpp)Ru(Me_4phen)_2][PF_6]_4$ ($[\mathbf{P_{Me}}][PF_6]_4$), and $[(Me_4phen)_2Ru(tatpp)][PF_6]_2$ ($[\mathbf{MP_{Me}}][PF_6]_2$). Moreover, this chapter demonstrates the ability of these analogues to cleave DNA via the same mechanism as observed for $\mathbf{MP}^{2+}$ and $\mathbf{P}^{4+}$.

In chapter 3, the complex lipophilicity is quantified by determination of the partition coefficients (log *P*) via the shake-flask method in PBS at pH 7.4 and octanol, as well as in deionized water and octanol. As expected, the lipophilicity of the complexes increased with the lipophilicity of the ancillary ligands. The effects of the structural changes on the cytotoxicity of the RPCs in terms of IC_{50} values is examined in numerous malignant cell lines including H358, CCL228, MCF-7, HCC2450, H522, H1993, H2073, H322, H2122,

H460, and PANC1, as well as the normal cell line, MCF-10. Structure-cytotoxicity relationships are discussed as applicable. One analogue, $[(Ph_2phen)_2Ru(tatpp)]Cl_2$, was submitted and accepted for screening against the NCI-60 panel through the Developmental Therapeutics Program of the National Cancer Institute. These results are also presented.

Furthermore, the effects of the structural changes on the mouse acute toxicity after IP injection is examined by determination of the maximum tolerable dose (MTD). As hypothesized, the more lipophilic ruthenium complexes: $\mathbf{P_{Ph}}^{4+}$, $\mathbf{P_{Me}}^{4+}$, $\mathbf{MP_{Me}}^{2+}$, $\mathbf{MP_{Ph}}^{2+}$ showed no acute animal toxicity at doses up to 160 mg drug/Kg mouse in this screen. Pharmacokinetic data related to the rate of three ruthenium drugs accumulation in blood serum after IP injection in rats was attempted. Three RPCs with very different log *P* values were administered IP to 3 groups of three rats and blood samples drawn at several time intervals following injection. The data are weak in that large differences were observed in the absolute values of [Ru] in serum per animal within a given group. Nonetheless, this data is presented in that the trends observed are supportive of the peak blood concentration model.

Chapter 2

SYNTHESIS, CHARCTERIZATION, AND DNA ACTIVITY OF DIFFERENT LIPOPHILICITIES

2.1 Introduction

In the early 1950's, Dwyer and coworkers examined the biological activity of coordinatively saturated ruthenium polypyridyl complexes (RPCs).[50] In this seminal work, they discovered promising cytotoxicity against malignant cell lines as well as bacteriostatic, bacteriocidal, and anti-viral activity.[50] The homoleptic parent complex, ruthenium(II) tris-1,10-phenanthroline, was shown to exhibit great stability *in vivo*.[22] Experiments in which albino rats were injected IP with radiolabeled $[^{106}Ru(phen)_3]ClO_4$ revealed that the complex did not remain in the animal for longer than a day and was excreted in urine unmetabolized.[21]

Moreover, the dissociation of dicationic ruthenium complexes was minimal in concentrated bases and acids,[18] leading them to conclude that the active biological agent was the intact complex. Dwyer and coworkers also established that RPCs had neurotoxic side effects in mice, including death, when administered at sufficient doses via IP injection. Subsequent studies showed the RPCs to be potent competitive inhibitors of acetylcholinesterase (AChE) with the Λ enantiomer of ruthenium(II) tris-1,10-phenanthroline being a better inhibitor of AChE and a more potent neurotoxin than the Δ enantiomer.[22] In a preliminary study, they also showed some influence of complex lipophilicity on the AChE inhibition and animal neurotoxicity.[22]

Later work by MacDonnell's group showed that RPCs containing the tatpp ligand are promising chemotherapeutic agents as they bind and cleave DNA *in vitro*, exhibit low micromolar cytotoxicity against numerous malignant cell lines but 100 μM cytotoxicity towards nonmalignant (immortalised) cells, and show relatively low acute animal toxicity

at therapeutically relevant doses. This is in striking contrast to nearly all other RPCs including, $[Ru(bpy)_3]^{2+}$, $[Ru(phen)_3]^{2+}$, $[Ru(phen)_2(dppz)]^{2+}$, and numerous analogues, which can bind DNA but do not induce DNA cleavage, may or may not be particularly cytotoxic towards malignant cell lines, show little difference in cytotoxicity against malignant and normal cells, and are frequently neurotoxic even at modest doses.[26, 51]

Ultimately, the DNA cleavage activity of the tatpp-based RPCs has been shown to be caused by the redox activity of the tatpp ligand *in vitro*. In situ reduction of this ligand places a reactive radical intermediate in the immediate vicinity of the DNA deoxyribose units, leading to H-atom abstraction and strand scission.[26] This enhanced reactivity is postulated to be the cause of the enhanced anticancer properties between these complexes and other RPCs which lack bioreducible ligands.

In this chapter, we present the synthesis and characterization of several analogues of $\mathbf{MP}^{2+}$ and $\mathbf{P}^{4+}$ in which the terminal phenanthroline ligand has been replaced with more lipophilic analogues. These complexes include: $[(Ph_2phen)_2Ru(tatpp)Ru(Ph_2phen)_2]\,[PF_6]_4$ ($\mathbf{P_{Ph}}^{4+}$), $[(Ph_2phen)_2Ru(tatpp)][PF_6]_2$ ($\mathbf{MP_{Ph}}^{2+}$), $[(Me_4phen)_2Ru(tatpp)Ru(Me_4phen)_2]\,[PF_6]_4$ ($\mathbf{P_{Me}}^{4+}$), and $[(Me_4phen)_2Ru(tatpp)][PF_6]_2$ ($\mathbf{MP_{Me}}^{2+}$), which are shown in Figures 2.1 and 2.2. In general, these complexes were prepared in a manner similar to the $[(phen)_2Ru(tatpp)Ru(phen)_2]\,[PF_6]_4$, and $[(phen)_2Ru(tatpp)][PF_6]_2$ complexes. All the analogues were all examined for DNA cleavage activity *in vitro* to determine if the structural changes impacted this function.

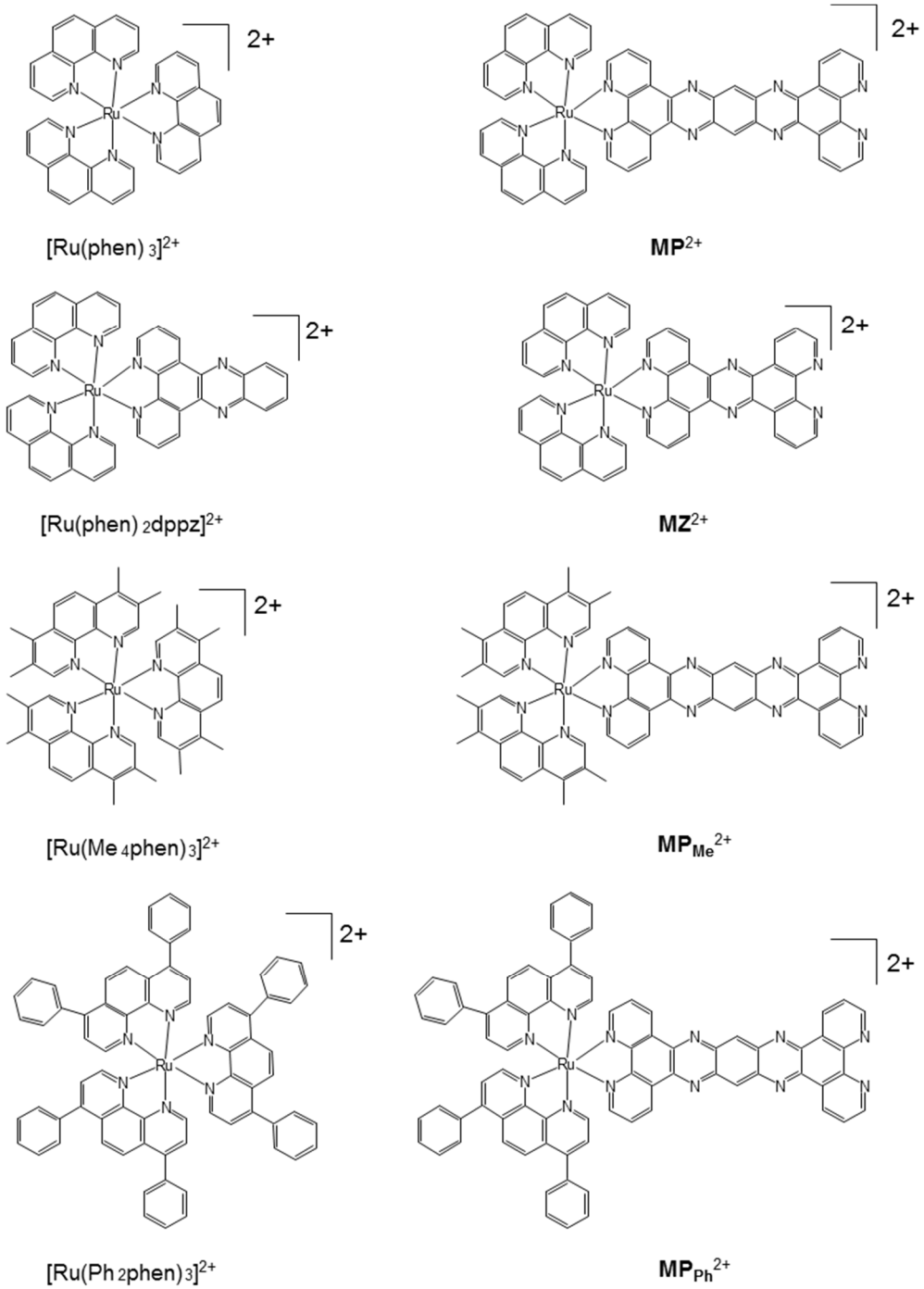

Figure 2.1 Chemical structures and shorthand notation of several key monomeric ruthenium polypyridyl complexes prepared and used in this study

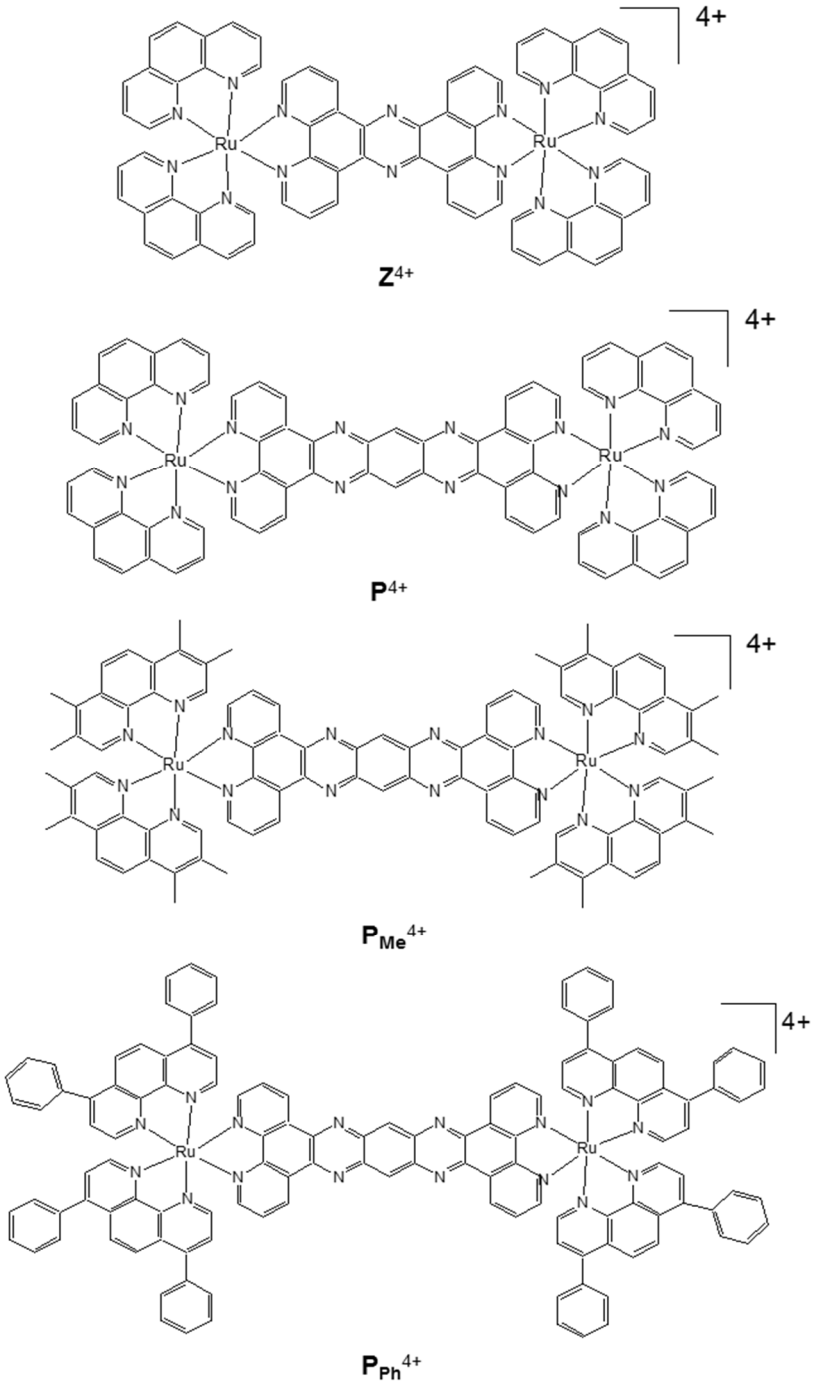

Figure 2.2 Chemical structures and shorthand notation of several key dimeric ruthenium polypyridyl complexes prepared and used in this study

2.2 Experimental- Synthesis

2.2.1 Chemicals

Tetrabutyl ammonium chloride hydrate, ethanol, lithium chloride, chloroform, 4,7-diphenyl-1,10-phenanthroline (Ph_2phen), 3,4,7,8-tetramethylphen-1,10phenanthroline (Me_4phen), ammonium hexafluorophosphate, N,N-diethylformamide, acetonitrile were purchased from Aldrich and were used as received. Ruthenium(III) chloride trihydrate was purchased from Pressure Chemical Co and was used as received. 1,10-Phenanthroline-5,6-dione (phendione) was synthesized based on literature procedures.[52] 11,12-diaminodipyrido[3,2-a:2',3'-c]phenazine (dadppz) and 4,5-dinitro-o-phenylene-diamine, 9,11,20,22-tetraazatetrapyrido[3,2-a:2',3'-c:3'',2''-l:2''',3'''-n]-pentacene (tatpp) were prepared as previously described in the literature.[53,54,55] $Ru(Me_4phen)_2Cl_2$ and $Ru(Ph_2phen)_2Cl_2$ were prepared in analogous fashion to $Ru(bpy)_2Cl_2$ reported previously in literature by Sullivan *et al*.[56]

$[(phen)_2Ru(tatpp)Ru(phen)_2][PF_6]_4$ [54] and $[Ru(phen)_2(phendione)][PF_6]_2$ [57] were prepared according to literature procedures. The following homoleptic ruthenium(II) complexes $[Ru(Ph_2phen)_3]Cl_2$ and $[Ru(Me_4phen)_3]Cl_2$ were prepared by using a modified procedure that was described before in the literature.[58] All organic solvents were of analytical grade and used as received unless stated otherwise.

2.2.2 Instrumentation

^{1}H NMR spectra were obtained on JEOL Eclipse Plus 300 or 500 MHz Spectrometers using either CD_3CN, $(CD_3)_2CO$ and CD_3Cl as the solvent, and referenced to the residual ^{1}H signals in the solvent using TMS as the standard for zero ppm.

2.2.3 Synthesis

2.2.3.1 $[(Ph_2phen)_2Ru(dndppz)][PF_6]_2$

$[(Ph_2phen)_2Ru(phendione)]Cl_2$ (0.14 g, 0.13 mmol) and 4,5-dinitro-1,2-phenylenediamine (0.026 g, 0.13 mmol) were dissolved in a mixture of 50 mL of absolute ethanol and 5 mL of glacial acetic acid in 100 mL round bottomed flask. The solution was refluxed overnight and then cooled down to room temperature. Product was isolated upon the addition of aqueous NH_4PF_6, filtered and washed with water and dried in the vacuum at 60 ^oC. Yield: 162 mg (87%). ^1H NMR (δ, CD_3COCD_3, 500 MHz): 9.79 (d, J = 5.2 Hz, 2H), 9.26 (s, 2H), 8.73 (d, J = 7.7 Hz, 4H), 8.64 (d, J = 7.7 Hz, 2H), 8.33 (s, 4H), 8.06 (dd, J_1 = 8.6 Hz, J_2 = 5.3 Hz, 4H), 7.78 (apparent triplet, J_1 = 8.4 Hz, J_2 = 8.2 Hz, 2H), 7.57-7.75 (multiplet, 20H). This complex was used in the following step after changed to chloride salt by using the following metathesis procedure.

2.2.3.1.1 Metathesis Procedure

The chloride salt of the complex was prepared from the hexafluorophosphate salt by adding a concentrated solution of n-tetrabutylammonium chloride in acetone to a concentrated solution of the complex in minimum amount of acetone. The resulting precipitate was filtered immediately, washed with acetone and dried in vacuo at 60 °C for 1 to 2 h. The hexafluorophosphate salt of the complex was prepared from the chloride salt by dissolving the complex in a minimum amount of water and adding a concentrated aqueous solution of ammonium hexafluorophosphate. The resulting precipitate was filtered and washed with water, then ethanol, and dried in vacuo at 60 °C for 1 to 2 h.

2.2.3.2 $[(Ph_2phen)_2Ru(dadppz)][PF_6]_2$

$[(Ph_2phen)_2Ru(dndppz)]Cl_2$ (0.1 g, 0.082 mmol) was dissolved in 50 mL of ethanol in a 200 mL glass pressure vessel. To this solution, 0.05 g of 10% Pd/C was added and the vessel

was placed in the Parr hydrogenation apparatus. The resulting slurry was pressurized to 5 atm H_2 and allowed to react for 24 h at room temperature with mechanical agitation. After the pressure was relieved, the resulting solution was filtered through a pad of Celite. The pad was washed twice with 5 mL of ethanol and the combined filtrates were reduced in volume to approximately 5 mL under the reduced pressure. To the concentrated filtrate, a concentrated aqueous solution of NH_4PF_6 was added, which precipitated the product. The product was filtered, washed with water, and dried in vacuo at 60 °C for 1 h. This complex was changed to chloride salt by using the general metathesis procedure as described previously. Yield: 90 mg (80%). ^{1}H NMR (δ, CD_3CN, 500 MHz): 9.54 (d, *J* = 8 .5 Hz, 2H), 8.25 (d, *J* = 8.0 Hz, 2H), 8.23 (d, *J* = 7.7 Hz, 4H), 8.18 (s, 4H), 8.16 (d, *J* = 8.2 Hz, 4H), 7.78 (apparent triplet, 2H), 7.57-7.63 (multiplet, 20H), 7.30 (s, 2H), 5.24 (br s, 4H).

2.2.3.3 $[(Ph_2phen)_2Ru(phendione)][PF_6]_2$

This complex was prepared in an analogous fashion to $[Ru(phen)_2phendione][PF_6]_2$.[57]

A mixture of $Ru(Ph_2phen)_2Cl_2$ (0.05 g, 0.06 mmol) and 1,10-phenanthroline-5,6-dione (0.013 g, 0.06 mmol) was dissolved in 50 mL of ethanol and refluxed for 5 h. After cooling the product was precipitated by addition of aqueous NH_4PF_6. The product was filtered, washed with ethanol (20 mL) followed by washing with water and dried in vacuum at 60 °C for 1h. The complex was changed to chloride salt by using the general metathesis procedure as described previously. Yield: 68 mg (90%). Anal. Calcd for $C_{60}H_{38}F_{12}N_6P_2RuO_2$: C, 56.92; H, 3.03; N, 6.64; Found C, 57.42; H, 2.96; N, 6.50. ^{1}H NMR (δ,CD_3CN, 500 MHz): 7.54-7.64(m , 36H, H_{Ph}), 7.78 (d, 2H, *J* = 6.0 Hz, H_c), 8.11 (d, 2H, *J* = 6.0 Hz, H_c), 8.19 (d, 2H, H_3, H_9), 8.21 (s, 2H, H_5, H_6), 8.26 (d, 2H, *J* = 6.0 Hz, H_2, H_9) 8.41 (d, *J* = 6.0 Hz, 3.0 Hz, H_a). ESI-MS (m/z): 1121.20 $[[Ru(Ph_2phen)_2(phendione)]^{2+}\text{-}PF_6]^+$, 488.33 $[Ru(Ph_2phen)_2(phendione)]^{2+}\text{-}2PF_6]^{2+}$.

2.2.3.4 [$Ru(Me_4phen)_2Cl_2$]

This complex was prepared in analogous fashion to $Ru(bpy)_2Cl_2$ reported by Sullivan *et al*.[56] with slight modification. Me_4phen ligand (0.56 g, 2.37 mmol), $RuCl_3 \cdot 3H_2O$ (0.1g, 0.38 mmol) and LiCl (0.11g, 2.6 mmol) were dissolved into 20 mL of dimethylformamide (DMF). The solution was refluxed overnight for 14 h under nitrogen. The mixture was allowed to cool to room temperature and the product was precipitated by adding water (~30 mL). The precipitate was then washed with copious amounts of water followed by washing with diethyl ether and allowed to dry at room temperature. Yield: 245 mg (98%).

2.2.3.5 [$(Me_4phen)_2Ru(phendione)][PF_6]_2$

This complex was prepared in an analogous fashion to $[Ru(phen)_2phendione][PF_6]_2$.[57]

A mixture of $(Me_4phen)_2RuCl_2$ (0.2 g, 0.31 mmol) and 1,10-phenanthroline-5,6-dione (0.062 g, 0.31 mmol) was dissolved in 50 mL of ethanol and refluxed for 5 h. After cooling the reaction mixture to room temperature, the product was precipitated out with an excess amount of aqueous NH_4PF_6. The product was filtered, washed with ethanol followed by washing with water and dried in vacuum at 60 °C for 1h. $[(Me_4phen)_2Ru(phendione)][PF_6]_2$ was changed to chloride salt by using the general metathesis procedure as described previously. Yield: 240 mg (71%). ^{1}H NMR (δ,CD_3CN, 500 MHz): 8.43 (dd, 2H, J_1 = 6.0 Hz, J_2 = 3.0 Hz, H_a), 8.36 (d, J = 3.0 Hz, 4H, H_2, H_9), 7.90 (s, 2H, H_6), 7.79 (dd, 2H, J_1 = 6.0 Hz, J_2 = 3.0 Hz H_c), 7.60 (s, 2H, H_5), 7.42 (dd, 2H, J_1 = 6.0 Hz, J_2 = 3.0 Hz, H_b), 2.77 (d), 2.36 (br. s, CH_3). ESI-MS (m/z): 929.27 $[[(Me_4phen)_2Ru(phendione)]^{2+}\text{-}PF_6]^+$, 392.87 $[[(Me_4phen)_2Ru(phendione)]^{2+}\text{-}2PF6]^{2+}$.

2.2.3.6 $[(Me_4phen)_2Ru(tatpp)][PF_6]_2$, $[\mathbf{MP_{Me}}][PF_6]_2$

$[(Me_4phen)_2Ru(phendione)]Cl_2$ (0.1 g, 0.12 mmol) and 11,12-diaminodipyridophenazine, (dadppz, 0.04 g, 0.13 mmol) were dissolved in mixture of 5 mL of glacial acetic acid and 50 mL of absolute ethanol in 100 mL round bottomed flask. The reaction mixture was refluxed overnight and then cooled down to room temperature. The addition of saturated aqueous NH_4PF_6 to the solution resulted in a precipitate, which was isolated by filtration and washed with 100 mL of water followed by drying under vacuum at 60 °C for 1 h. $[\mathbf{MP_{Me}}][PF_6]_2$ was changed to chloride salt by using the general metathesis procedure as described previously. Yield: 115 mg (71%). Anal. Calcd for $C_{66}H_{42}F_{12}N_{12}P_2Ru{\cdot}2H_2O$: C, 53.72; H, 3.64; N, 12.13; Found C, 53.79; H, 3.34; N, 11.91. ^{1}H NMR (δ, CD_3CN, 500 MHz): 9.95 (d, 2H, J = 10.0 Hz, H_c), 9.62 (s, 2H, H_h), 9.60 (d, 2H, J = 9.5 Hz, $H_{c'}$), 9.25 (d, 2H, J = 8.0 Hz, H_a), 8.38 (s, 4H, H_3,H_4), 8.32 (dd, 2H, J_1 = 5.0 Hz, J_2 = 10.0 Hz, H_b), 8.05 (d, 2H J = 9.0 Hz, $H_{a'}$), 7.91 (s, 4H, H_1), 7.75 (dd, 4H, J_1 = 4.5 Hz, J_2 = 9.8 Hz, $H_{b'}$), 7.73 (s, 4H, H_4), 2.77 (d, 12H, CH_3), 2.23 (s, 12H, CH_3). ESI-MS (m/z): 529.60 $[M\text{-}2PF_6]^{2+}$.

2.2.3.7 $[(Ph_2phen)_2Ru(tatpp)][PF_6]_2$, $[\mathbf{MP_{Ph}}][PF_6]_2$

Method 1:

$[(Ph_2phen)_2Ru(phendione)]Cl_2$ (0.14 g, 0.13 mmol) and dadppz (0.04 g, 0.13 mmol) were dissolved together at the same time in 50 mL mixture of glacial acetic acid and absolute ethanol (10:90). The solution was heated to reflux for 12 h and then cooled down to room temperature. The addition of aqueous NH_4PF_6 solution resulted in a precipitate, which was isolated by filtration and washed with water and dried under vacuo at 60 °C for 1 h. $[\mathbf{MP_{Ph}}][PF_6]_2$ was changed to chloride salt by using the general metathesis procedure as described previously. Yield: 120 mg (60%). Anal. Calcd for $C_{78}H_{46}F_{12}N_{12}P_2Ru$: C, 60.74; H, 3.01; N, 10.90; Found C, 59.16; H, 2.94; N, 10.87. ^{1}H NMR (δ, CD_3CN, 500 MHz): 9.96,

(d, J = 10.0 Hz, H_c), 9.74 (d, J = 10.0 Hz, $H_{c'}$), 9.67 (s, H_h), 9.30 (br s, H_a), 8.37 (d, J = 10.0 Hz, H_a), 8.31 (d, J = 5.0 Hz, H_1), 8.23 (d, J = 5.0 Hz, H_6), 8.20 (d, J = 10.0 Hz, H_3, H_4), 8.17 (br d, J = 5.0 Hz, H_b), 7.89 (dd, J_1 = 5.0 Hz, J_2 = 1.8 Hz $H_{b'}$), 7.59-7.63 (m, Ph). ^{1}H NMR (δ, 500 MHz, CD_3CN), 4[PF_6]$_2$: $ZnBF_4$(1:5) : 9.94 (d, J = 7.4 Hz, H_c), 9.71 (d, J = 8.0 Hz, $H_{c'}$), 9.62 (s, H_h), 9.23, (d, 2H, J = 5.0 Hz, H_a), 8.38 (d, J = 5.0 Hz, $H_{a'}$), 8.32 (d, J = 5.0 Hz, H_1), 8.32 (d, J = 8.0 Hz, 3.5 Hz, H_b), 8.24 (d, J = 10.0 Hz, H_2, H_5), 8.23 (d, J = 5.0 Hz, H_6), 8.18 (d, J = 10.0 Hz, H_3, H_4), 8.15 (br. s), 7.88 (dd, J_1 = = 5.0 Hz, J_2 = 1.8 Hz $H_{b'}$), 7.57-7.60 (m, Ph). ESI-MS (m/z): 1397 [M-PF_6]$^+$, 626 [[M-2PF_6] $^{2+}$.

Method 2:

[(Ph_2phen)$_2$Ru(dadppz)]Cl_2 (0.1 g, 0.087 mmol) and phendione (0.018 g, 0.069 mmol) were dissolved in a mixture of 50 mL of absolute ethanol and 5 mL of glacial acetic acid in 100 mL round bottomed flask. The solution was refluxed overnight and then cooled down to room temperature. Product was isolated upon the addition of aqueous NH_4PF_6, filtered, and washed with water and dried in the vacuum at 60 ^{o}C for 1 h. Yield = 63.8 mg (60%). The product is identical in all respects to that obtained by method 1.

2.2.3.8 [(Me_4phen)$_2$Ru(tatpp)Ru(Me_4phen)$_2$][PF_6]$_4$, [$\mathbf{P_{Me}}$][PF_6]$_4$

A mixture of tatpp (0.1 g, 0.021 mmol) and Ru(Me_4phen)$_2Cl_2$ (0.32 g, 1.36 mmol) was suspended in 30 mL of a 1:1 ethanol-water mixture and refluxed for 7 days under N_2. The mixture was then stored at 4°C for 12 h and filtered. The addition of aqueous NH_4PF_6 resulted in a precipitate, which was isolated by filtration and washed with 10 mL of water (3×) and 10 mL of ethanol (3×). The crude product was further purified by repeated metatheses between the chloride and hexafluorophosphate salts using the general metathesis procedure that described previously. Yield: 158 mg (34%). Anal. Calcd for $C_{94}H_{78}F_{24}N_{16}P_4Ru_2$.: C, 51.00; H, 3.55; N, 10.12; Found C, 50.71; H, 3.34; N, 9.74. ^{1}H NMR

(δ, 500 MHz, CD_3CN) δ:9.65 (s, 2H, H_h), 9.62 (d, *J* = 10.0 Hz, 4H, H_c), 8.38 (s, 8H, H_3,H_4), 8.04 (d, *J* = 5.0 Hz, 4H, H_a), 7.87 (s, 4H, H_1), 7.74 (dd, J_1= 3.5 Hz, 4H, J_2 =10.0 Hz, H_b), 7.71 (s, 4H, H_4), 2.77 (d, 24H, CH_3), 2.23 (s, 24H, CH_3). ESI-MS (m/z): 409 $[M-4PF_6]^{4+}$.

2.2.3.9 $[(Ph_2phen)_2Ru(tatpp)Ru(Ph_2phen)_2][PF_6]_4$, $[\mathbf{P_{Ph}}][PF_6]_4$

A mixture of tatpp (0.1 g, 0.21 mmol) and $(Ph_2phen)_2RuCl_2$ (0.42 g, 0.5 mmol) was suspended in 30 mL of a 1:1 ethanol-water mixture and refluxed for 7 days under N_2. The mixture was then stored at 4°C for 12 h and filtered. The addition of aqueous NH_4PF_6 resulted in a precipitate, which was isolated by filtration and washed with 10 mL of water (3x) and 10 mL of ethanol (3x). The crude product was further purified by repeated metatheses between the chloride and hexafluorophosphate salts using the general metathesis method that described previously. Yield: 270 mg (41%). Anal. Calcd for $C_{126}H_{78}F_{24}N_{16}P_4Ru_2$: C, 58.25; H, 3.03; N, 8.63; Found C, 57.18; H, 2.46; N, 8.67. ^{1}H NMR (δ, CD_3COCD_3, 500 MHz): 9.79 (d, *J* = 10.0 Hz, 4H, H_c), 9.28 (s, 4H, H_h), 8.74 (d, *J* = 5.0 Hz, 8H, H_1,H_6), 8.64 (d, *J* = 10.0 Hz, 4H, H_a), 8.34 (s, 8H), 8.06(dd, J_1 = 5.0 Hz, J_2 = 10.0 Hz, 4H, H_b), 7.78-7.80 (dd, J_1 = 5.0 Hz, J_2 = 10.0 Hz, 8H, H_2,H_5), 7.61-7.66(m, 40H, Ph). ESI-MS (m/z): 712.47 $[M-3PF_6]^{3+}$, 504.61 $[M-2PF_6]^{4+}$.

2.3 DNA Cleavage Assay

2.3.1 Reagents

Tris-Cl, EDTA (ethylenediamintetraacetic acid), Tris-acetate, agarose, ethidium bromide, dimethyl sulfoxide (DMSO) and glutathione (GSH) were used as received from Sigma Aldrich. Supercoiled plasmid pUC18 was obtained from Bayou Biolabs. Millipore water was used to prepare all buffers.

2.3.2 Sample Preparation for the DNA Cleavage Assay

Samples were prepared for stock solutions of Ru complex, supercoiled pUC18 DNA, GSH, and buffer as depicted in Table 2.1. Once the solutions were made up, the final concentrations of [DNA] = 0.154 mM, [GSH] = 0.513 mM, and [Ru complex] = 0.0128 mM.

2.3.3 Sample Workup and Analysis

Prepared samples were left to incubate for 12 hours at room temperature in dark place. The cleavage reaction was stopped by adding 3 µL sodium acetate and 80 µL ethanol to precipitate the DNA in each tube. The solutions were then kept in a -20 °C refrigerator overnight. The samples were centrifuged at 4 °C at 13,000 rpm for 30 minutes. After centrifugation, the supernatant was removed and the precipitant vacuum dried for 30 to 60 minutes. Thereafter, 40 µL of phosphate buffer (4 mM Na_3PO_4 and 50 mM NaCl) and 12 µL loading buffer (30% glycerol in distilled water with 0.1% w/v bromophenol blue) were added to all the samples. The samples were mixed thoroughly and 6 µL of each was loaded into a well of a 1% agarose gel (0.4 g of agarose, 40 mL of Tris-HCl EDTA buffer (40 mM Tris-Cl, 1 mM EDTA, pH 8.0), and 4.0 µL ethidium bromide). The gel was subjected to electrophoresis at 120 V for 1 hours using TAE buffer (40 mM Tris-acetate, 1 mM EDTA, pH 8.0). The same cleavage reaction was performed under low [O_2] condition in a glovebox (N_2 atm) to determine how DNA cleavage was affected under hypoxic condition. Equilibration of degassed buffer solutions with the glovebox atm which had an [O_2] of 4.0 µM as measured by PO_2 sensitive electrode.[59]

Table 2.1 Experimental design for the DNA cleavage assay. Tube number identifies the lane in an agarose gel that would be used to analyze that sample

Tube	1	2	3	4	5	6	7	8	9	10	11	12	13	14
DNA	4 µL	4 µL	4 µL	4 µL	4 µL	4 µL	4 µL	4 µL	4 µL	4 µL	4 µL	4 µL	4 µL	4 µL
GSH		8 µL		8 µL		8 µL		8 µL		8 µL		8 µL		8 µL
$[P]Cl_4$			8 µL	8 µL										
$[MP]Cl_2$					8 µL	8 µL								
$[P_{Ph}]Cl_4$							8 µL	8 µL						
$[MP_{Ph}]Cl_2$									8 µL	8 µL				
$[P_{Me}]Cl_4$											8 µL	8 µL		
$[MP_{Me}]Cl_2$													8 µL	8 µL
Buffer	36 µL	28 µL	28 µL	20 µL	28 µL	20 µL	28 µL	20 µL	28 µL	20 µL	28 µL	20 µL	28 µL	20 µL
Total Volume	40 µL	40 µL	40 µL	40 µL	40 µL	40 µL	40 µL	40 µL	40 µL	40 µL	40 µL	40 µL	40 µL	40 µL

- Buffer = phosphate buffer (4 mM Na_3PO_4 and 50 mM NaCl)
- Final concentrations: [DNA] = 0.154 mM, [Ru complex] = 0.0128 mM, [GSH] = 0.513 mM
- **[P]**Cl_4 = **[MP]**Cl_2 = **[P_{Ph}]**Cl_4= **[MP_{Ph}]**Cl_2 **=** **[P_{Me}]**Cl_4 **=** **[MP_{Me}]**Cl_2 **=** 0.0128 mM

2.4 Results and Discussion

2.4.1 Synthesis of Ruthenium Polypyridyl Complexes

Two mononuclear $[(L\text{-}L)_2Ru(tatpp)]^{2+}$ and two dinuclear $[(L\text{-}L)_2Ru(tatpp)Ru(L\text{-}L)_2]^{4+}$, RPCs containing the 9,11,20,22-tetraazatetrapyrido [3,2-a:2',3'-c:3'',2''-l:2''',3'''-n]pentacene (tatpp) ligand were synthesized, where L-L is 3,4,7,8 tetramethyl-1,10-phenanthroline (Me_4phen) and 4,7-diphenyl-1,10-phenanthroline (Ph_2phen).

The most direct route to prepare the dinuclear tatpp complexes is to prepare a slurry of tatpp with two equivalents of $Ru(L\text{-}L)_2Cl_2$ in refluxing ethanol and water (50:50),[54] as shown in Figure 2.3. The sparing solubility of tatpp leads to long reaction times (up to seven days), and moderate yields. The pure dinuclear compounds were obtained by repeated metatheses between the hexafluorophosphate salt and the chloride salt. The yield varied among the analogues with 65% for $[(phen)_2Ru(tatpp)Ru(phen)_2]^{4+}$ ($\mathbf{P^{4+}}$),[54] 34% for $[(Me_4phen)_2Ru(tatpp)Ru(Me_4phen)_2]^{4+}$ ($\mathbf{P_{Me}^{4+}}$), and 41% for $[(Ph_2phen)_2Ru(tatpp)Ru(Ph_2phen)_2]^{4+}$ ($\mathbf{P_{Ph}^{4+}}$).

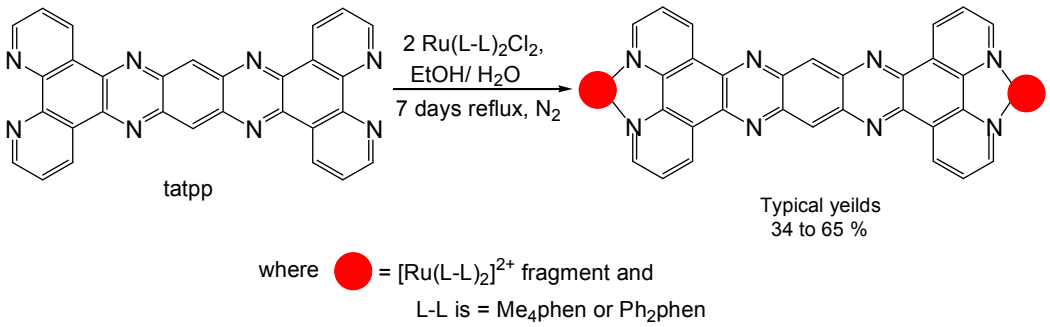

Figure 2.3 Synthetic route for Ru(II) dinuclear complexes

Attempts to synthesize the mono-metallated Ru(II) complexes using the direct route by refluxing one equivalent of $Ru(L\text{-}L)_2Cl_2$ with tatpp invariably gave the dimer, as the solubility of the mono-metallated complex results in facile addition of the second metal center. Instead, we examined two alternative approaches in which the tatpp ligand is built up onto the metal complex, as outlined in Figure 2.4. We had difficulty preparing dadppz from the condensation reaction between freshly prepared 1,2,4,5-tetraaminobenzene and phendione as described by Warnmark *et al*.,[60] a problem that was also noted by Mattay and co-workers in a separate study.[61,62] Instead, they prepared dadppz using protected diamines, such as 4,5-dinitro-*o*-phenylenediamine or 4,5-diamino-N^1,N^2-ditosyl-*o*-phenylenediamine, to prepare a protected form of the dadppz.[62,61] Subsequent reduction of the dinitro species or detosylation for the latter species yielded pure dadppz, respectively.

Synthesis of mononuclear complexes was done by the condensation of 11,12-diaminodipyrido[3,2-a:2',3'-c]phenazine with $[(L\text{-}L)_2Ru(phendione)]^{2+}$ overnight in ethanol (method 1) to obtain 60 to 71% yield as shown in Figure 2.4. In another route $[(L\text{-}L)_2Ru(phendione)]^{2+}$ coupled with 1,2-diamino-4,5-dinitrobenzene to obtain $[(L\text{-}L)_2Ru(dinitro\text{-}dppz)]^{2+}$ (method 2), which are further reduced to $[(L\text{-}L)_2Ru(diamino\text{-}dppz)]^{2+}$ using H_2 atm over Pd/C as a catalyst. In the last step $[(L\text{-}L)_2Ru(diamino\text{-}dppz)]^{2+}$ was coupled with one equivalent of phendione in glacial acetic acid and ethanol (1:1) to obtain mononuclear ruthenium complexes. While both methods work, method 2 is less desirable route as the expensive ruthenium complexes are carried through more synthetic procedures and risk additional losses. Method 1 is more efficient as it carries pure material between the multiple sequences of the reaction compared to method 2.

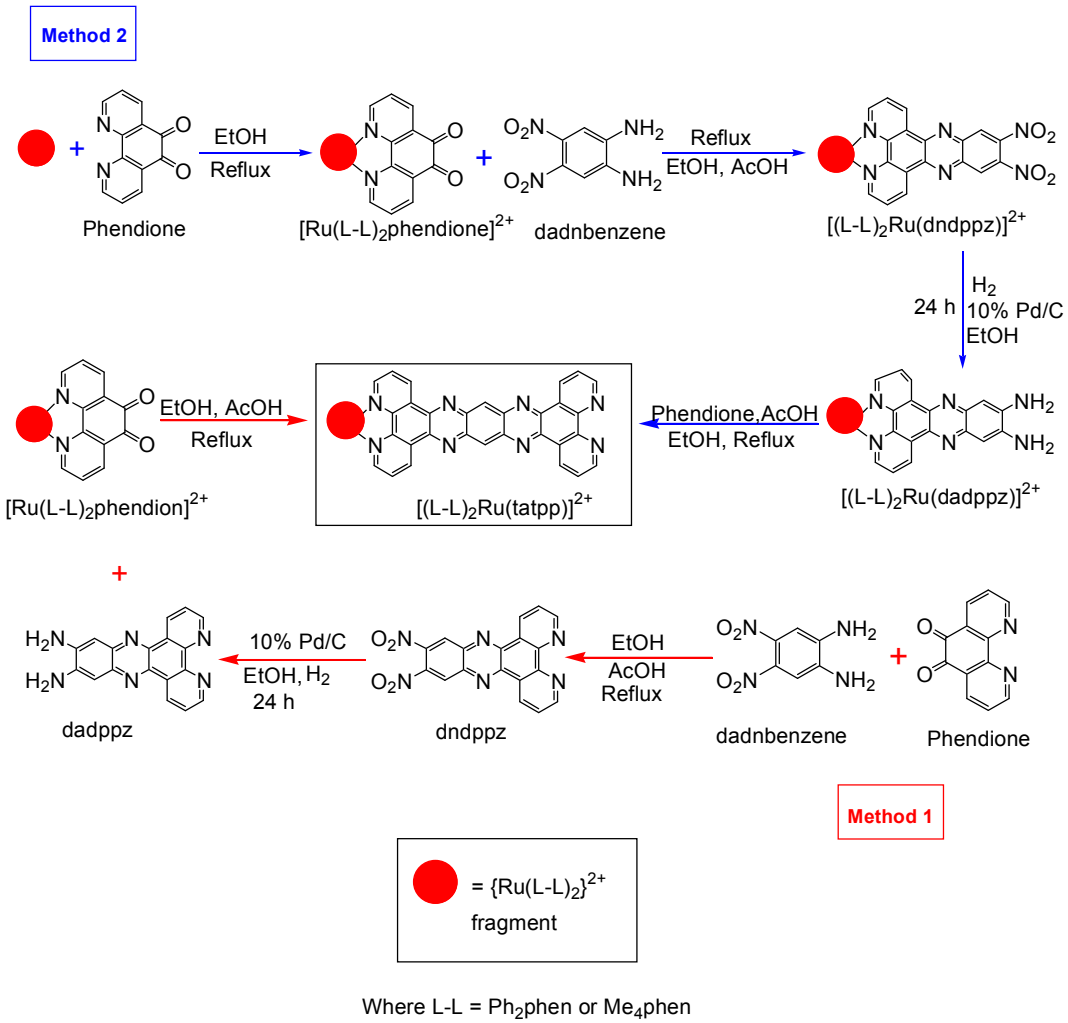

Where L-L = Ph_2phen or Me_4phen

Figure 2.4 Synthetic route for Ru(II) mononuclear complexes

^{1}H NMR

^{1}H NMR of the dinuclear and mononuclear ruthenium(II) complexes, were taken in CD_3COCD_3 or CD_3CN. Despite the stereochemical complexity of the dinuclear complexes prepared by the ligand displacement method, the NMR spectra of the diastereomers are indistinguishable, which was reported earlier as being due to the large distances between stereocenters in complexes like $\mathbf{P}^{4+}$.[54] As with $\mathbf{P}^{4+}$, the ^{1}H NMR of $\mathbf{P_{Ph}}^{4+}$, and $\mathbf{P_{Me}}^{4+}$ are surprisingly simple as the complexes have relatively high symmetry (C_{2h} for $\Delta\Lambda$). The tatpp peaks in $\mathbf{P_{Ph}}^{4+}$, and $\mathbf{P_{Me}}^{4+}$, show essentially the same chemical shifts as seen in $\mathbf{P}^{4+}$,[54] for which the most diagnostic peak is a doublet for H_c (see Figure 2.5 and 2.6). This peak comes downfield between 9.6 and 9.8 ppm and is indicative of pyrazine ring formation in the condensation reactions. The H_c proton of tatpp ligand is observed at 9.79 ppm and 9.62 ppm for $\mathbf{P_{Ph}}^{4+}$ and $\mathbf{P_{Me}}^{4+}$, respectively as shown in Figures 2.5 and 2.6. Similarly, a singlet for H_d is observed at 9.8 ppm for $\mathbf{P}^{4+}$ which is shifted downfield because of its location between that adjacent aza nitrogens. In both dinuclear complexes, $\mathbf{P_{Ph}}^{4+}$ and $\mathbf{P_{Me}}^{4+}$, a sharp singlet H_d is observed at 9.28 and 9.65 ppm respectively. The data comparing the tatpp chemical shifts are collected in Table 2.2. The most prominent changes the various NMR spectra are associated with the substitution of the phen ligands, as expected.

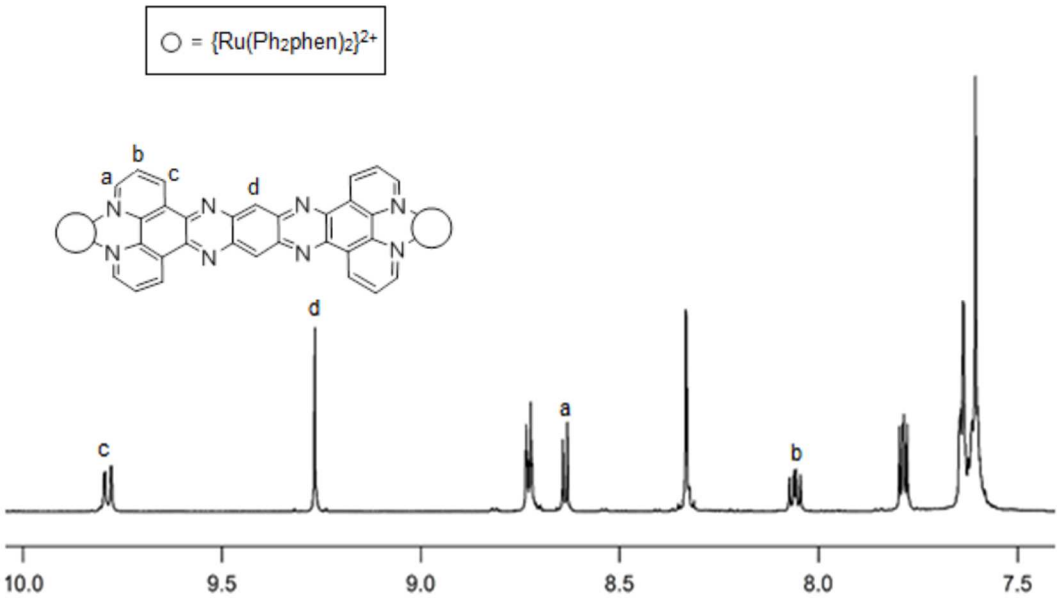

Figure 2.5 ^{1}H NMR spectrum of $[(Ph_2phen)_2Ru(tatpp)Ru(Ph_2phen)_2]^{4+}$

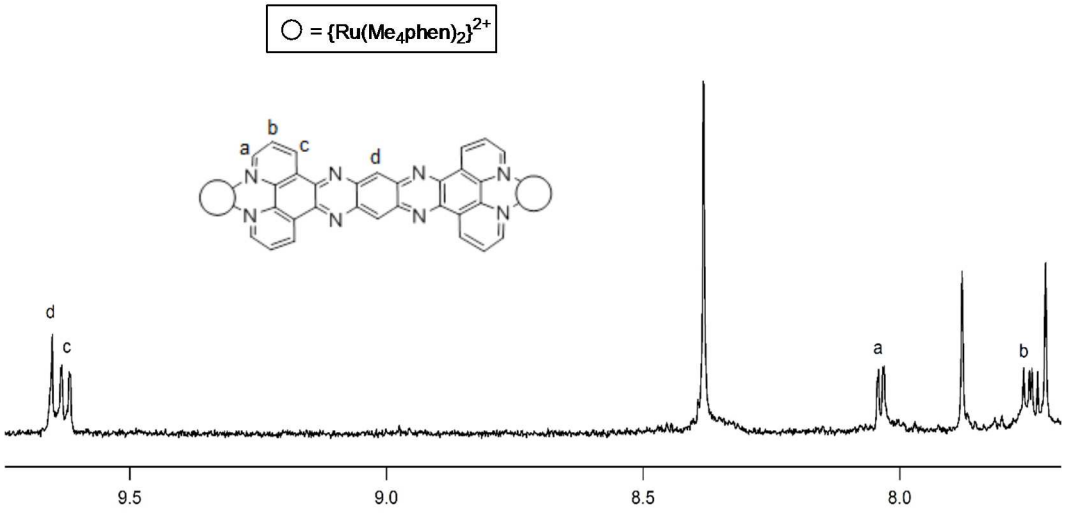

Figure 2.6 ^{1}H NMR spectrum of $[(Me_4phen)_2Ru(tatpp)Ru(Me_4phen)_2]^{4+}$

(extended downfield region)

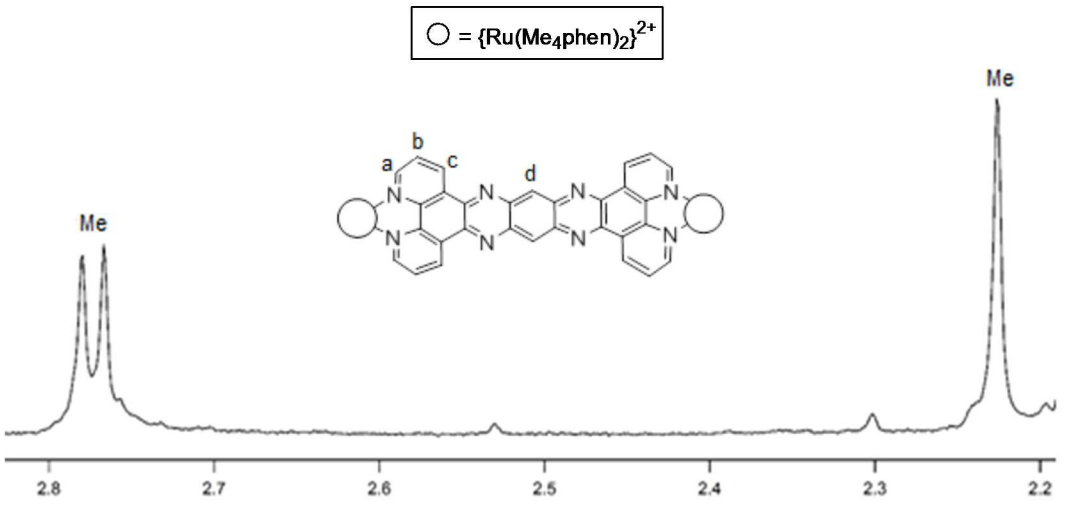

Figure 2.7 ^{1}H NMR spectrum of $[(Me_4phen)_2Ru(tatpp)Ru(Me_4phen)_2]^{4+}$

(extended upfield region)

The phenyl protons in $\mathbf{P_{Ph}}^{4+}$ were observed as a multiplet between 7.61-7.66 ppm as seen in Figure 2.5. The methyl protons in in $\mathbf{P_{Me}}^{4+}$ were observed as a broad singlet at 2.23 ppm, and a doublet at 2.77 ppm as shown in Figure 2.7. While the NMR data for the dinuclear complexes is straightforward, the presence of the large planar tatpp ligand in the mononuclear complexes complicates the spectra as π-π aggregation is evident in both the NMR and mass-spectroscopic data. As reported previously for the monomer $[(bpy)_2Ru(tatpp)][PF_6]_2$, the proton NMR for these complexes are concentration dependent due to the formation of π-stacked aggregates in MeCN.[63] Such aggregation appears common in complexes with large planar aromatic ligands[64,65] and has been reported for $[(phen)_2Ru(tpphz)]^{2+}$,[66,52,67] as well as a number of related complexes containing large planar aromatic ligands.[68,69,70] As is typical for all these compounds, π-stacking shifts the resonant absorptions for protons associated with the stacking moiety, tatpp in this case, upfield and broadens the peak(s).

Coordination of Zn(II) ions to the open diimine site on the tatpp ligand in monomer complexes $\mathbf{MP}^{2+}$, $\mathbf{MP_{Ph}}^{2+}$ and $\mathbf{MP_{Me}}^{2+}$ provides a convenient way to break-up the π-aggregates and simplify the ^{1}H NMR spectra.[63] Addition of a 5-fold excess of Zn(II) relative to the monomeric Ru complexes favors formation of a simple $(Ru\text{-}tatpp\text{-}Zn)^{4+}$, heterodimer of the general structure $[(L\text{-}L)_2Ru(tatpp)Zn(MeCN)_x]^{4+}$ ($\mathbf{MP}^{4+}$, $\mathbf{MP_{Ph}}^{4+}$, $\mathbf{MP_{Me}}^{4+}$), the data for which is collected in Table 2.2. This is seen in Figure 2.8 for $\mathbf{MP_{Ph}}^{2+}$ and Figure 2.9 for $\mathbf{MP_{Me}}^{2+}$. In particular, $H_{a'}$ shifts downfield by 1.04, 1.18 ,0.86 and 1.22 ppm in $[(phen)_2Ru(tatpp)Zn(MeCN)_x]^{4+}$ ($[\mathbf{MP}\text{-}Zn]^{4+}$), $[(Ph_2phen)_2Ru(tatpp)Zn(MeCN)_x]^{4+}$ ($[\mathbf{MP_{Ph}}\text{-}Zn]^{4+}$), and $[(Me_4phen)_2Ru(tatpp)Zn(MeCN)_x]^{4+}$ ($[\mathbf{MP_{Me}}\text{-}Zn]^{4+}$) respectively as compare to H_a (Table 2.2). The peaks due to the auxiliary ligands 1,10-phenanthroline, 3,4,7,8 tetramethyl-1,10-phenanthroline, 4,7-diphenyl-1,10-phenanthroline on the Ru(II) ions are

observed at almost identical chemical shifts to their respective dimer and are largely unaffected by Zn(II) coordination.

Mass spectrometry:

ESI-MS is a powerful technique to observe non-covalent polymeric aggregations, such as those proposed as the source of peak broadening in the ^{1}H NMR spectra in the absence of Zn^{2+}. The singly charged mononuclear complex [**MP** - $1PF_6$]$^+$ is observed at 1093 m/z and [**MP** - $2PF_6$]$^{2+}$ is at 474.0 m/z, respectively. Parent ion peaks at 529.6 for [$\mathbf{MP_{Me}}$ - $2PF_6$]$^+$ and at 1397 and 626 for [$\mathbf{MP_{Ph}}$ - PF_6]$^+$ and [$\mathbf{MP_{Ph}}$ - PF_6]$^{2+}$ respectively. The ESI-MS mass spectra for the dinuclear complexes do not indicate any formation of π--stacked aggregates. ESI-MS data of dinuclear complexes [$\mathbf{P_{Ph}}$][PF_6]$_4$ and [$\mathbf{P_{Me}}$][PF_6]$_4$ shows parent ion peak with m/z of 409 and 504.6 respectively, which correspond well with the calculated m/z ratios for the $\mathbf{P_{Ph}}^{4+}$, and $\mathbf{P_{Me}}^{4+}$ cation with loss of four associated PF_6^- counterions.

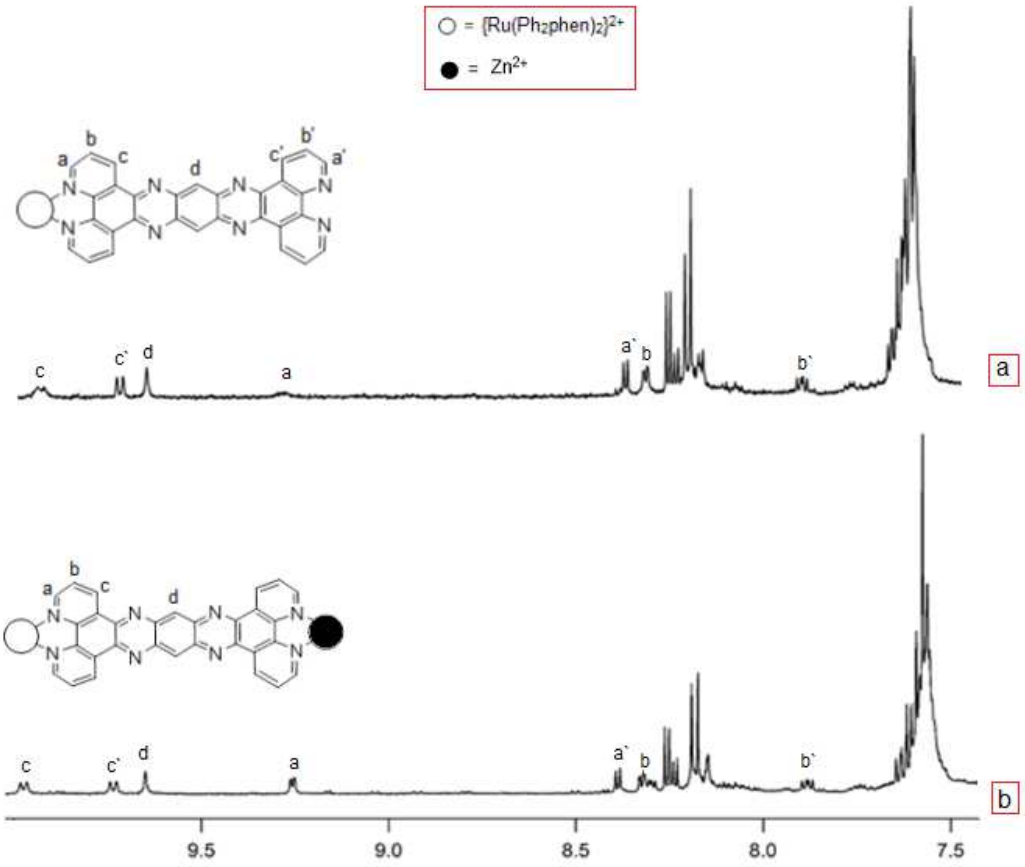

Figure 2.8 ^{1}H NMR spectrum of (a) $[(Ph_2phen)_2Ru(tatpp)]^{2+}$ in the absence of $Zn(BF_4)_2$ and (b) $[(Ph_2phen)_2Ru(tatpp)]^{2+}$ with excess $Zn(BF_4)_2$

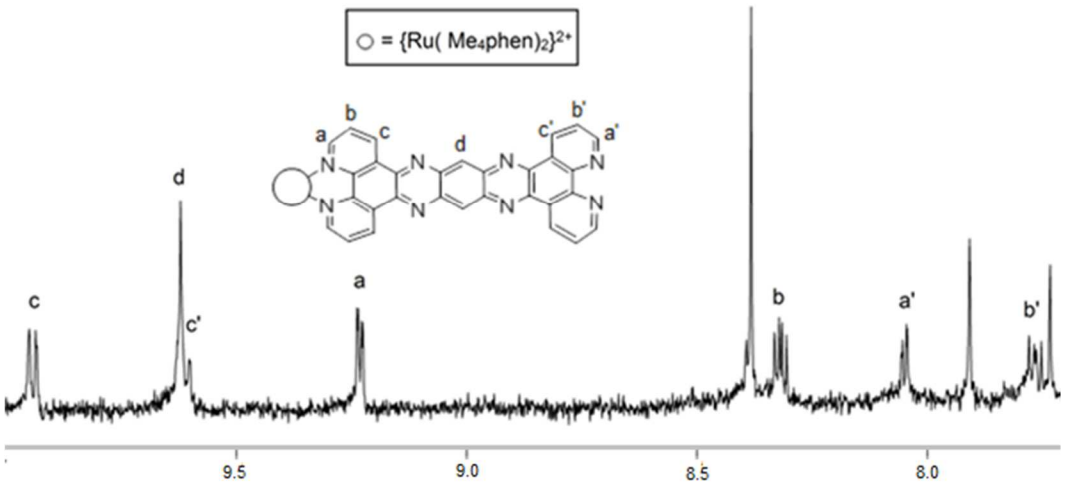

Figure 2.9 ^{1}H NMR spectrum of $[(Me_4phen)_2Ru(tatpp)]^{2+}$ with excess $Zn(BF_4)_2$

(expended down field region)

Table 2.2 ^{1}H NMR chemical shifts in ppm for ruthenium(II) complexes and tatpp in MeCN-d_3

Complex δ	$MP^{2+\ 54}$	MP_{Ph}^{2+}	MP_{Me}^{2+}	$P^{4+\ 54}$	P_{Ph}^{4+}	MP_{Me}^{4+}	Tatpp (with excess $Zn(BF_4)_2$
H_a Ru	8.19	8.38	8.02	8.15	8.32	8.04	
H_b Ru	7.82	7.90	7.76	7.82	7.89	7.74	
H_c Ru	9.81	9.71	9.59	9.70	9.73	9.63	
H_a Zn	9.37	9.24	9.24				9.27
H_b Zn	8.48	8.32	8.32				8.35
H_c Zn	10.1	9.94	9.96				9.99
H_a Ru	8.20	8.3					
H_b Ru	7.82	7.91					
H_c Ru	9.48	9.74					
$H_{a'}$	9.20	9.31 br.					
$H_{b'}$	9.18	8.32					
$H_{c'}$	9.89	9.97					
H_d	9.28	9.67		9.70	9.69	9.65	
H_d-Zn	9.78	9.62	9.62				9.66

2.4.2 DNA Cleavage of Ruthenium Polypyridyl Complexes

While substitution of the phenanthroline ligands in $\mathbf{P}^{4+}$ and $\mathbf{MP}^{2+}$ should not impact the DNA cleavage activity, this is not guaranteed, therefore, complexes $\mathbf{P_{Ph}}^{4+}$, $\mathbf{MP_{Ph}}^{2+}$, $\mathbf{P_{Me}}^{4+}$, $\mathbf{MP_{Me}}^{2+}$ were all examined for DNA cleavage activity using a standard plasmid cleavage assay. All complexes were incubated with supercoiled pUC18 DNA (1 μg/1 μL, 0.154 mM DNA base pairs) for 12 h and the products examined using agarose gel DNA electrophoresis. The gel is used to separate the three different topological confirmations (Form I, Form II and Form III) of the plasmid DNA pUC18. If supercoiled (Form I) undergoes a single strand nick, it will be converted to circular plasmid (Form II) and if undergoes a double strand nick, it will be converted to a linear plasmid (Form III) as shown in Figure 2.10.

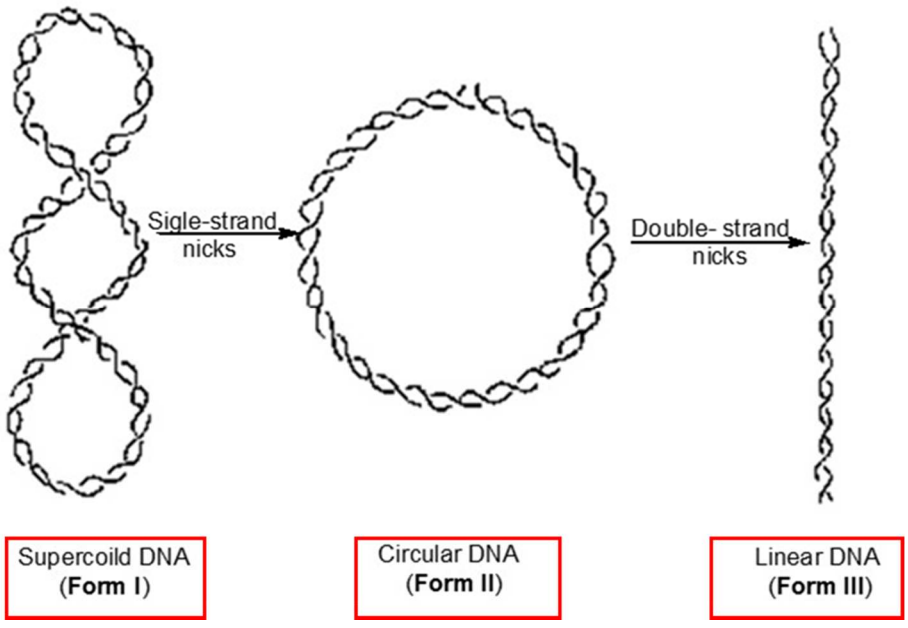

Figure 2.10 Topological confirmation of the plasmid DNA pUC18

The ability of tatpp-based RPCs to bind to DNA have been examined in earlier studies. [29,71,72] Previous work had established that $\mathbf{P}^{4+}$ and $\mathbf{MP}^{2+}$, were DNA cleavage agents in the presence of GSH and that they showed potentiated DNA cleavage under hypoxia conditions.[28,27] This oxygen sensitive DNA cleavage activity is almost apparent in line calls as revealed by an increase in their potency as cytotoxic agents for H358 tumor cells are under hypoxia (1% O_2) compared to H358 cells under normoxic conditions.[26]

The mechanism of DNA cleavage has been shown to be related to reduction of the intercalated Ru complex.[59] Formation of a tatpp-based radical in the immediate vicinity of the DNA leads to H-atom abstraction from the deoxyribose backbone, ultimately leading to strand scission.

As with $\mathbf{MP}^{2+}$ and $\mathbf{P}^{4+}$, the new analogues were examined for DNA cleavage activity under normoxia (~200 μM O_2), and hypoxia (~ 4 μM O_2) in the presence or absence of GSH. These gels are shown in Figures 2.11, 2.12 (normoxia) and 2.13, 2.14 (hypoxia). For the experiments conducted under normoxia, it was clear that the presence of GSH was essential for cleavage activity, as seen for $\mathbf{P_{Ph}}^{4+}$, $\mathbf{MP_{Ph}}^{2+}$ in Figure 2.11 and for $\mathbf{P_{Me}}^{4+}$ and $\mathbf{MP_{Me}}^{2+}$ in Figure 2.12. All complexes were inactive in the absence of the reducing agent. It also was shown that the DNA cleavage activity was enhanced under hypoxia conditions. Moreover, mononuclear Ru(II) complexes have shown greater cleavage activity compared to the dinuclear complexes as revealed in Figure 2.13 and 2.14.

This data show that all the novel lipophilic Ru(II) complexes sustain their DNA cleavage activity upon changing their terminal ligands to Ph_2phen and Me_4phen.

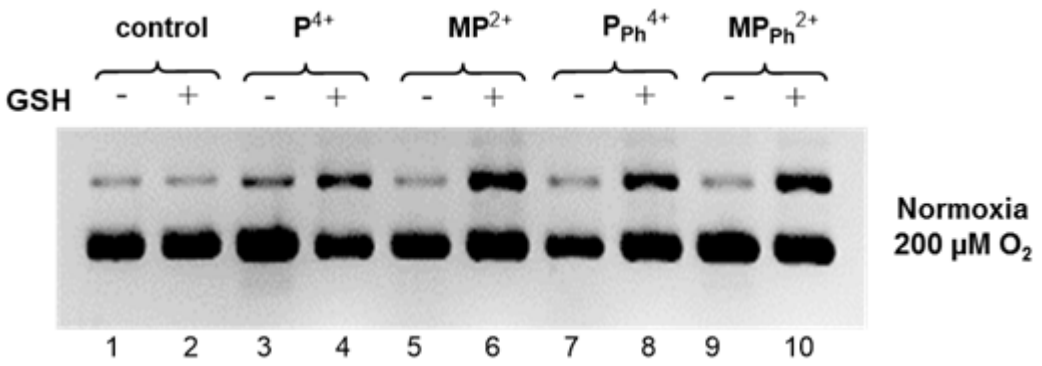

Figure 2.11 1% Agarose gel exhibiting conversion of supercoiled pUC18 plasmid DNA (0.154 μM bp) to circular DNA upon treatment with of ruthenium complexes $\mathbf{P}^{4+}$, $\mathbf{MP}^{2+}$, $\mathbf{P_{Ph}}^{4+}$ and $\mathbf{MP_{Ph}}^{2+}$ (final concentration 0.0128 μM) with and without mM GSH (51 μM) under normoxic conditions at 20 °C for 12 h in phosphate buffer (4 mM Na_3PO_4 and 50 mM NaCl) at pH 7.35

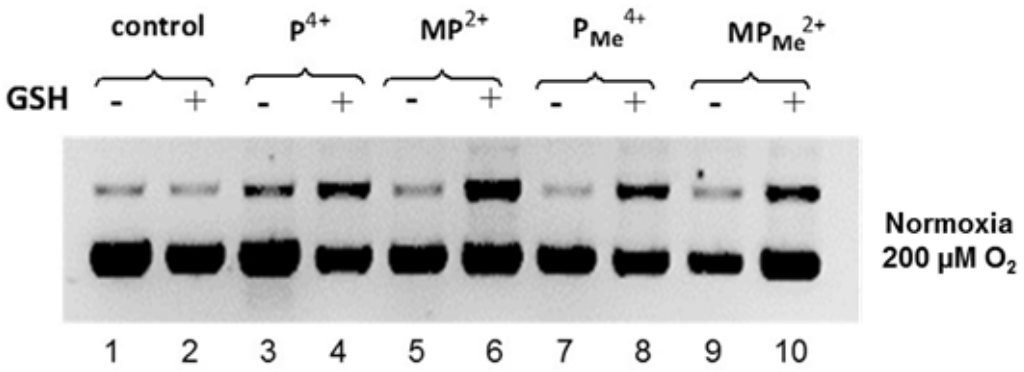

Figure 2.12 1% Agarose gel exhibiting conversion of supercoiled pUC18 plasmid DNA (0.154 mM bp) to circular DNA upon treatment with 0.0128 mM of ruthenium complexes $\mathbf{P}^{4+}$, $\mathbf{MP}^{2+}$, $\mathbf{P_{Me}}^{4+}$ and $\mathbf{MP_{Me}}^{2+}$ with and without 0.513 mM GSH under normoxic conditions at 20 °C for 12 h in phosphate buffer (4 mM Na_3PO_4 and 50 mM NaCl) at pH 7.35

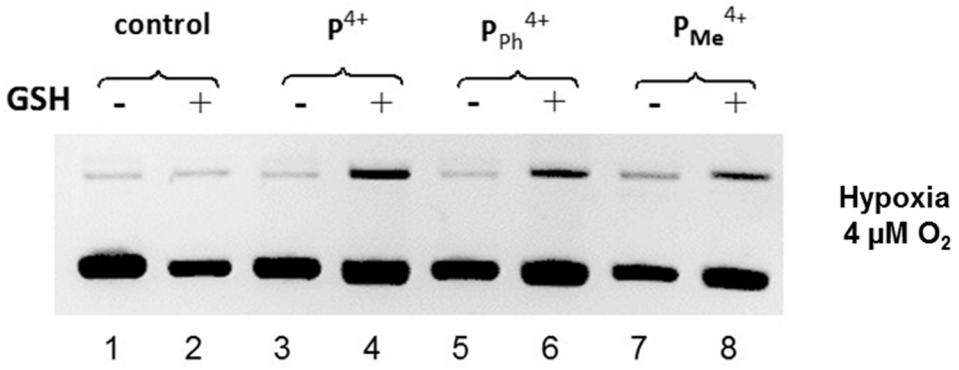

Figure 2.13 1% Agarose gel exhibiting conversion of supercoiled pUC18 plasmid DNA (0.154 mM bp) to circular DNA upon treatment with 0.0128 mM of ruthenium complexes $\mathbf{P}^{4+}$, $\mathbf{P_{Ph}}^{4+}$ and $\mathbf{P_{Me}}^{4+}$ with and without 0.513 mM GSH under hypoxic conditions at 20 °C for 12 h in phosphate buffer (4 mM Na_3PO_4 and 50 mM NaCl) at pH 7.35

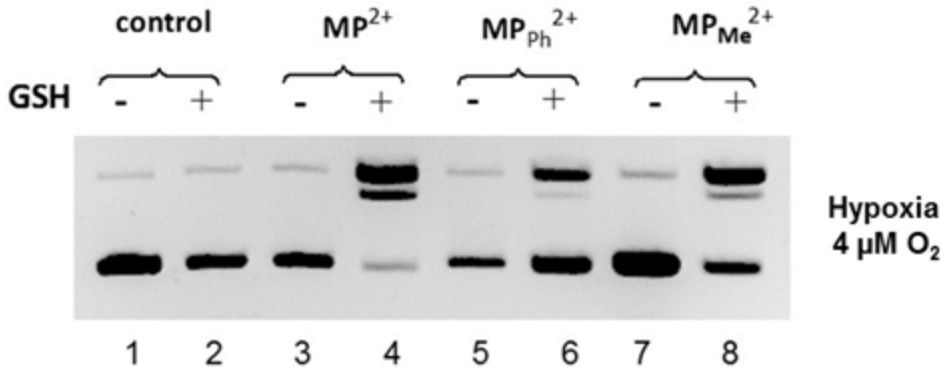

Figure 2.14 1% Agarose gel exhibiting conversion of supercoiled pUC18 plasmid DNA (0.154 mM bp) to circular DNA upon treatment with 0.0128 mM of ruthenium complexes **MP**$^{2+}$, **MP$_{Ph}$**$^{2+}$ and **MP$_{Me}$**$^{2+}$ with and without 0.513 mM GSH under hypoxic conditions at 20 °C for 12 h in phosphate buffer (4 mM Na_3PO_4 and 50 mM NaCl) at pH 7.35

2.5 Conclusion

We have synthesized four new lipophilic Ru(II) complexes and characterized them by NMR, MS and CHN. While the dinuclear complexes can be prepared in a one-step assembly reaction, the mononuclear complexes require a more elaborate synthesis. Two routes in which the tatpp ligand is built up onto a $[(L\text{-}L)_2Ru(phendione]^{2+}$ starting complex were explored, with the route in which a diaminodppz unit is coupled to the $[(L\text{-}L)_2Ru(phendione]^{2+}$ ultimately being favored as it involves the least amount of manipulation of the more expensive metal complex. DNA cleavage studies on $\mathbf{P_{Ph}}^{4+}$, $\mathbf{P_{Me}}^{4+}$, $\mathbf{MP_{Ph}}^{2+}$ and $\mathbf{MP_{Me}}^{2+}$ showed that all of the new derivatives behave similarly to $\mathbf{P}^{4+}$ and $\mathbf{MP}^{2+}$ in that they require GSH to cleave DNA and show potentiated DNA cleavage under low O_2 conditions. This data reveals that they should, in principle, be similarly effective as cytotoxic agents with any differences observed being largely due to the ancillary ligands.

Chapter 3

CYTOTOXICITY AND LIPOPHILICITY OF RUTHENIUM POLYPYRIDYL COMPLEXES

3.1 Introduction:

Ruthenium(II) polypyridyl complexes (RPCs) have been utilized for numerous applications including sensors, photosensitizers, and biological probes for over 30 years because of their favorable redox and photophysical properties as well as their synthetic variability and inherent stability.[73,74,75,76,77,78,79,80] Polyazine ligands such as dppz (dipyrido[3,2-*a*:2',3'-*c*]phenazine), tatpp, tpphz (tetrapyrido[3,2-*a*:2‘,3‘-*c*:3‘‘,2‘‘-*h*:2‘‘‘,3‘‘‘-*j*]phenazine), and tatpq (9,11,20,22-tetraazatetrapyrido [3,2-a:2',3'-c:3'',2''-l:2''',3'''-n]pentacene-10,21-quinone), illustrated in Figure 3.1, are of special interest as they comprise a series of closely related structures which have shown interesting properties upon interacting with DNA.[81,82,83,84,85,86,87] Ruthenium(II) complexes of the dppz and tpphz ligands complexes are known to act as molecular light switches which luminesce upon intercalation into DNA or in non-protic solvents.[88,89,90,91]

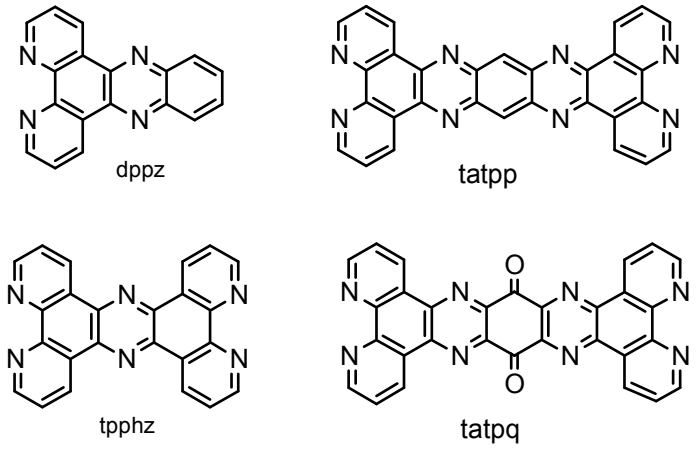

Figure 3.1 Chemical structures and abbreviations for the diimine ligands

This field has expanded considerably in the past decade, with numerous groups exploring substitutionally-inert ruthenium polypyridyl complexes as potential cytotoxic agents (drugs) for cancer therapy and can broadly be divided into two groups: those exploring light-activated ruthenium-based drugs (aka photodynamic therapy) and those simply examining the innate cytotoxicity of the complexes in the absence of external activation. The photodynamic approach can offer certain advantages if the unactivated complex can be modified to have limited deleterious side-effects or toxicity and become active only when irradiated.[92], However, such a strategy implies that one knows where the cancer is and can direct light to activate the drug complex in this location.[93] Drugs that find and destroy cancer cells wherever they are found are systemic. This is especially important in situations where a cancer is suspected to have metastasized but is still too small to detect. These drugs must work without external activation; seeking out these metastases and eliminating them before they cause a reoccurrence.

While RPCs activated by light are generally known to induce cell damage via activation of O_2 to form reactive oxygen species (ROS)[94] or via ligand loss such that the metal forms adducts with biological substrates,[2] the mechanisms and targets by which non-externally activated ruthenium complexes induce cell death are much less understood. At present, there is no consensus on the cellular target: the nuclear DNA,[95,96,97] mitochondria,[98,99,100] and cell membrane[101,37,95,102] are all postulated to be putative targets. Furthermore, it is possible that some or all of these targets are involved when RPCs are used; this depends on the structure characterization and activity of these drugs.

The initial examination of the biological activity of RPCs began in earnest in the 1950's with the work of Dwyer and coworkers. They examined the bacteriostatic, virostatic, mammalian cell cytotoxicity, and even anti-tumor properties of simple $[Ru(diimine)_3]^{2+}$ and $[Ru(diimine)_2(acac)]^{+}$ complexes[18] and further established that potency in a number of

applications, including cytotoxicity, was enhanced by either increasing the lipophilicity of the diimine ligand or lowering the overall charge to +1.[19,18] In 2008, Barton and coworkers reported enhanced cellular uptake of the more lipophilic ruthenium(II) complex $[(Ph_2phen)_2Ru(dppz)]^{2+}$ over the $[(phen)_2Ru(dppz)]^{2+}$ analogue; this enhanced cellular uptake was postulated to be a result of better transport through the cell membrane.[101] Dwyer's early work also established that $[Ru(phen)_3]^{2+}$ and related polypyridyl complexes are competitive inhibitors of AChE and that inhibition of this particular enzyme was responsible for their observed acute toxicity in mice at relatively low dosages.[103]

Recently, Meggers and coworkers expanded on this theme by examining heteroleptic ruthenium(II) polypyridyl complexes as AChE inhibitors. Upon proper optimization of the heteroleptic ligands, they were able to increase the inhibitory power of the simple homoleptic complex by 50-fold.[24] Meggars has gone on to show that heteroleptic Ru(II) complexes with monodentate ligands represent a rich area to explore for biologically active metal complexes, including the development of several complexes which show good cytotoxicity towards malignant cell lines and a melanoma spheroid model.[104]

As described in chapter 2, we have focused on the tatpp-based complexes $[(phen)_2Ru(tatpp)]^{2+}$ (**MP**$^{2+}$) and $[(phen)_2Ru(tatpp)Ru(phen)_2]^{4+}$ (**P**$^{4+}$), as potential anti-cancer drug candidates based on their ability to bind and cleave DNA and to regress tumor growth in mice with H358 xenografts.[26] While we are not certain that the DNA cleavage observed *in vitro* is responsible for the tumor regression observed *in vivo*, we postulate this connection. Presently, there is a significant and increasing amount of data supporting that different RPCs, and our tatpp-based RPCs in particular, show promise as investigational new drugs, which could possibly be taken into human clinical studies. However, there is noticeable lack in pharmacokinetic (PK), pharmacodynamic (PD) and toxicological studies.

Aside from the Dwyer early reports, the toxicity of these complexes in mammals is largely unexplored.

Dwyer and coworkers were pioneers in this area, as they reported on the minimal lethal doses of $[M(phen)_3][ClO_4]_2$, where M = Ru(II), Ni(II), and Fe(II); $[Os(bpy)_3][ClO_4]_2$, $[Ru(bpy)_3]I_2$, $[Ru(terpy)_2][ClO_4]_2$, and $[Ru(terpy)_2]I_2$ in mice when the complex was administered via intraperitoneal (IP) injection.[18] In general, doses higher than 18 mg complex/Kg mouse were toxic and in many cases doses as low as 3 mg/Kg were too much. They further showed that the toxicity of the Λ enantiomers of $[M(phen)_3]^{2+}$ complexes was twice that of the Δ enantiomers, in cases where the enantiomers were resolved, but there was no difference in toxicity between enantiomers for $[Os(bpy)_3][ClO_4]_2$ and $[Ru(bpy)_3]I_2$.[18] When toxicity was observed, symptoms appeared within minutes of the injection: the mice exhibited hind limb paralysis, labored breathing, tonic-clonic seizures, and, ultimately death, in short order, all of which are characteristic signs of acute neurotoxicity.[22]

Dwyer and coworkers postulated that it is the rate of drug perfusion through tissue and into the blood that dictates the toxicity. Slower perfusion is hypothesized to limit the peak blood concentration and, therefore, reduce drug toxicity toward the nervous system.[22] In this respect, Dwyer's work has demonstrated that the mechanism of acute toxicity in animals has less to do with how the complexes affect singular cells, and more to do with the effect on the systems' biology, such as poisoning of the central nervous system.[22]

Ultimately, the development of a drug from the ruthenium polypyridyl platform will depend on the therapeutic index of the individual drug, which is a measure of the toxicity to therapeutic benefit ratio. In early studies, it was not easy to determine the therapeutic index, but it is obvious that the lower the acute toxicity, the better this index will be. Given the promising anti-tumor activity of $\mathbf{P}^{4+}$ and $\mathbf{MP}^{2+}$ and relatively modest MTDs,[26] we decided to prepare a number of derivatives in which the terminal 1,10-phenanthroline ligands were

replaced with more lipophilic ligands. The synthesis of these and the parent complexes and the synthetic strategies used to prepare them were described in chapter 2, as was an analysis of their ability to similarly cleave DNA.

In this chapter, we examined the cytotoxicity and acute mammalian toxicity that these and some additional closely-related RPCs in an attempt to discern what structure-activity relationships exist, especially those that may be related to the complex lipophilicity and charge. It is postulated that complexes with higher lipophilicity will more easily penetrate the cell membrane and therefore show enhanced cytotoxicity over their more hydrophilic counterparts. It is also postulated that the more lipophilic complexes will be the slower in entering the bloodstream after IP injection. Slower build up was suggested by apparent renal clearance, evident in the observation of orange color in the mouse urine after injection. These observations indicate that increasing complex lipophilicity lowers peak blood concentration. We have observed that our tatpp-based complexes display the same type of neurotoxicity that Dwyer observed for $[Ru(phen)_3]^{2+}$ and related RPCs; thus controlling their peak blood concentration may be critical in any clinical application.

3.2 Experimental

3.2.1 Determination of the Partition Coefficient (log $P_{O/W}$)

3.2.1.1 Reagents

0.01 M Phosphate Buffered Saline (PBS) which contains the following: 0.027 M potassium chloride, 0.137 M sodium chloride, and 0.00176 M potassium phosphate, was prepared in lab at pH 7.4, 1-octanol was purchased from Sigma-Aldrich.

3.2.1.2 Instrumentation

Hewlett -Packard HP8453A spectrophotometer.

3.2.1.3 Partition Coefficient Experiment

The lipophilicity of the ruthenium(II) complexes was determined by using the shake-flask technique[105] with 1-octanol ($CH_3(CH_2)_7OH$) and PBS (PBS buffer instead of pure water is generally considered more appropriate model of blood serum, as 10 mM PBS (pH 7.4) better approximates the ionic strength and pH of blood plasma). 33.3 x 10^{-5} M of the solute was dissolved first in octanol and PBS, then the two saturated phases were shaken for 30 minutes at room temperature and let to set and equilibrate for 24 hours. After this period, the distribution of the complex in each solvent was measured using a Hewlett -Packard HP8453A spectrophotometer. The corresponding concentration of the solute in each solvent was determined by using Beer's law from the absorbance of the measured spectra; the concentration was then used in calculating the partition coefficient. The partition coefficient ($P_{O/W}$) is the ratio of the equilibrium concentration of the dissolved compound in two phases:

$$\log P_{o/w} = \log ([\text{solute}]\text{octanol} / [\text{solute}]\text{water})$$

The log *P* of the ruthenium complexes was also obtained for a biphasic solution of DI water and 1-octanol using the same general procedure as above.

3.2.2 Cytotoxicity Screening

3.2.2.1 Reagents

Dulbecco's Modified Eagle Medium (DMEM), RPMI-1640 Medium, fetal bovine serum (FBS), penicillin/streptomycin solution (P/S), L-glutamine, Trypsin-EDTA were purchased from Sigma-Aldrich. DMSO, phenazine methosulfate (PMS), 3-(4,5-dimethylthiazol-2-yl)-2,5-diphenyltetrazolium bromide (MTT), and 3-(4,5-dimethylthiazol-2-yl)-5-(3-carboxymethoxyphenyl)-2-(4-sulfophenyl)-2H-tetrazolium (MTS) were obtained

from Sigma. 0.01 M PBS was prepared in lab at pH 7.4. Colony fixation staining solution was glutaraldehyde 6.0% (vol/vol), crystal violet 0.5% (wt/vol) in H_2O.

3.2.2.2 Instrumentation

The absorbances of the MTT plates were analyzed using a microplate reader (Fluostar-omega, BMG Labtech). The absorbances of the MTS plates were measured using Spectra Max 190 (Molecular Devices).

3.2.2.3 Cell Culture and Cell Lines for MTT Assay

The cell lines, non-small cell lung cancer (NSCLC) line (H358), breast cancer (MCF-7), colon cancer (CCL228) and breast epithelial cell line (MCF-10), were kindly donated by Dr. Mandal Subhrangsa. The MCF-7, CCL228, MCF-10 were grown and maintained in DMEM that was supplemented with 10% FBS, 1% L-glutamine, and 1% Penicillin/streptomycin solution. H358 was grown and maintained in RPMI-1640 medium that was supplemented with 10% FBS, 1% L-glutamine, and 1% Penicillin /streptomycin solution. All the cells were cultured at 37°C in a humidified atmosphere of 5% CO_2. Cells were grown on cover slips for microscopy experiments and in 96 well microtiter plates for cell viability and cytotoxicity assays.

3.2.2.4 MTT Assay

For the cytotoxicity measurements, ~2 x 10^4 cells were seeded into each well of a 96-well microtiter plate, grown for 24 h, then treated with varying concentration (0 to 50 μM final concentration) of [**MP**]Cl_2, [**P**]Cl_4, [$\mathbf{P_{Ph}}$]Cl_4, [$\mathbf{MP_{Ph}}$]Cl_2, [$\mathbf{P_{Me}}$]Cl_4, [$\mathbf{MP_{Me}}$]Cl_2, [Ru(phen)$_3$]Cl_2, [Ru(Ph$_2$phen)$_3$]Cl_2, [Ru(Me$_4$phen)$_3$]Cl_2, [Ru(phen)$_3$]Cl_2, [**Z**]Cl_4, [**MZ**]Cl_2, [Ru(phen)$_2$dppz]Cl_2, and cisplatin. The plates were then left to incubate for an additional 96 h. Each of the metal complexes was initially dissolved in DMSO to make a concentrated stock solution (100 mM) that was then diluted in culture media prior to treatment of the cells. Each reaction was performed in five parallel replicates. Control cells were treated

with an equivalent amount of DMSO (final DMSO concentration in culture was less than 0.1% v/v). After 96 h of incubation, the cell viability was analyzed by using 30 μL MTT (stock 5 mg ml^{-1} in PBS), added to each well and incubated for 4 h under normal growth condition to allow the viable cells to convert MTT to formazan. The cell culture supernatants were then removed and replaced with 100 μL DMSO for 1 h with continuous shaking to dissolve the formazan crystals at room temperature. The absorbance of the lysates was directly measured at 560 nm using a microplate reader. The percentage viable cells (calculated based on absorbance of the control untreated sample) were plotted as a function of concentration of the complexes to obtain the IC_{50} values. Three separate experiments were done to determine the IC_{50} for each drug.

3.2.2.5 Cell Culture and Cell Lines for MTS and Clonogenic Assays

The cell lines, NSCLC, HCC2450 (squamous cell carcinoma), H522 (adenocarcinoma; epithelium), H322 (Caucasian bronchioalveolar carcinoma), H1993 (adenocarcinoma; epithelium), H460 (carcinoma; epithelium), H2073 (adenocarcinoma; epithelium), H2122 (adenocarcinoma), and pancreatic cancer (PANC1), were kindly donated by Dr. Rolf Brekken. All cell lines were grown and maintained in RPMI-1640 or DMEM that was supplemented with 10% FBS, and 1% L-glutamine. All cells were cultured at 37°C in a humidified atmosphere of 5% CO_2. Cells were grown in T-flask for microscopy experiments and in 96-well microtiter plates for cell viability.

3.2.2.6 MTS Assay

For the cytotoxicity measurements, ~2000 cells were seeded into each well of a 96-well microtiter plate, grown for 24 h, then treated with varying concentration (100 to 0.1 μM final concentration) of [**P**]Cl_4, [M**P**]Cl_2 and [Ru(phen)$_2$dppz]Cl_2 complexes for an additional 96 h. Drugs were added in 4-fold dilutions with a maximum dose of 100 μM. Each metal complex was initially dissolved in DMSO to make a concentrated stock solution

(100 mM) that was then diluted in culture media prior to treatment of the cells. Each drug was given at 8 drug concentrations per assay. Each reaction was performed in eight parallel replicates. Control cells were treated with an equivalent amount of medium. After 96 h of incubation, relative cell number was determined by incubating for 1 to 3 hours at 37°C in the presence of MTS (Promega, Madison, WI), final concentration 333 mg/ml. The absorbance was directly measured at 490 nm using a Spectra Max 190 (Molecular Devices). Each plate contained eight replicates per concentration and was repeated at least 4 times. Two separate experiments were done to determine the IC_{50} for each drug. The drug sensitivity curves and each IC_{50} were calculated using in-house software, DIVISA.

3.2.2.7 Clonogenic Assay

Colony formation survival test was accomplished by seeding ~ 500 cells per well in 6-well plate after adding 2 mL of media to each well. After adding the cells, the plate was gently tapped few times to aid in even the distribution of the cells. The drug was added after 24 h of plating the cells. The plate was placed in the incubator 2 to 4 weeks to allow the cells to grow. This period of time can be varied based on type of the cells. The end of the assay was determined when control colonies have approximately 50 cells per colony. The assay was completed by fixing and staining the colonies.

3.2.2.7.1 Fixation and Staining of Colonies

The medium was removed and the formed cell colonies were stained by using crystal violet solution (50 mg crystal violet in 30% ethanol). Stain was left for at least 30 minutes and then removed. Plates were rinsed by gently immersing them in tap water. Plates were left to dry at room temperature and then counted.

3.2.2.7.2 Counting the Colonies

Colonies were counted with a Gel Doc-XR Imager (Bio-Rad Laboratories) using the colony counting program.

3.2.3 Animal Study: Maximum Tolerable dose

3.2.3.1 Chemicals

The following ruthenium(II) complexes: [$\mathbf{P_{Me}}$]Cl_4, [$\mathbf{MP_{Me}}$]Cl_2, [$\mathbf{P_{Ph}}$]Cl_4, [$\mathbf{MP_{Ph}}$]Cl_2, [**MP**]Cl_2, [**P**]Cl_4, [**Z**]Cl_4, [**MZ**]Cl_2, [Ru(phen)$_3$]Cl_2, [Ru(Ph_2phen)$_3$]Cl_2, [Ru(Me_4phen)$_3$]Cl_2, and [Ru(phen)dppz]Cl_2 were synthesized in the laboratory as described previously in chapter 2. Phosphate buffered saline (PBS) (10X) was purchased from Bio-Rad. Dimethyl sulfoxide (DMSO) was used as received from Sigma Aldrich.

3.2.3.2 Experiment

The animal study was carried out according to the protocol approved by the Institutional Animal Care and Use Committee (IACUC A08.018, approved 2/20/08). Male Balb/c mice, twelve to fourteen weeks of age, were obtained from an established colony at the UTA Animal Care Facility. The Balb/C mice are commonly-used inbred laboratory mice noted for their white fur and red eyes (albinos) and have been widely adopted for cancer research. The animals were housed in a temperature controlled room and allowed to acclimate before treatment. RPCs were screened for acute toxicity by IP injection; three mice were designated for each complex. One group of four mice were used as control. Stock solutions of ruthenium complexes were prepared using PBS buffer at pH 7.4, and 2% DMSO. A typical experiment was conducted as follows: A single mouse (~ 27 g) was given a single dose of 90 µL of 6.0 mg/mL (20 mg drug/Kg mouse) via IP injection and monitored for 2 hours for any toxic symptoms and/or death. If all three mice survived the treatment, two additional mice were treated at the same dose and examined for 24 h. If the mice survived the treatment, the dose was escalated to 90 µL of a 12 mg/mL (40 mg/Kg) and monitored for 24 h. If the mouse survived this treatment, the dose was again escalated to 90 µL of a 18 mg/mL (60 mg/Kg) and monitored for 24 h. Further dose escalations to 90 uL of a 24 mg/mL (80 mg/Kg) or a 48 mg/mL (160 mg/Kg) were done if needed. If at any

stage any of the mice showed signs of toxicity, morbidity or death, the experiment was stopped and the previous tolerable dose was considered the MTD for this compound.

3.2.4 Pharmacokinetic study

3.2.4.1 Reagents

0.1X Dulbecco`s Phosphate Buffered Saline (DPBS), DMSO, and dipotassium ethylenediaminetetraacetic acid anticoagulant (K_2EDTA).

3.2.4.2 Instrumentation for Ru Analysis

The concentrations of ruthenium were analyzed using inductively coupled plasma mass spectrometry Thermo Scientific X Series II ICP-MS. The data were further processed using vendor supplied software (Thermo Plasma Lab, version 2.5.5.290).

3.2.4.3 Experiment

The animal dosing and blood collection were performed by Charles River Laboratories under contract. Nine male Wister Han rats were allowed to acclimate before treatment. The animals were placed into three groups of three rats per group. All animals were fasted overnight before dosing and food was returned 4 hours post dose. Each animal in groups 1 through 3 received a single IP injection of 5 mg/Kg dose at a dose volume of 0.8 mL/Kg as presented in Table 3.1. Following dosing, the animals were observed for any clinically relevant abnormalities and all animals appeared normal at the time of each observation. At the following times post injection: 0.15, 0.5, 1, 1.5, 2, 3, 9, 12, 18, and 24 h, 300 μL of whole blood sample was taken via jugular vein catheter. The blood was separated into plasma, whole blood cells and flash frozen on dry ice. These samples were shipped to UTA for Ru analysis by ICP-MS. After the final blood collection, all animals were euthanized via CO_2 asphyxiation in accordance with accepted American Veterinary Medical Association (AVMA) guidelines.

Table 3.1 Study design

Group	No. of Rats	Compound	Dose Level mg/Kg	Dose Conc. mg/mL	Dose Vol. mL/Kg	Dose Medium	Dose Route
1	3	$[Ru(phen)_2dppz]^{2+}$	5	6.25	0.8	4% DMSO, 96% 0.1x DPBS	IP
2	3	$\mathbf{MP}^{2+}$	5	6.25	0.8	4% DMSO, 96% 0.1x DPBS	IP
3	3	$\mathbf{MP_{Ph}}^{2+}$	5	6.25	0.8	4% DMSO, 96% 0.1x DPBS	IP

3.2.4.4 Dose Administration

For Group 1, 16.58 mg of compound $[Ru(phen)_2dppz]^{2+}$ was combined with 53.1 µL of DMSO to produce a thick, red 312.5 mg/mL stock solution. Because the stock solution was too thick to pipette, it was further diluted down with an additional 53.1 µL of DMSO to produce a red 156.2 mg/mL stock solution. From that, 80 µL was added to 1.92 mL of 0.1X DPBS to produce a clear red dosing solution at a target concentration of 6.25 mg/mL for IP dosing. To ensure homogeneity, the dose formulations were stirred continuously on a magnetic stir plate until the completion of dosing. The dose site was shaved in preparation for dose administration and was marked with indelible ink for dose site collection. The same procedure was followed for all the other complexes. Dose concentration was varied based on the rat weight as seen in Table 3.2

Table 3.2 Dose administration

Compound	Rat Sex	Rat Weight (Kg)	Dose Route	Dose Concentration (mg/Kg)
$[Ru(phen)_2dppz]^{2+}$	M	0.334	IP	5.052
$[Ru(phen)_2dppz]^{2+}$	M	0.343	IP	4.920
$[Ru(phen)_2dppz]^{2+}$	M	0.338	IP	4.993
$\mathbf{MP}^{2+}$	M	0.324	IP	5.015
$\mathbf{MP}^{2+}$	M	0.293	IP	4.906
$\mathbf{MP}^{2+}$	M	0.349	IP	5.014
$\mathbf{MP_{Ph}}^{2+}$	M	0.323	IP	5.031
$\mathbf{MP_{Ph}}^{2+}$	M	0.316	IP	4.945
$\mathbf{MP_{Ph}}^{2+}$	M	0.305	IP	4.918

3.2.4.5 Collection of Blood Samples

All blood samples were collected by way of jugular vein catheter. Blood samples were collected from each animal at 0.15, 0.5, 1, 1.5, 2, 3, 6, 9, 12, 18, and 24 hours after IP dosing. 300 µL of whole blood sample was collected at each time point and placed into tube containing K_2EDTA anticoagulant. All whole blood samples were placed on wet ice immediately after collection and were centrifuged at 2200 x g for 10 minutes at 2– 8 ºC to isolate plasma. The resulting plasma was transferred to individual polypropylene tubes in a 96-well plate format and instantly placed on dry ice. The residual red blood cells were also frozen after plasma collection and both the plasma and residual red blood cells were stored at nominally -70 °C.

3.2.4.6 Evaluation of Ruthenium Content by Using ICP-MS

ICP-MS quantification was performed on a single quadruple instrument of 0.7 amu mass resolution (X-Series II, ICP-MS, Thermo Fisher Scientific). The results are reported as average ± standard deviation (n=3). Operational parameters for the ICP–MS are shown in the Table 3.3. The data were processed through vendor supplied software (Thermo PlasmaLab, ver. 2.5.9.300). An ASX-520 CETAC Autosamplers performed sample delivery. Ruthenium standards were prepared from 0 ppb to 100 ppb of Ru. All data were interpreted in terms of a 5-point calibration with check standards run daily.

Table 3.3 Operation parameter of ICP-MS

Parameter	Value
RF power	1400 W
Cooling gas flow (Argon)	13.0 L/min
Auxiliary gas flow (Argon)	0.8 L/min
Nebulizer gas flow (Argon)	0.8 L/min
Spray chamber temperature	3 °C
Interface cones	Nickel
Expansion chamber pressure	1.9 mbar
Analyzer chamber pressure	3.6×10^{-7} mbar
Nebulizer back pressure	2.1 bar
Sampling depth	150 mm
Detector mode	Pulse Counting
Resolution	Standard
Elements monitored	^{101}Ru, ^{102}Ru, ^{104}Ru
Integration time/mass	170 ms
Software	Thermo PlasmaLab, version 2.5.9.300

3.3 Results and Discussion

3.3.1 Lipophilicity of Ruthenium Polypyridyl Complexes

The lipophilicity was measured by determining the log $P_{O/W}$ value for the following ruthenium(II) complexes: [**MP**$_{Ph}$]Cl_2, , [**P$_{Me}$**]Cl_4, [**MP**]Cl_2, [**P**]Cl_4, [Ru(Ph_2phen)$_3$)]Cl_2, [**P$_{Ph}$**]Cl_4, [**MP$_{Me}$**]Cl_2, [Ru(Me4phen)$_3$)]Cl_2 [Ru(phen)$_3$)]Cl_2, [Ru(phen)$_2$dppz]Cl_2, [**MZ**]Cl_2 and [**Z**]Cl_4 and the data collected in Table 3.4. The log *P* data was obtained under two different aqueous phase compositions. One set of data reveal the partition coefficient when deionized (DI) water was used and another set when 0.1 M PBS buffer at pH 7.4 was used.

The data was arranged in order of decreasing lipophilicity in the octanol/PBS system with [**MP**$_{Ph}$]Cl_2 being the most lipophilic and [**Z**]Cl_4 the least lipophilic. As can been seen Table 3.4, the *log P* values in the PBS/octanol system are higher than those in the water/octanol system, which is most likely due to the lower ionic strength of the pure water system, but, in general, the trends are the same in both systems.

As shown in Figure 3.2, the log *P* values are different by five order of magnitude from 2.5 for the most lipophilic ruthenium complexes to -2.0 for the least ones. The trend of the lipophilicity data comes to an agreement with the data of Barton *et al*. where it was found that the complexes containing the Ph_2phen ancillary ligands are the most lipophilic followed by complexes containing the Me_4phen and that least lipophilic are the ones containing phen ligands.[38] The lipophilicity of the RPCs may have a correlation with the cytotoxicity and that will have important effects on the biological activity.[106]

Table 3.4 Log *P* values of Ru(II) polypyridyl complexes

Ruthenium Complex	log *P*, PBS (pH 7.4)	log *P*, DI water
$\mathbf{MP_{Ph}}^{2+}$	2.3	1.6
$[Ru(Ph_2phen)_3]^{2+}$	1.9	1.4
$\mathbf{P_{Ph}}^{4+}$	1.7	0.46
$[Ru(Me_4phen)_3]^{2+}$	1.6	-0.9
$\mathbf{MP_{Me}}^{2+}$	1.5	-0.6
$\mathbf{P_{Me}}^{4+}$	1.0	-1.4
$[(phen)_2Ru(dppz)]^{2+}$	0.2	-1.3
$\mathbf{MZ}^{2+}$	-0.18	-0.9
$\mathbf{MP}^{2+}$	-0.4	-1.4
$\mathbf{P}^{4+}$	-0.6	-1.0
$[Ru(phen)_3]^{2+}$	-1.1	-1.5
$\mathbf{Z}^{4+}$	-1.9	-1.26

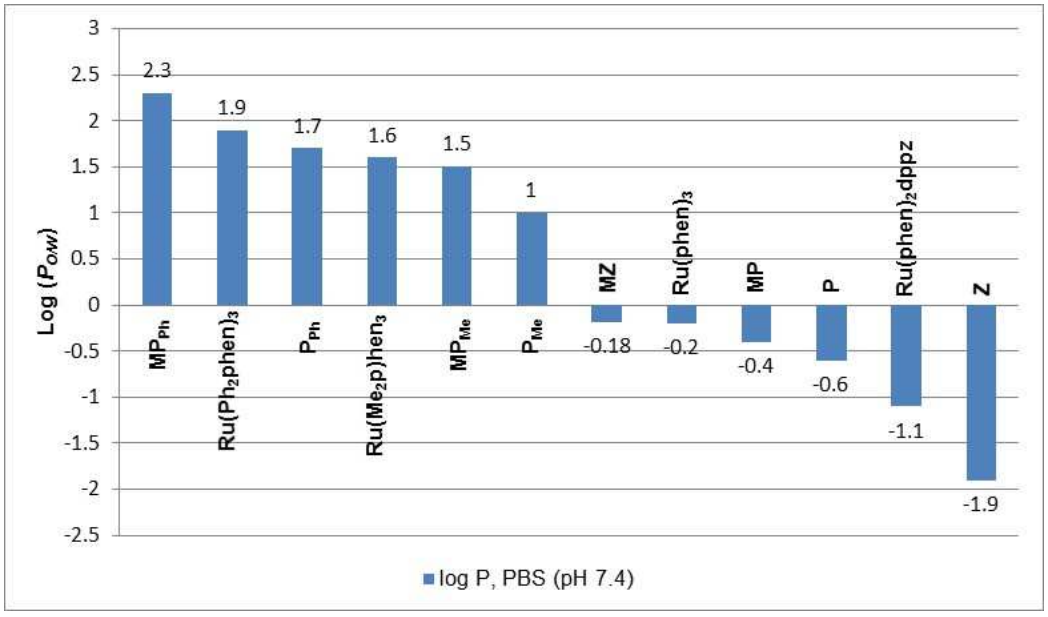

Figure 3.2 Lipophilicity trend of Ru(II) polypyridyl complexes

3.3.2 Cytotoxicity of Ruthenium Polypyridyl Complexes

3.3.2.1 Cytotoxicity (MTT)

The cytotoxicities of the following RPCs: [**MP**]Cl_2, [**P**]Cl_4, [$\mathbf{P_{Ph}}$]Cl_4, [$\mathbf{MP_{Ph}}$]Cl_2, [$\mathbf{P_{Me}}$]Cl_4, [$\mathbf{MP_{Me}}$]Cl_2, [Ru(phen)$_3$]Cl_2, [Ru(Ph$_2$phen)$_3$]Cl_2, [Ru(Me$_4$phen)$_3$]Cl_2, [Ru(phen)$_3$]Cl_2, [**Z**]Cl_4, [**MZ**]Cl_2, [Ru(phen)$_2$dppz]Cl_2, and cisplatin were evaluated in cancerous and non-cancerous human cell lines using a standard MTT assay and the data summarized in Table 3.5. In MTT, the yellow tatrazole was reduced to purple formazan in living cells. The amount of formazan present after 4 h incubation is correlated with the number of living cells and thus can be used to help quantify the cytotoxicity of various drugs. One lane of cells is not treated with drugs (negative control) and another lane is treated with cisplatin as a positive control.

The first screen was an evaluation of the complexes against MCF-7 breast cancer cell line. The data in the form of a bar graph indicating the IC_{50} values for all the complexes screened, arranged according to their log *P* values, is shown in Figure 3.3. The IC_{50}'s of the dinuclear and mononuclear complexes [$\mathbf{P_{Ph}}$]Cl_4 and [$\mathbf{MP_{Ph}}$]Cl_2 are 1.4 μM and 2.13 μM, respectively, and were noticeably lower than the other tatpp-based complexes. Only [Ru(Ph$_2$phen)$_3$]$^{2+}$ showed a similarly low IC_{50} and was also one of the most lipophilic complexes tested. If we only consider the tatpp-based complexes (indicated by red bars in Figure 3.3) we observe that the less lipophilic tetramethyl-phen complexes were less cytotoxic but this trend does not continue. The even less lipophilic [**P**]Cl_4 and [**MP**]Cl_2 show significantly better cytotoxicity than the Me$_4$phen derivatives. We note that aside from [Ru(Ph$_2$phen)$_3$]Cl_2, all the other non-tatpp based RPCs are not particularly cytotoxic regardless of the log *P* value, reinforcing the importance of the redox-active tatpp ligand for much of the observed cytotoxicity.

A screen against a non-malignant breast epithelial cell line, MCF-10, is particularly revealing, as seen in Figure 3.4. Every RPC except $[Ru(Ph_2phen)_3]Cl_2$ showed much less cytotoxicity. This data shows that $[Ru(Ph_2phen)_3]Cl_2$ is not selective for malignant over non-malignant cells whereas the tatpp-based complexes, in general, show good selectivity. The selectivity index, calculated as shown below, is a measure of this discrimination:

Selectivity Index (**SI**) = IC_{50} MCF-10/ IC_{50} MCF-7

Using the data from Figures 3.3 and 3.4, we plotted the SI of each complex in Figure 3.5 and 3.6. With a SI of 71, $[\mathbf{MP_{Ph}}]Cl_2$ is the most pronounced, however most of the tatpp complexes have SI closer to 10 and the remaining RPCs show no selectivity, with SI's of 1. Even cisplatin has a modest SI of 2.5 in this experiment, which is in part a reflection of its modest cytotoxicity towards MCF-7.

Two additional cell lines were screened: non-small cell lung carcinoma (H358) and colorectal cancer cell line (CCL228). These data are shown in graph format in Figures 3.7 and 3.8. The most striking findings here are that $[\mathbf{MP_{Ph}}]Cl_2$ and $[\mathbf{P_{Ph}}]Cl_4$ are considerably less active against these two cell lines than seen for MCF-7. In contrast, the cytotoxicity of $[\mathbf{P}]Cl_4$ and $[\mathbf{MP}]Cl_2$ are similar in all three lines, shown in Figure 3.9, indicating that while the lipophilic phenyl-phen derivatives are more active in breast cancer cells, the phen analogues show a broader spectrum of activity. As with MCF-7 and MCF-10, the $[Ru(Ph_2phen)_3]Cl_2$ complex is very cytotoxic against H359 and CCL228, indicating that this particular RPC is a potent cytocidyl agent regardless of the cell type examined. The reason for this broad spectrum cytotoxicity is not immediately apparent, but it seems likely that the root of its cytotoxic properties differ from the tatpp-based complexes.

As mentioned previously, the data in Figures 3.3 to 3.9 are plotted versus complex lipophilicity and aside from a weak correlation of decreasing lipophilicity leading to decreasing cytotoxicity, there is no strong connection between these two parameters.

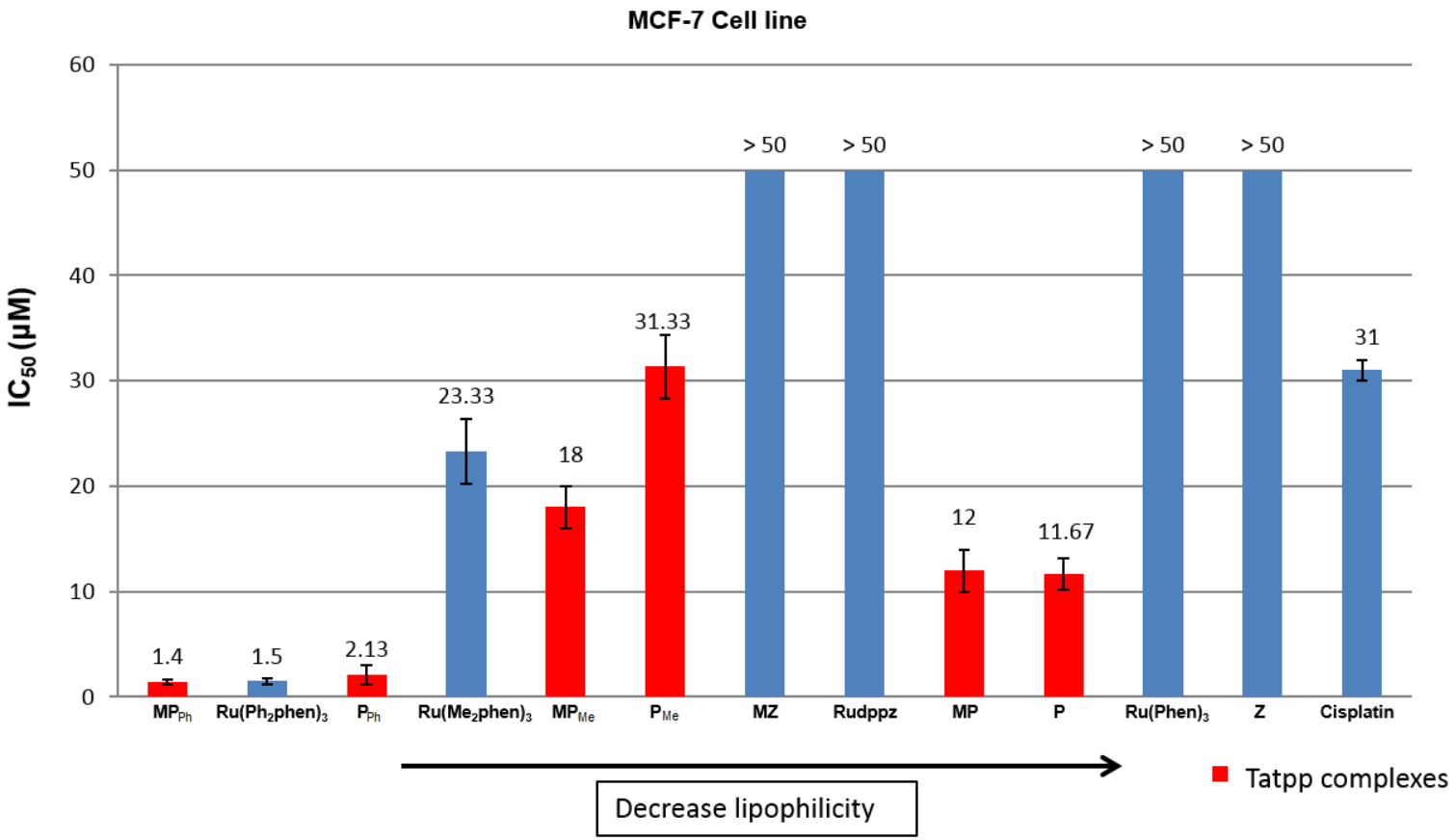

Figure 3.3 IC_{50} of Ru(II) polypyridyl complexes against breast cancer cell line MCF-7

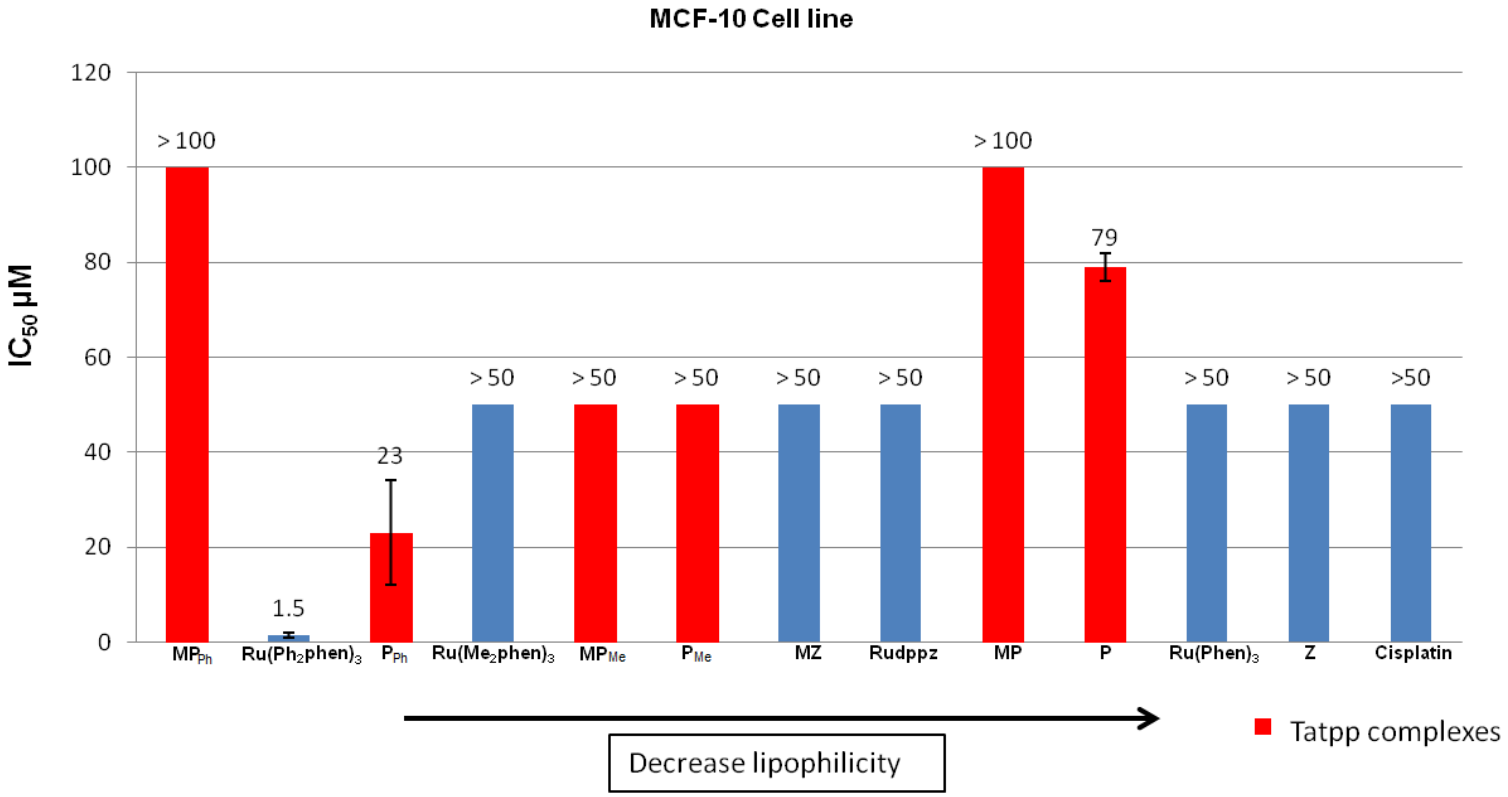

Figure 3.4 IC_{50} of Ru(II) polypyridyl complexes against a non-malignant breast epithelial cell line MCF-10

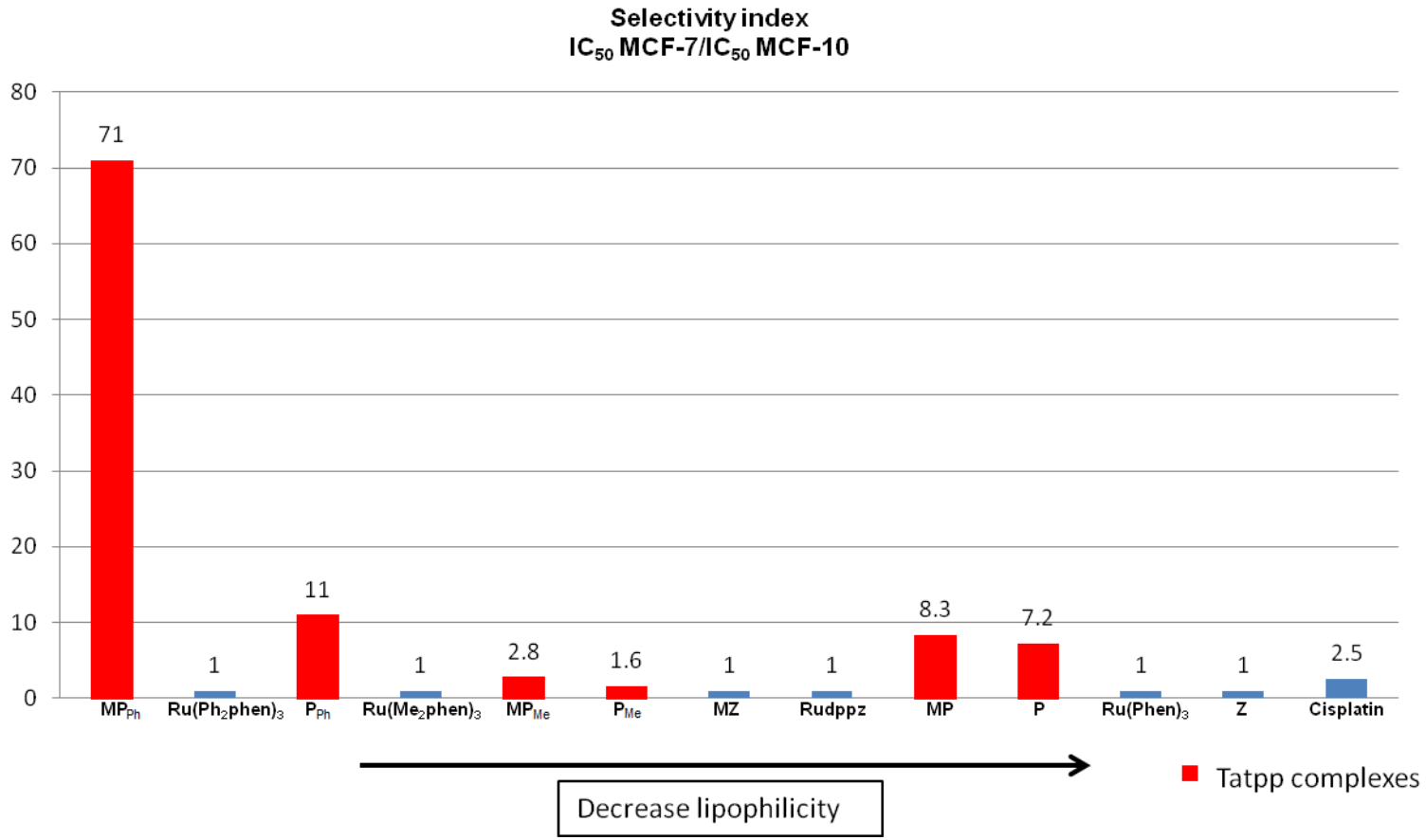

Figure 3.5 Selectivity Index (SI): IC_{50} MCF-10/ IC_{50} MCF-7

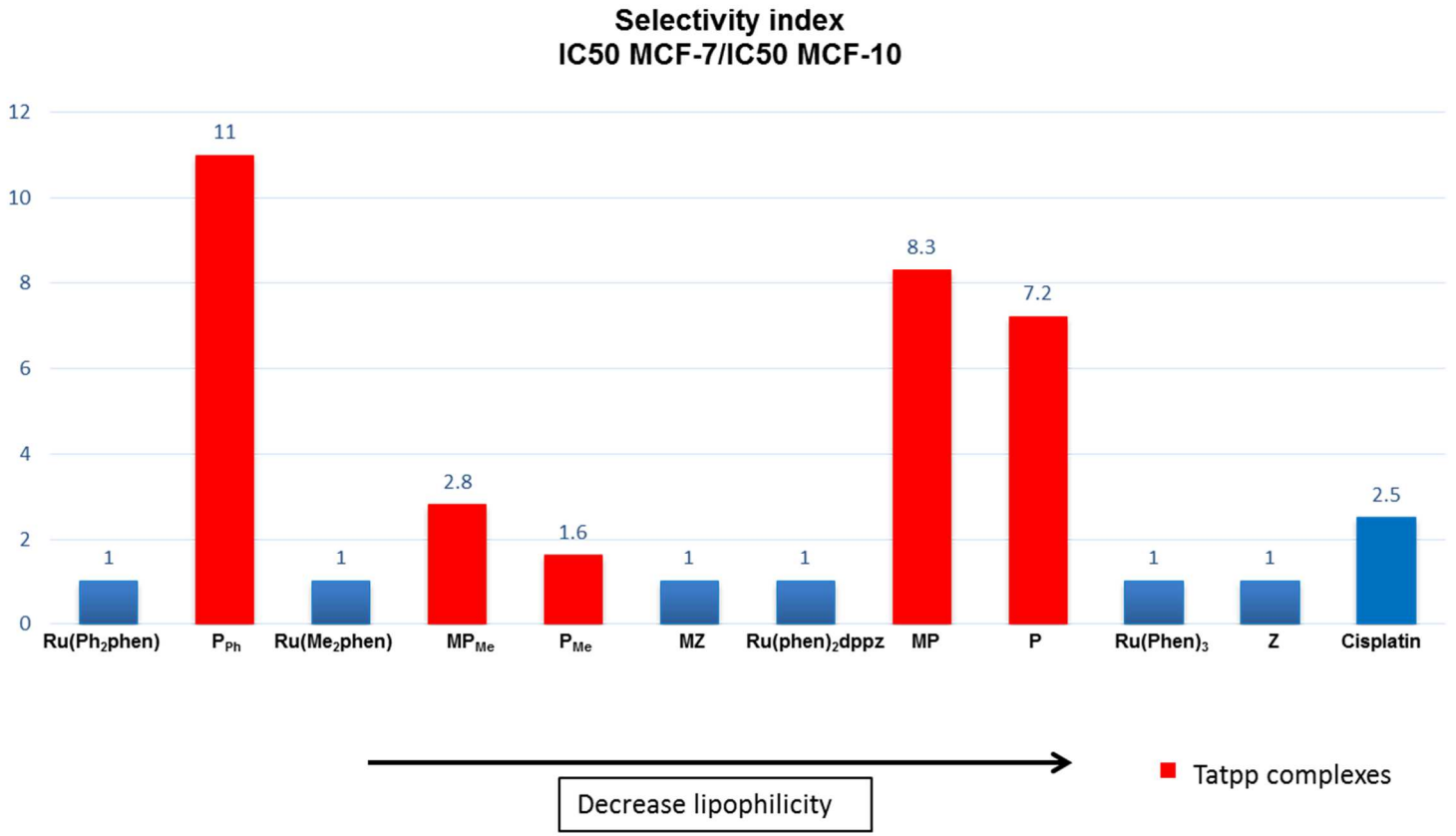

Figure 3.6 Selectivity Index (SI): IC_{50} MCF-10/ IC_{50} MCF-7 (**MP_{Ph}** excluded**)**

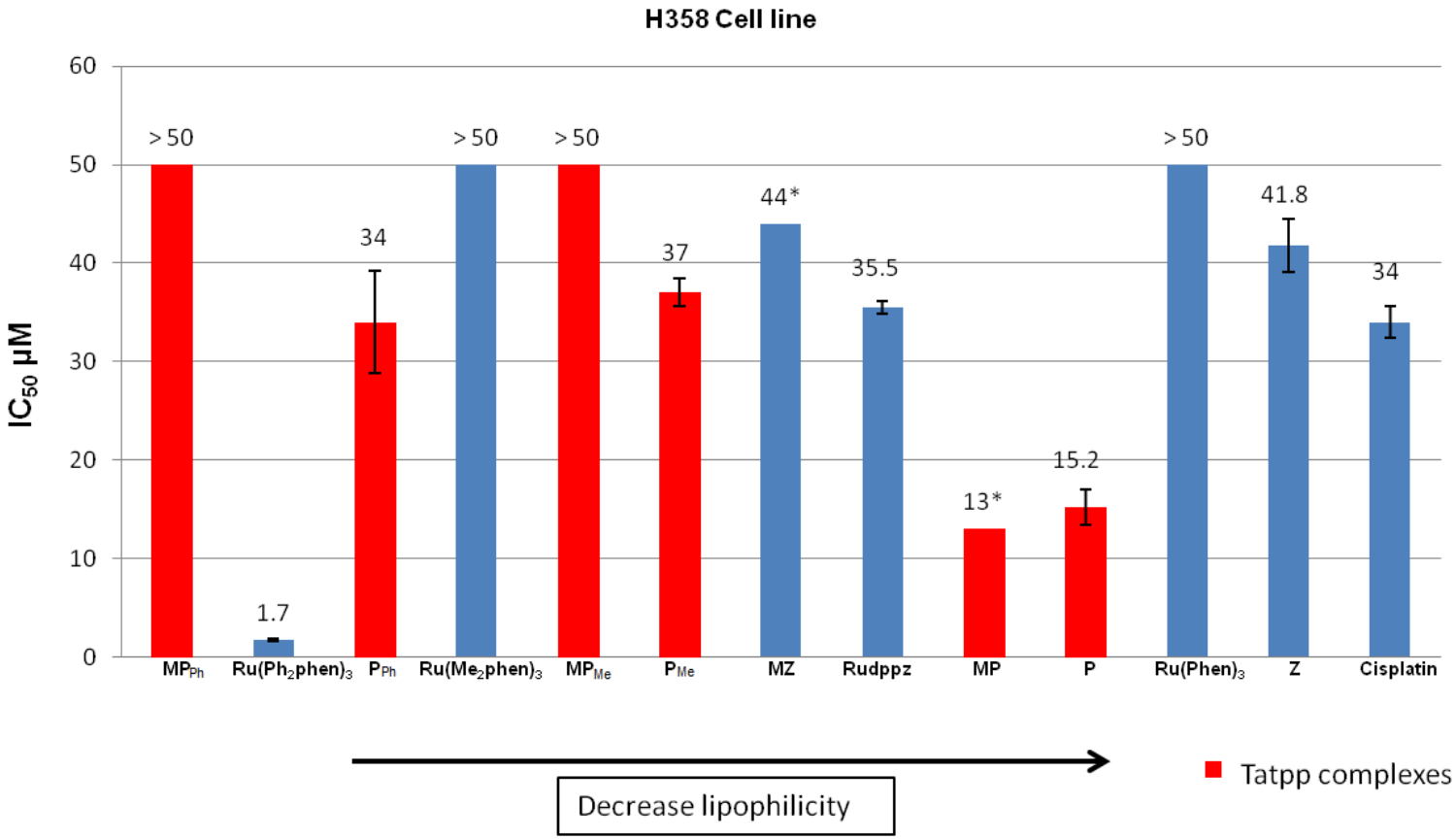

Figure 3.7 IC_{50} of Ru(II) polypyridyl complexes against non-small cell lung cancer (NSCLC) cell line H358 (Bronchioalveolar), * Yadav *et al*. results

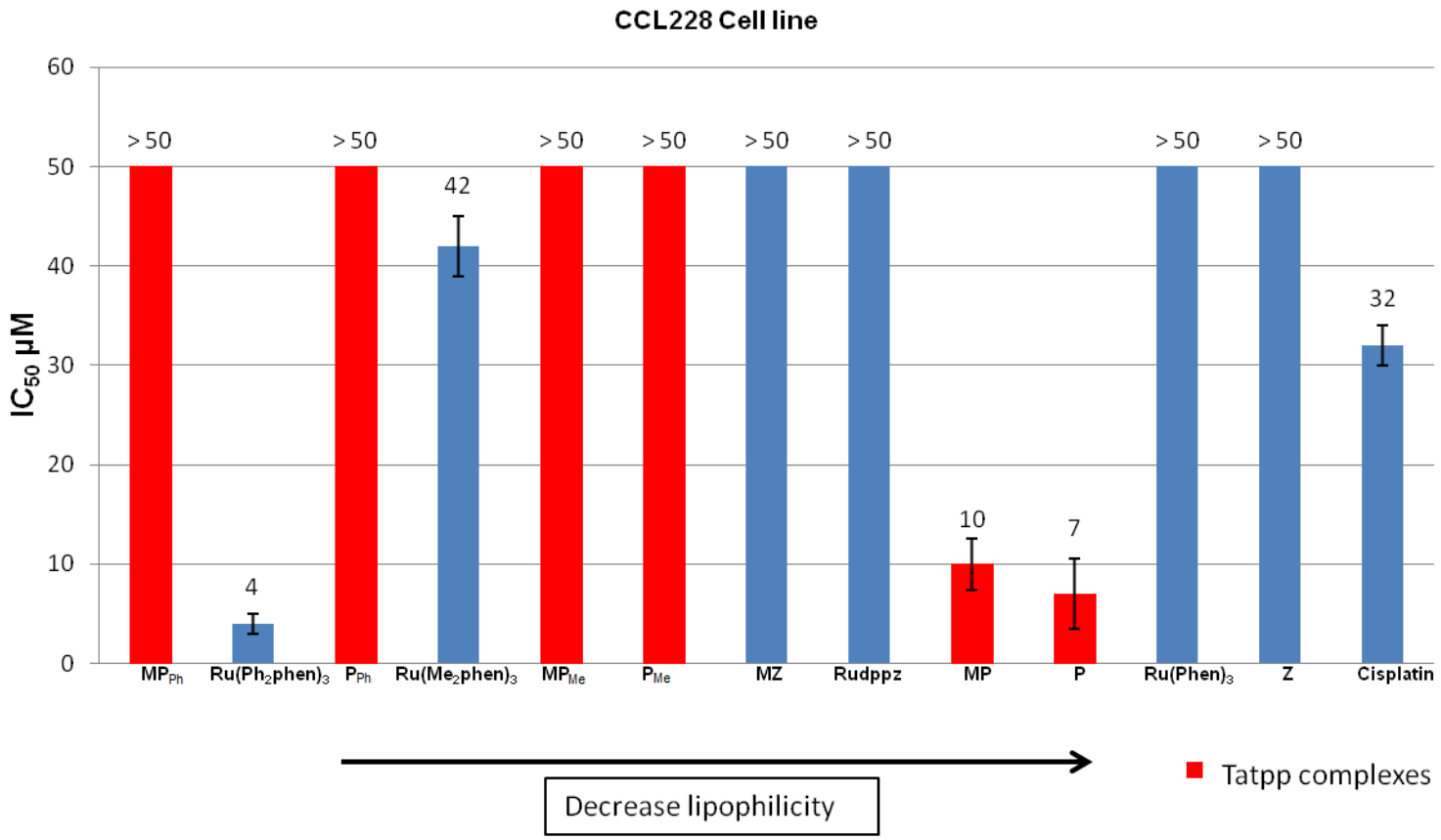

Figure 3.8 IC_{50} of Ru(II) polypyridyl complexes against colon cancer cell line CCL228

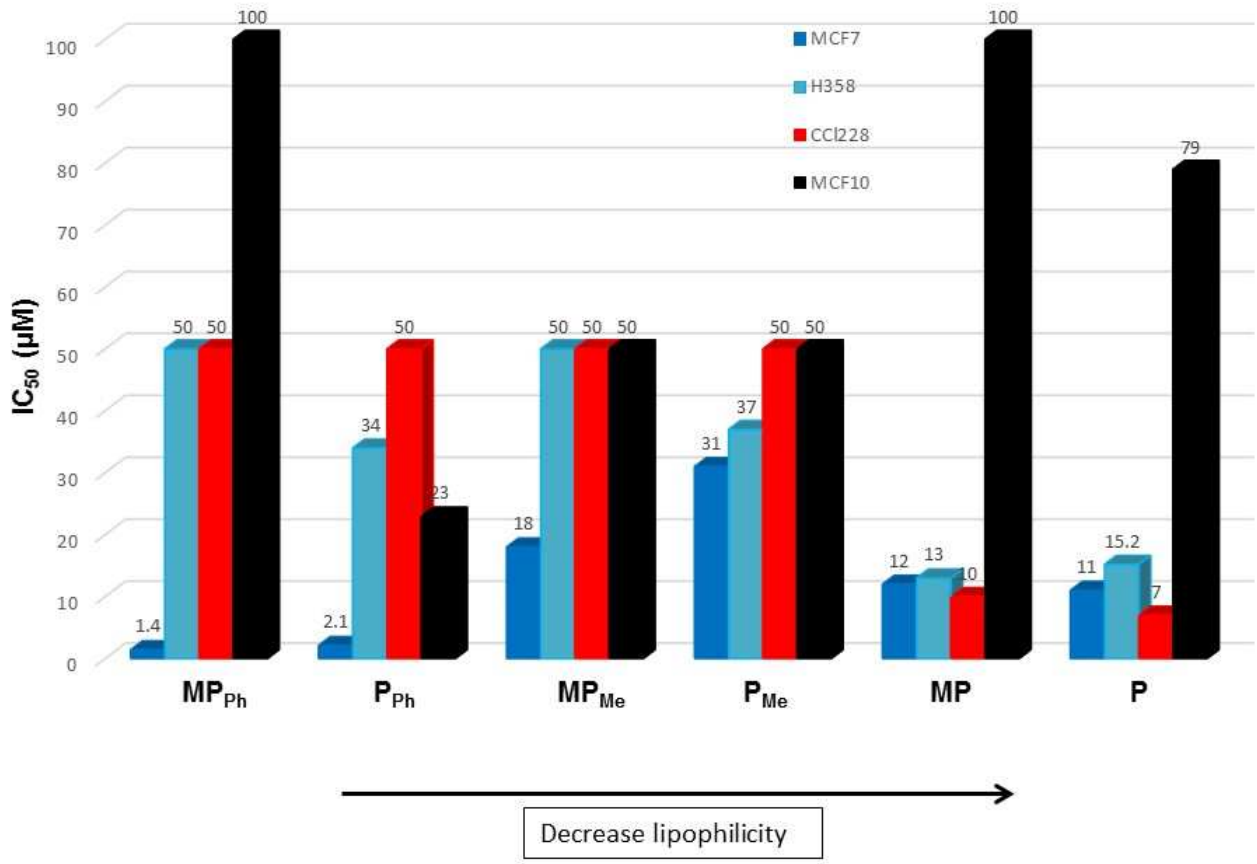

Figure 3.9 IC_{50} of Ru(II) polypyridyl complexes against cancerous cell line (MCF-7, H358, CCL228) and non-cancerous cell line (MCF-10) for tatpp-based Ru(II) complexes

Table 3.5 Cytotoxicity results of Ru(II) complexes against cancerous and non-cancerous cell lines

Complex	IC_{50}/μM	IC_{50}/μM	IC_{50}/μM	IC_{50}/μM	Selectivity Index
	MCF-7	CCL228	H358	MCF-10	IC_{50} MCF-10/ IC_{50} MCF-7
$[MP_{Ph}]Cl_2$	1.4 ± 0.2	> 50	> 50	> 100	> 71
$[P_{Ph}]Cl_4$	2.1 ± 0.9	>50	34 ± 5.2	23 ± 11	11
$[Ru(Ph_2phen)_3]Cl_2$	1.5 ± 0.2	4.0 ± 1.0	1.7 ± 0.1	1.5 ± 0.5	1.0
$[Ru(Me_4phen)_3]Cl_2$	23 ± 3.0	42 ± 3.0	> 50	> 50	> 2.2
$[MP_{Me}]Cl_2$	18 ± 2.0	> 50	> 50	> 50	> 2.8
$[P_{Me}]Cl_4$	31 ± 3.0	>50	37 ± 1.4	> 50	> 1.6
$[MZ]Cl_2$	> 50	> 50	44*	> 50	> 1.0
$[Ru(phen)_2dppz]Cl_2$	> 50	> 50	35 ± 0.7	> 50	> 1.0
$[MP]Cl_2$	12 ± 2.0	10 ± 2.6	13*	> 100	> 8.3
$[P]Cl_4$	11 ± 1.5	7.0 ± 3.5	15 ± 1.8*	79 ± 3.0	7.2
$[Ru(Phen)_3]Cl_2$	> 50	> 50	> 50	> 50	> 1.0
$[Z]Cl_4$	> 50	> 50	41 ± 2.7*	> 50	> 1.0
Cisplatin	20 ± 1.2	32 ± 2.0	34 ± 1.6	> 50	> 2.5

3.3.2.2 Cytotoxicity (MTS)

The cytotoxicity of three specific RPCs was extended to evaluate NSCLC lines HCC2450, H522, H1993, H2073, H322, H2122, H460 and pancreatic cancer (PANC1) cell line using standard MTS assay. This chromogenic assay was used to see if the compounds have effects on cell proliferation or cell death in an expanded panel and as a function of PO_2. MTS produces formazan in the presence of phenazine methosulfate (PMS). The results from this study are given in Table 3.6.

Table 3.6 IC_{50} values for RPCs against a number of cell lines (MTS Assay) under normoxic and hypoxic conditions (< 2% O_2)

		$\mathbf{P^{4+}}$	$\mathbf{MP^{2+}}$	$\mathbf{[Ru(phen)_2dppz]^{2+}}$
Cell Line		**IC_{50} (μM)**	**IC_{50} (μM)**	**IC_{50} (μM)**
	Condition			
H1993	**Normoxic**	2 ± 0.3	100 ± 20	31 ± 21
H1993	**Hypoxic**	4*	100*	64*
HCC2450	**Normoxic**	10 ± 40	100 ± 20	41 ± 19
HCC2450	**Hypoxic**	25 ± 49	82 ± 25	33 ± 2.1
H2073	**Normoxic**	50 ± 39	100 ± 16	12 ± 21
H322	**Normoxic**	11 ± 9.9	100 ± 38	76
PANC1	**Normoxic**	25*	100*	43*

All Experiments were carried out in triplicated except those with * notation.

We found that $\mathbf{P^{4+}}$ is more effective at treating platinum-resistant cell lines than $\mathbf{MP^{2+}}$ and $[Ru(phen)_2dppz]^{2+}$. Treated cells grown under hypoxic conditions did not show an increase in sensitivity related to those under normoxia, as shown in Table 3.6. In fact, the two tatpp-based RPCs showed less effectiveness under hypoxia, which contrasts earlier data with H358. [26] However, it is noticeable the $\mathbf{P^{4+}}$ was considerably more effective than $\mathbf{MP^{2+}}$ or $[Ru(phen)_2dppz]^{2+}$. We also evaluated the activity of RPCs against pancreatic

cancer cell line (PANC1). It was found that **MP**$^{2+}$ and [Ru(phen)$_2$dppz]$^{2+}$ have poor cytotoxicity against this cell line compared to **P**$^{2+}$ but, in general, all the RPCs are largely ineffective toward PANC1.

Of the NSCLC lines, H358, H1993, HCC2450 and H322 are considered to be somewhat poorly sensitive to cisplatin with IC_{50}'s of 15, 9, 11, 18.5 μM, respectively, whereas H2073 is very sensitive with an IC_{50} of 1.7 μM.[107] It is notable the **P**$^{4+}$ shows good activity, as measured by IC_{50} values, against platinum-resistant lines whereas neither **MP**$^{2+}$ nor [Ru(phen)$_2$dppz]$^{2+}$ is particularly effective. This suggests **P**$^{4+}$ may have some utility in treating platinum-resistant cancers. It is clear that the redox-active bridging ligand tatpp is an essential component at the most effective RPCs.

3.3.2.3 Colony Formation

Clonogenic assay or colony formation assay is an *in vitro* cell survival assay which tests the ability of a single cell to grow and form colony.[108,109] It is a more sensitive assay of drug cytotoxicity than MTT or MTS and reveals morphological changes to treated cells. We examined **P**$^{4+}$, **MP**$^{2+}$ and [Ru(phen)$_2$dppz]$^{2+}$ against two NSCLC cell lines: H1993 and HCC2450 using the clonogenic assay. Before treatment, cells were seeded out in appropriate dilutions to form colonies in 2-4 weeks. The cells were then inoculated with the drugs at different concentrations 24 h after the initial cell seeding. The cells were then incubated for 4 weeks to allow for colony formation, stained with crystal violet, and counted with a Gel Doc-XR Imager (Bio-Rad Laboratories) using the colony counting program. The IC_{50} data from these assays are summarized in Table 3.7.

The photographs in Figures 3.10 and 3.11 shown the plates after staining for all three complexes against both cell lines. Of the three RPCs examined, **P**$^{4+}$ inhibited colony formation the best by far. Surprisingly, [Ru(phen)$_2$dppz]$^{2+}$ was more effective than **MP**$^{2+}$ in inhibiting colony formation, which contrasts the data obtained via MTT or MTS assays.

The reasons for this are unclear, but the significantly longer incubation time of the clonogenic assay, 4 weeks contrasted to 4 days to the MTT or MTS assay, suggests that and $[Ru(phen)_2dppz]^{2+}$ is more active at longer treatment times. The data were consistent between the two cell lines and reveal a slightly greater cytotoxicity for $\mathbf{P}^{4+}$ than obtained via MTT or MTS methods. At least for $\mathbf{P}^{4+}$ greatest colony against H1993 and HCC2450 compared to and $[Ru(phen)_2dppz]^{2+}$ as shown in Figures 3.10 and 3.11. There was a great reduction in the colony numbers with $\mathbf{P}^{4+}$ complex compared to the control.

Table 3.7 Representation of the IC_{50} values of the colony formation assays of three independent experiments after four weeks

	$\mathbf{P}^{4+}$	$\mathbf{MP}^{2+}$	$\mathbf{[Ru(phen)_2dppz]^{2+}}$
	IC_{50} (µM)	**IC_{50} (µM)**	**IC_{50} (µM)**
Cell Line			
H1993	0.6 ± 0.2	3 ± 0.4	1 ± 0.5
HCC2450	0.8 ± 1.5	3 ± 0.9	3 ± 1.5

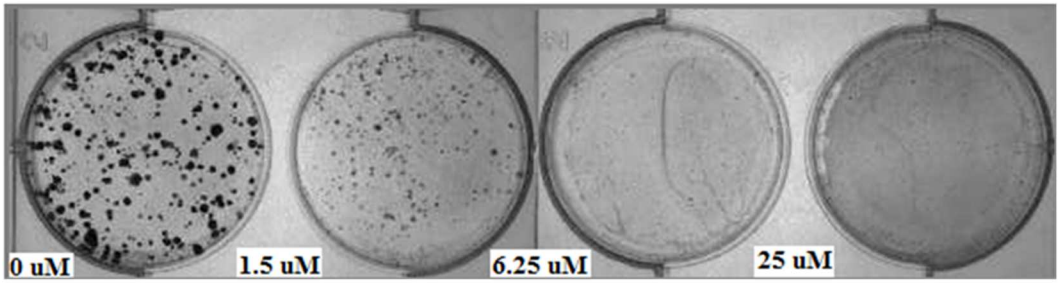

$[\mathbf{P}]^{4+}$

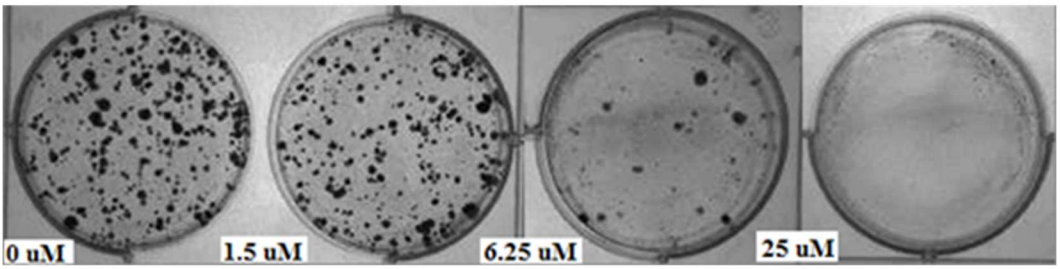

$[\mathbf{MP}]^{2+}$

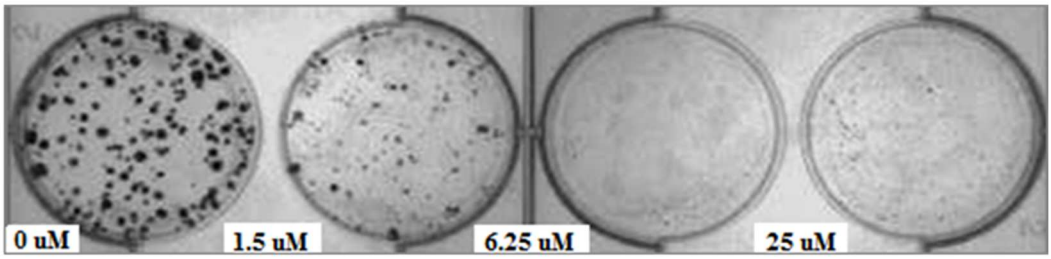

$[\mathbf{Ru(phen)_2dppz}]^{2+}$

Figure 3.10 Representative colony formation assay for H1993 cell line after four weeks of treatment with $\mathbf{P}^{4+}$, $\mathbf{MP}^{2+}$, and $[Ru(phen)_2dppz]^{2+}$

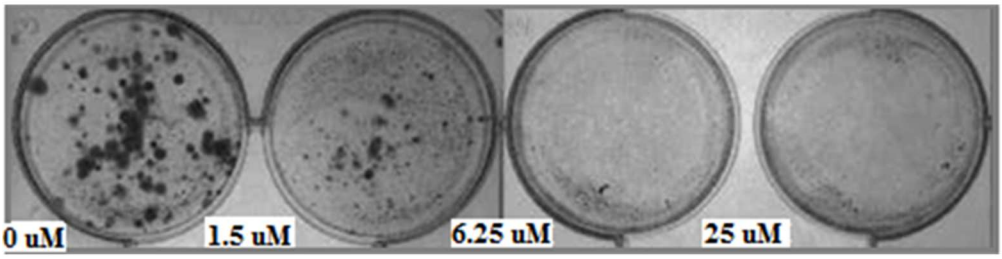

$[\mathbf{P}]^{2+}$

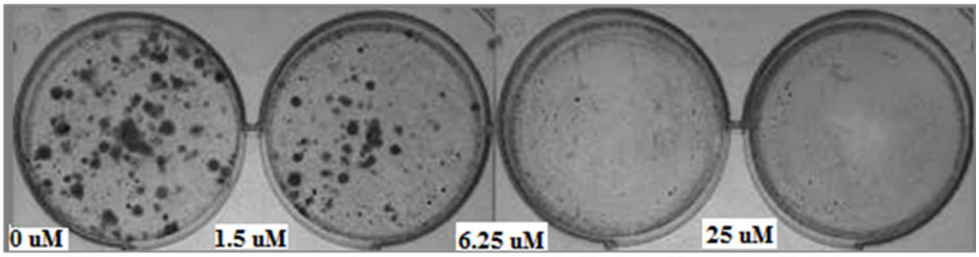

$[\mathbf{MP}]^{2+}$

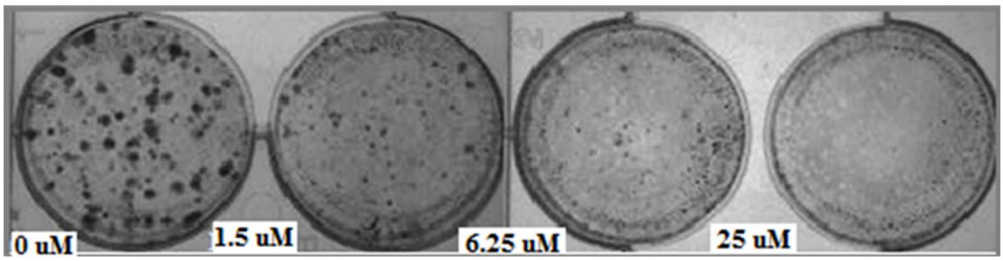

$[\mathbf{Ru(phen)_2dppz}]^{2+}$

Figure 3.11 Representative colony formation assay for HCC2450 cell line after four weeks of treatment with $\mathbf{P}^{4+}$, $\mathbf{MP}^{2+}$, and $[Ru(phen)_2dppz]^{2+}$

3.3.3 Animal Study

In this study, the maximum tolerated dose (MTD) reports the highest dose in milligrams drug per kilogram mouse that is tolerated without unacceptable toxicity; in this case, short term toxicity (24 h), and only uses 3 animals per compound. Death is not the only endpoint for an MTD study and therefore we define unacceptable toxicity as any dosage that causes morbidity in the animal. In addition to obvious signs of stress such as paralysis, seizures, and tremors, more subtle signs of toxicity including lethargy, labored breathing, or glassy eyes were also considered a toxic dose and the mouse was sacrificed. The MTD of the Ru(II) complexes was examined in male Balb/c mice. The data in Table 3.8 is organized in the order of descending lipophilicity.

As seen in Figure 3.12, the RPCs fall into two classes. RPCs with tatpp ligand are tolerated for better than those lacking a tatpp ligand. The reason for this is not clear, but it may have something to do with the redox-activity. As can be seen, the lipophilicity of the complexes does not correlate with the MTDs, with all non-tatpp RPCs showing acute toxicity at related low dosing. Among the tatpp RPCs, there may be a correlation with lipophilicity as the least lipophilic complex, $\mathbf{MP}^{2+}$, had a lower MTD than the non-lipophilic complexes but the single data point makes it hard to draw a firm conclusion. $\mathbf{MP}^{2+}$ complex showed signs of systemic toxicity including sickness and morbidity after treatment with 60 mg/Kg where the animal was sacrificed. The previous tolerable dose of 40 mg/Kg was considered the MTD for this compound. The differences in activity between $\mathbf{MP_{Me}}^{2+}$, $\mathbf{MP_{Ph}}^{2+}$ and $\mathbf{MP}^{2+}$ cationic complexes are most likely due to differences in penetration. $\mathbf{MP_{Me}}^{2+}$ and $\mathbf{MP_{Ph}}^{2+}$ are drastically more lipophilic than $\mathbf{MP}^{2+}$**,** as shown before in the partition coefficient experiment results Table 3.4. Dwyer and coworkers' study showed that increasing the lipophilicity of the ancillary ligand of the Ru(II) complexes can lower the animal toxicity; this is possibly due to the slow diffusion of the complex to the blood stream.[18,19] However,

$[Ru(Ph_2phen)_3]^{2+}$ (lipophilic complex) and $[Ru(phen)_3]^{2+}$ (hydrophilic complex) did not follow this trend; both of these are equally toxic at very low dose. It is clear that lipophilicity plays very important roles, but only in the presence of the tatpp bridging ligand as shown in Figure 3.12.

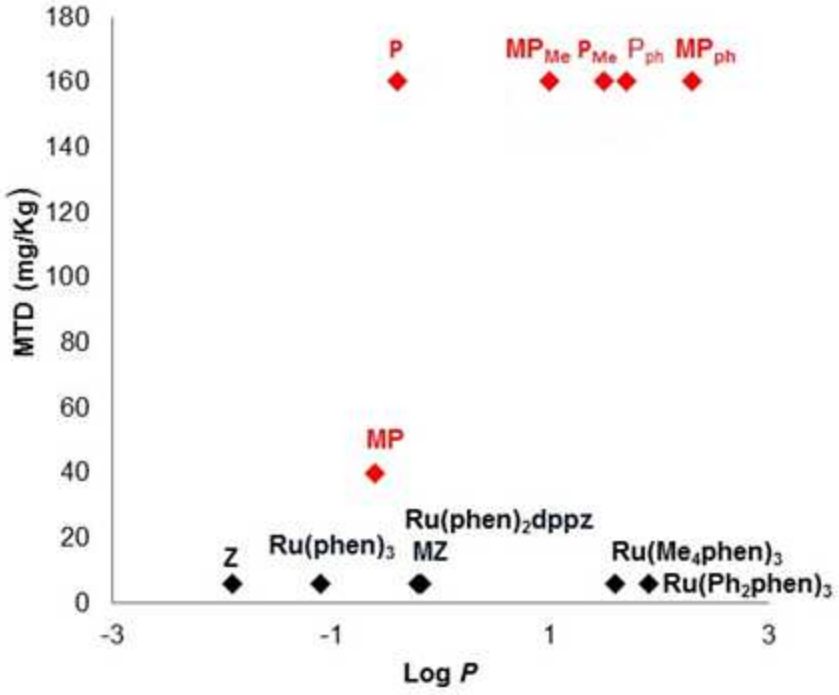

Figure 3.12 Maximum tolerable dose (mg/Kg) for Ru(II) polypyridyl complexes verse log *P* values

Table 3.8 Maximum tolerable dose (mg/Kg) for Ru(II) polypyridyl complexes administered to Balb/c mice

Compound	Maximum tolerable dose (mg/Kg)
$\mathbf{MP_{Ph}}^{2+}$	> 160
$[Ru(Ph_2phen)_3]^{2+}$	6
$\mathbf{P_{Ph}}^{4+}$	> 160
$[Ru(Me_4phen)_3]^{2+}$	6
$\mathbf{P_{Me}}^{4+}$	> 160
$\mathbf{MP_{Me}}^{2+}$	> 160
$[Ru(phen)_2dppz]^{2+}$	6
$\mathbf{MZ}^{2+}$	6
$\mathbf{P}^{4+}$	> 160
$\mathbf{MP}^{2+}$	40
$[Ru(phen)_3]^{2+}$	6
$\mathbf{Z}^{4+}$	6

3.3.4 Pharmacokinetic study

The following three Ru complexes: $[Ru(phen)_2dppz]^{2+}$, $\mathbf{MP}^{2+}$, and $\mathbf{MP_{Ph}}^{2+}$ were used in a PK study using male Wister Han rats. After IP dosing, blood samples were taken at various time intervals and separated the plasma and red blood cells. Each was then analyzed for Ru content by ICP-MS. One major characteristic that distinguishes ICP-MS from other spectroscopic instruments is its sensitivity.[110] Its sensitivity is well into the parts-per-billion (10^{-9}) to the parts-per-trillion (10^{-12}) range.[111] In our PK experiment, ICP-MS quantification was performed on a single quadrupole (X-Series II) instrument to determine the concentration of ruthenium in the plasma of Wister Han rats after IP administration. Before each analysis of the samples, the instrument was calibrated. The performance of the instrument was tested using standard plasma samples that were spiked with different concentrations of ruthenium from 0.00 to 100 ppb to evaluate the linearity of the calibration curve. 2% ultrapure concentrated nitric acid was used in preparation of standards, internal standards and samples. The blood pellets were digested and analyzed for ruthenium content.

Control samples in which RPCs were spiked into blood reveal the technique gives reliable data. The three RPCs were chosen because each is a dication and they have very different lipophilicities, with log *P* values of -1.9, -0.4, and 2.3 respectively. The raw data and a plot of the [Ru] versus the time for each RPC are shown in Tables 3.9, 3.10, and 3.11 and in Figures 3.13, 3.14, and 3.15 correspondingly. From the data, it is clear that the large standard deviation makes interpretation of the data difficult, but if we just consider the trends revealed, it appears that the temporal blood concentration of the RPCs does correlate with the lipophilicity of RPC. The least lipophilic complex, $[Ru(phen)_2dppz]^{2+}$, is seen to build up to a peak concentration of ~1000 ppb in 9 h, whereas $\mathbf{MP}^{2+}$ takes ~18 h to reach a maximum which peaks at ~400 ppb. The most lipophilic complex $\mathbf{MP_{Ph}}^{2+}$, never

reaches a peak in the 24 h observation period. Figure 3.16 shows the three profiles plotted together and reveals that, the greater the lipophilicity, the slower the build up in blood serum is. Importantly, the RBC fraction shows essentially no Ru content, indicating that all the complex is in the serum.

Table 3.9 Ruthenium concentration (ppb) in plasma for $[Ru(phen)_2dppz]^{2+}$ complex after IP injection in Wister Han rats

	Ru concentration (ppb)				Standard	Standard
Time/h	Exp#1	Exp#2	Exp# 3	Average	deviation	error
0.15	66	286	65	139	128	74
0.5	134	141	119	132	11	6
1	152	116	144	137	19	11
1.5	126	156	87	123	35	20
2	140	125	75	113	34	20
3	153	818	76	349	408	236
9	139	2622	14	925	1471	849
12	112	141	25	93	60	35
18	124	121	24	90	57	33
24	123	224	12	120	106	61

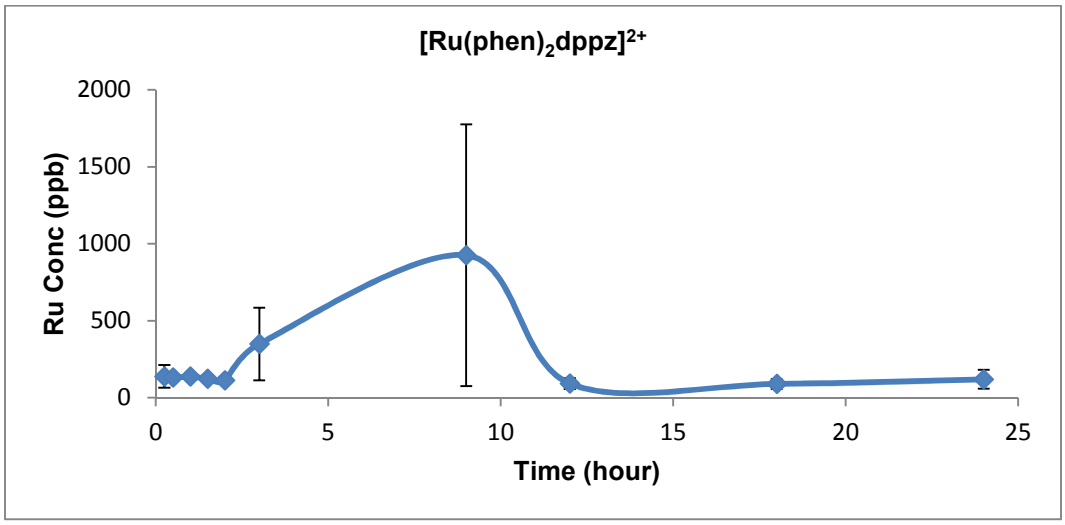

Figure 3.13 Rat blood concentration plasma ruthenium content as a function of time post IP injection in $[Ru(phen)_2dppz]^{2+}$

Table 3.10 Ruthenium concentration (ppb) in plasma for **MP**$^{2+}$ complex after IP injection in Wister Han rats

	Ru concentration (ppb)				Standard	Standard
Time/h	Exp#1	Exp#2	Exp# 3	Average	deviation	error
0.15	28	80	37	48	28	16
0.5	28	232	15	92	122	70
1	23	82	13	39	37	22
1.5	27	79	39	48	27	16
2	19	117	27	54	54	31
3	37	99	19	51	42	24
6	38	488	37	188	260	150
12	36	839	11	295	471	272
18	21	1020	19	353	577	333
24	27	148	21	65	71	41

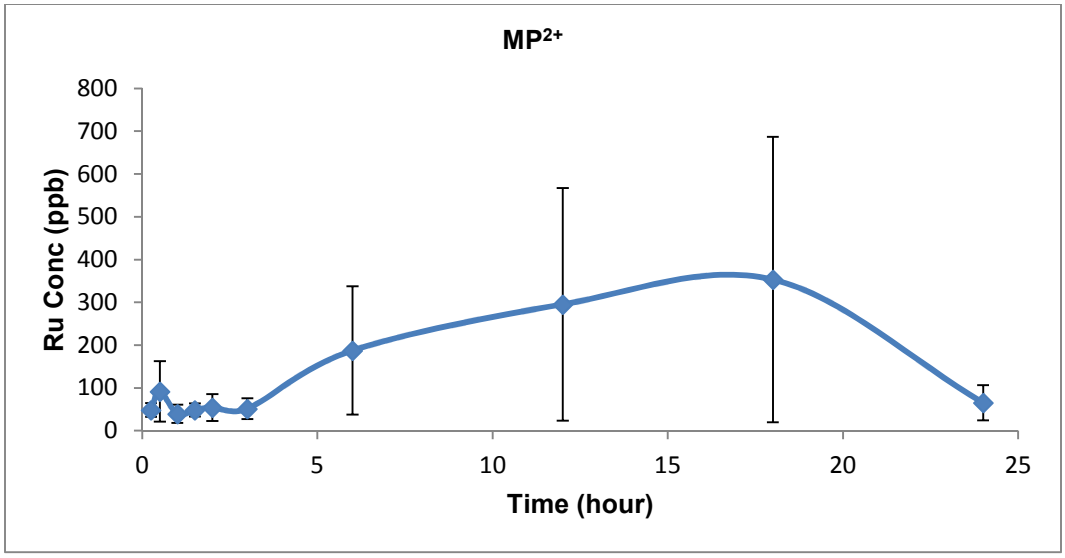

Figure 3.14 Rat blood concentration plasma ruthenium content as a function of time post IP injection in **MP**$^{2+}$

Table 3.11 Ruthenium concentration (ppb) in plasma for **MP$_{Ph}^{2+}$** complex after IP injection in Wister Han rats

	Ru concentration (ppb)				Standard	Standard
Time/h	Exp#1	Exp#2	Exp# 3	Average	deviation	error
0.15	39	256	40	112	125	72
0.5	78	167	46	97	63	36
1	54	301	46	133	145	84
1.5	38	244	88	124	107	62
2	52	120	124	99	40	23
3	62	192	42	99	81	47
6	90	122	87	100	19	11
12	73	562	151	262	263	152
18	54	330	845	410	401	232
24	46	1884	368	766	981	567

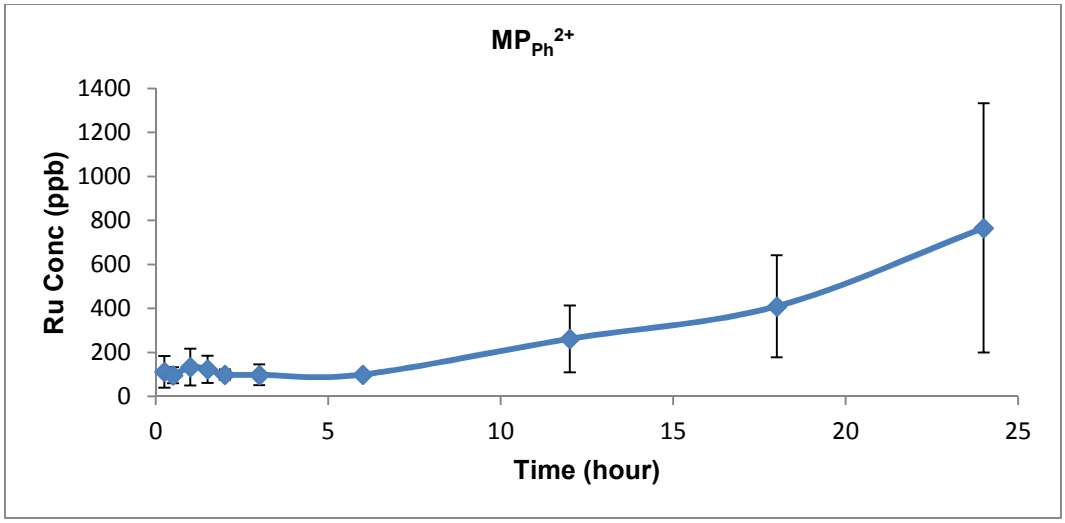

Figure 3.15 Rat blood concentration plasma ruthenium content as a function of time post IP injection in **MP$_{Ph}^{2+}$**

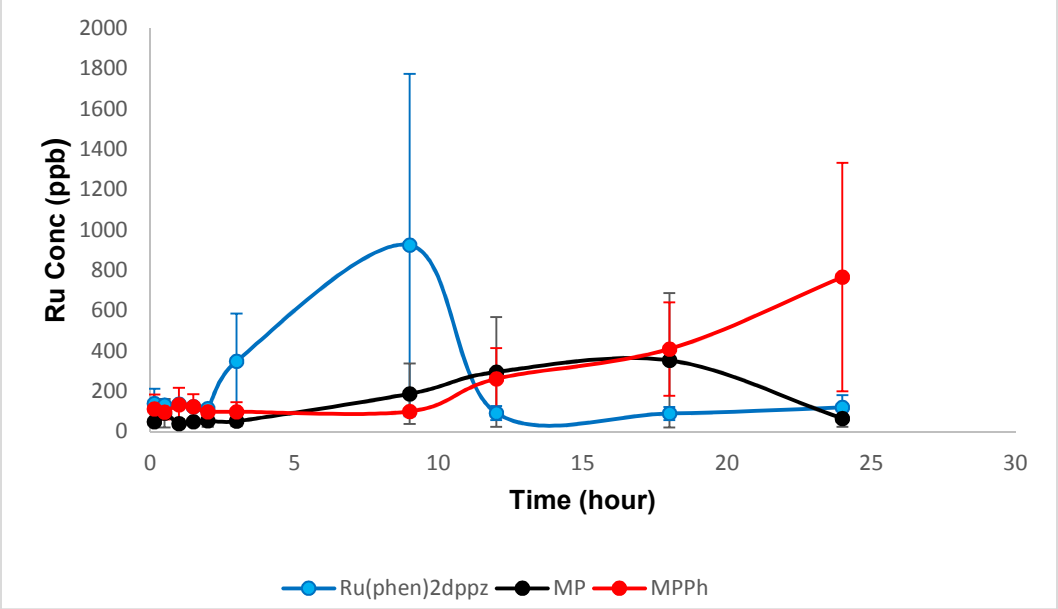

Figure 3.16 Rat blood concentration plasma ruthenium content as a function of time post IP injection in $[Ru(phen)_2dppz]^{2+}$, $\mathbf{MP}^{2+}$, and $\mathbf{MP_{Ph}}^{2+}$

*3.3.5 NCI Screen Data for [**MP$_{Ph}$**]Cl$_2$*

The compound [**MP$_{Ph}$**]Cl$_2$ was submitted for the NCI-60 cell panel testing and was accepted and assigned a reference number NSC 782009. The mean percentage of growth for cells treated with 10 μM complex was 118% which was too high to qualify the compound for further 5-dose testing. Nonetheless, this single dose data does provide a picture of the activity of this very lipophilic compound against 60 different cell lines and several cancer types. This data is plotted in Figure 3.17 and is reported as the percent growth inhibition relative to the mean of 118% (central vertical line) per cell line. As can be seen, [**MP$_{Ph}$**]Cl$_2$ was consistently better against colon cancer cells than other types of cells. Similar trends are seen for NSCLC, CNS, renal, and melanomas, but exceptions are noticeable. It appears to be less effective, on average, towards ovarian, breast, and prostate cancers.

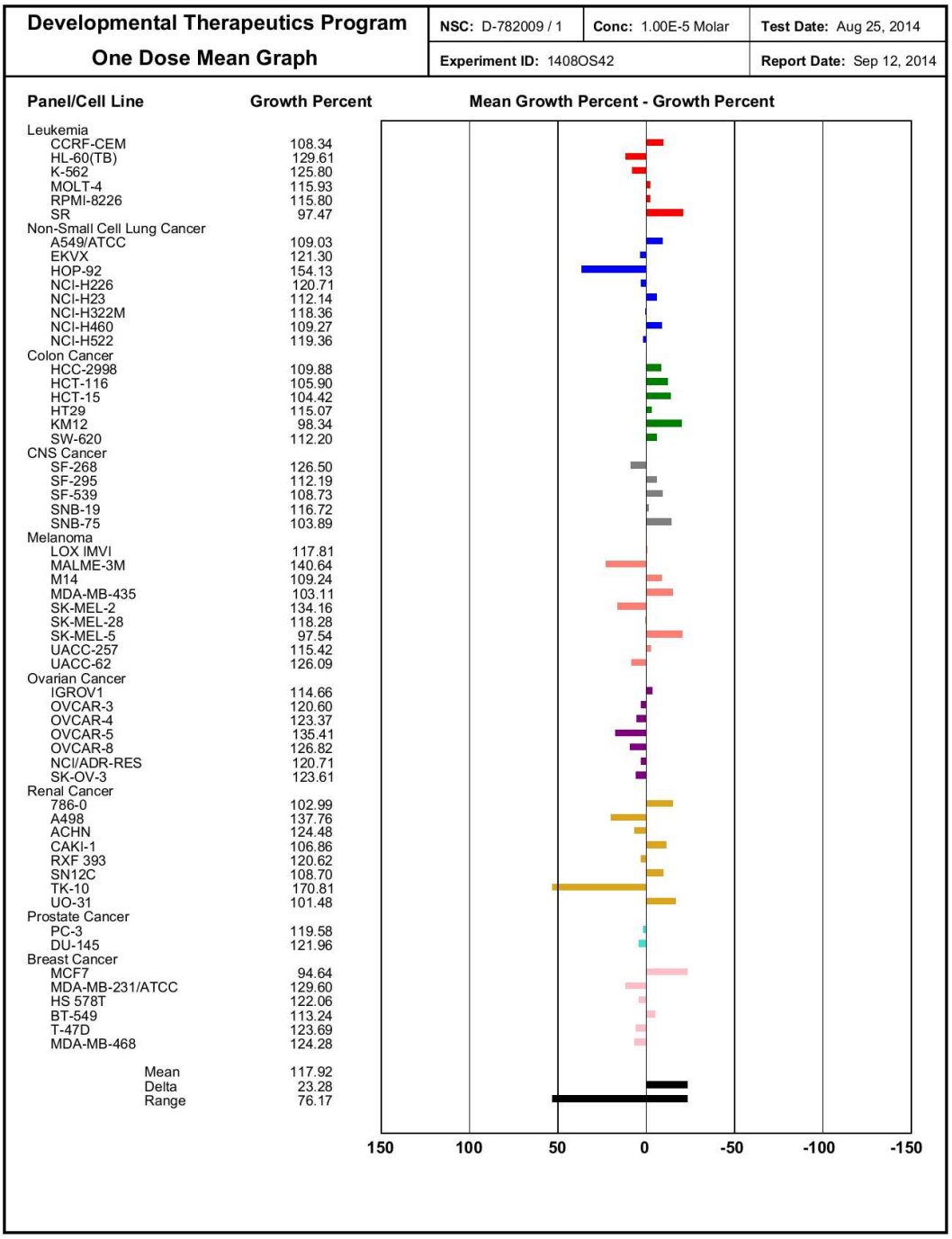

Figure 3.17 One dose mean graph for $\mathbf{MP_{Ph}}^{2+}$ (NSC 782009)

3.4 Conclusion

We have investigated the structure activity relationship of the Ru polypyridyl complexes by changing the lipophilicity of the ancillary ligands from phen to Ph_2phen or Me_4phen. It was found addition of the phenyl substituents results in a large increase in lipophilicity compared to complexes with unsubstituted 1,10-phenanthrolines. Methyl substituents on the phenanthroline ligands give complexes with an intermediate lipophilicity. There was a strong correlation between the tatpp-based compounds' lipophilicity and animal toxicity, as measured by the MTD. As the lipophilicity increased, animal toxicity decreased. All of the following RPCs: [$\mathbf{P_{Me}}$]Cl_4, [$\mathbf{MP_{Me}}$]Cl_2, [$\mathbf{P_{Ph}}$]Cl_4, [$\mathbf{MP_{Ph}}$]Cl_2 and [**P**]Cl_4, were very well tolerated at doses up to 160 mg compound per Kg mouse. [**MP**]Cl_2 complex exhibited signs of toxicity including sickness and morbidity after 60 mg/Kg, where the animal was sacrificed. In general, the [**MP**]Cl_2 complex is well tolerated with MTD value of 40 mg/Kg compared to other complexes. The low toxicity of the tatpp-based Ru(II) complexes may be due to a relatively slower rate of diffusion of these complexes into the blood stream. Pharmacokinetic data suggest that the lipophilic RPC takes more time to build up in blood stream than the hydrophilic ones. The distinct biological properties of theses tatpp-based ruthenium complexes increase their chances to advance into clinically used therapeutic agents.

The IC_{50} values were investigated and the tatpp-based complexes were found to have good cytotoxicity against most cancerous cell lines. Different cancer cell lines yield different response patterns regard the correlation of compound lipophilicity with cytotoxicity. While the general trend of increasing lipophilicity yielding better cytotoxicity seems to hold with MCF-7, is not seen with other cell line. The most lipophilic complexes, $\mathbf{P_{Ph}}^{4+}$ and $\mathbf{MP_{Ph}}^{2+}$, have shown high cytotoxicity against MCF-7 cell line with IC_{50} of 1.4 μM and 2.13 μM respectively. All tatpp-based RPCs have shown high SI against non-

cancerous cell line (MCF-10) compared to cisplatin that has SI of 2.5 in the same experiment. However, $\mathbf{P}^{4+}$ and $\mathbf{MP}^{2+}$ exhibited good cytotoxicity towards all three malignant cell lines and a respectable selectivity index. Also, we have found that $\mathbf{P}^{4+}$ is effective at treating platinum resistant cell lines such as H1993, HCC2450 and H322 compared to $\mathbf{MP}^{2+}$ and $[Ru(phen)_2dppz]^{2+}$ complexes, but none of these complexes were effective against pancreatic cell line, PANC1. This suggests $\mathbf{P}^{4+}$ may have some effectiveness in treating platinum-resistant cancers. It is clear that the redox-active bridging ligand tatpp is an important component in the most effective RPCs. In summary, all of the tatpp-based RPCs show promising antitumor activity.

Appendix A

^{1}H NMR of Ruthenium Polypyridyl Complexes

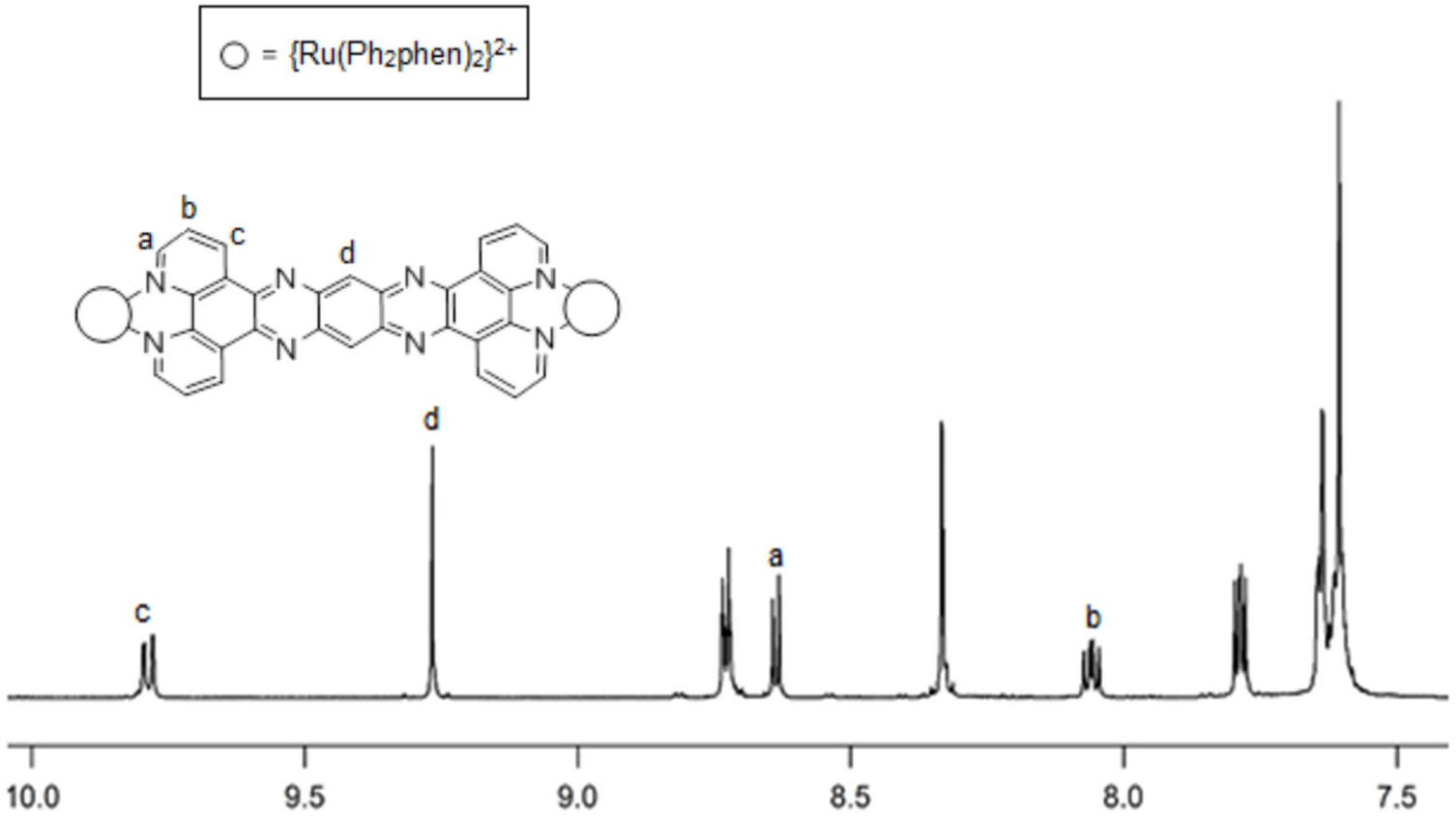

^{1}H NMR Spectrum of $[(Ph_2phen)_2Ru(tatpp)Ru(Ph_2phen)_2]^{4+}$

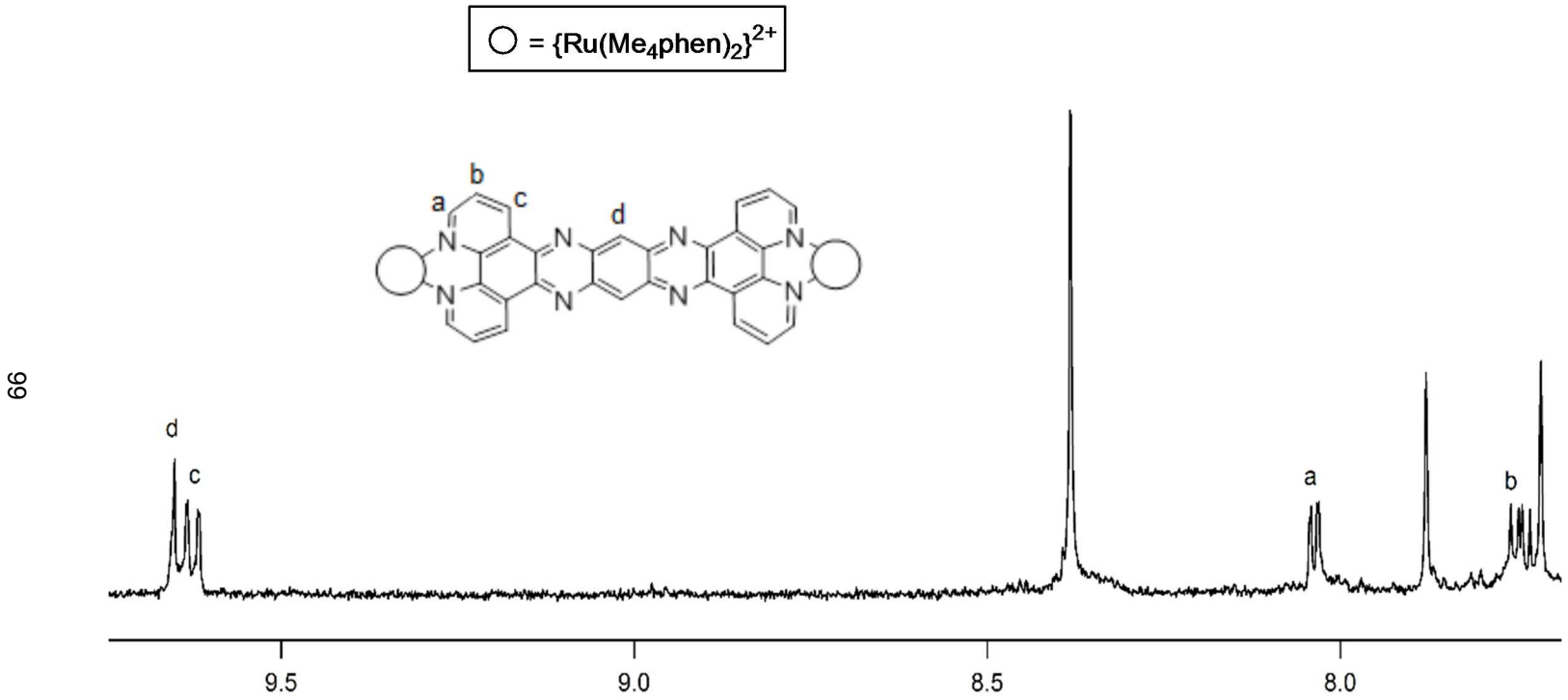

^{1}H NMR Spectrum of [(Me$_4$phen)$_2$Ru(tatpp)Ru(Me$_4$phen)$_2$]$^{4+}$

(expended down field region)

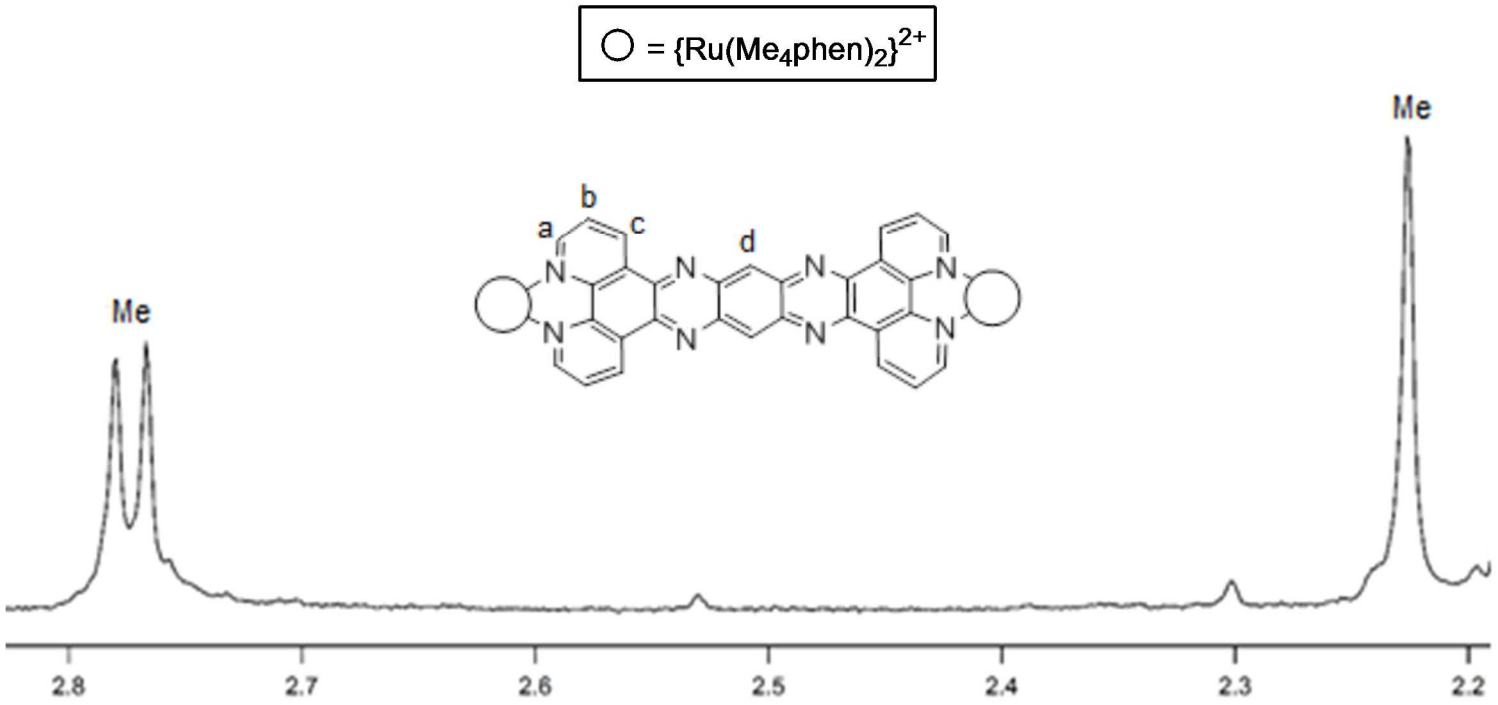

^{1}H NMR spectrum of $[(Me_4phen)_2Ru(tatpp)Ru(Me_4phen)_2]^{4+}$

(extended upfield region)

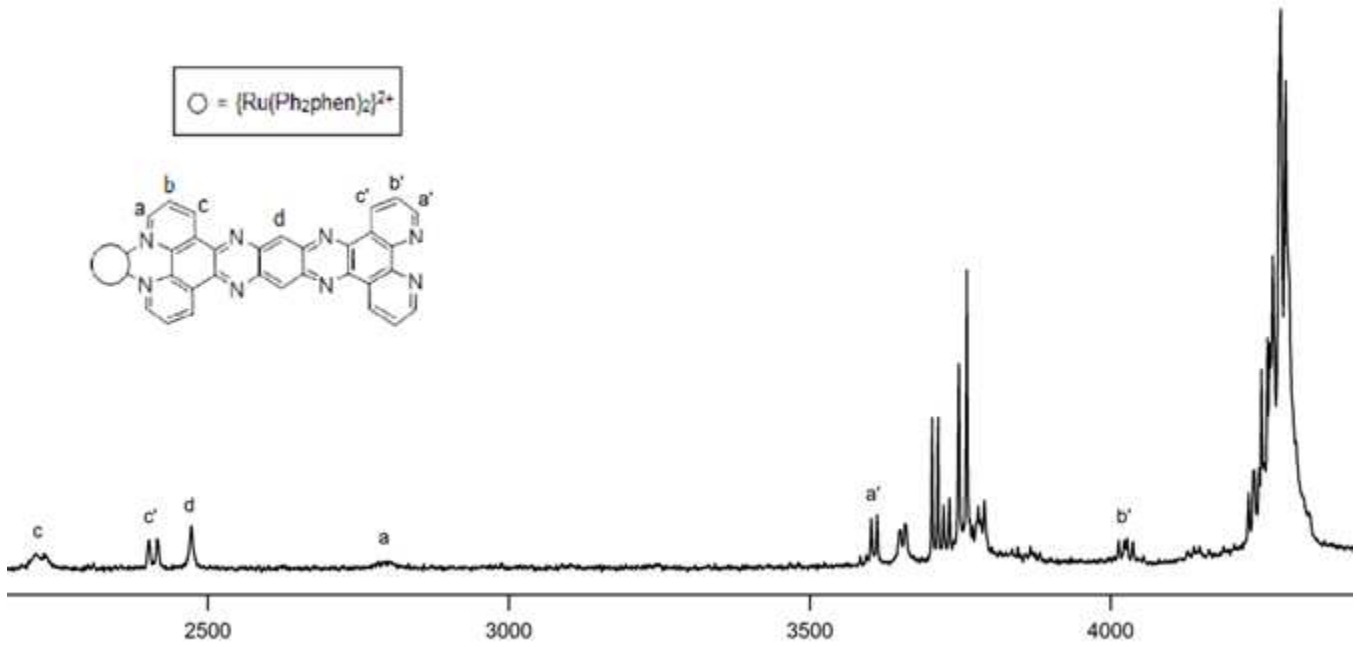

^{1}H NMR Spectrum of $[(Ph_2phen)_2Ru(tatpp)]^{2+}$ in the absence of $Zn(BF_4)_2$

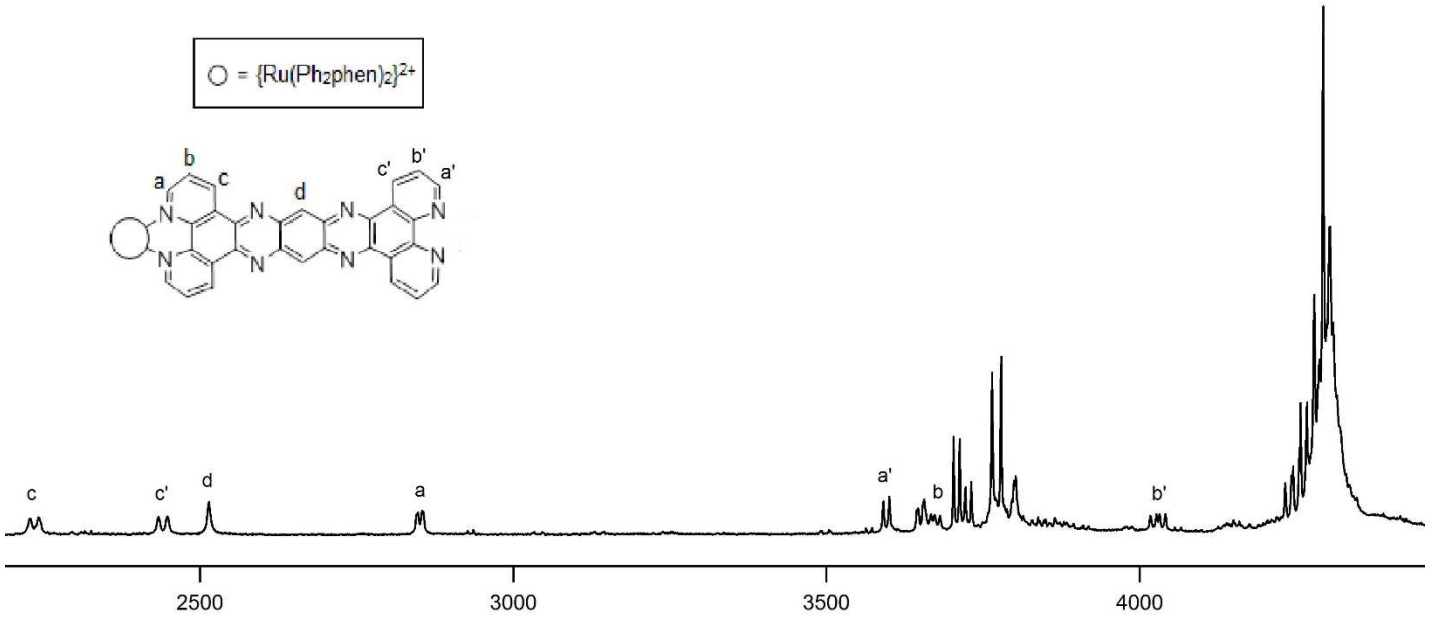

^{1}H NMR Spectrum of $[(Ph_2phen)_2Ru(tatpp)]^{2+}$ with excess $Zn(BF_4)$

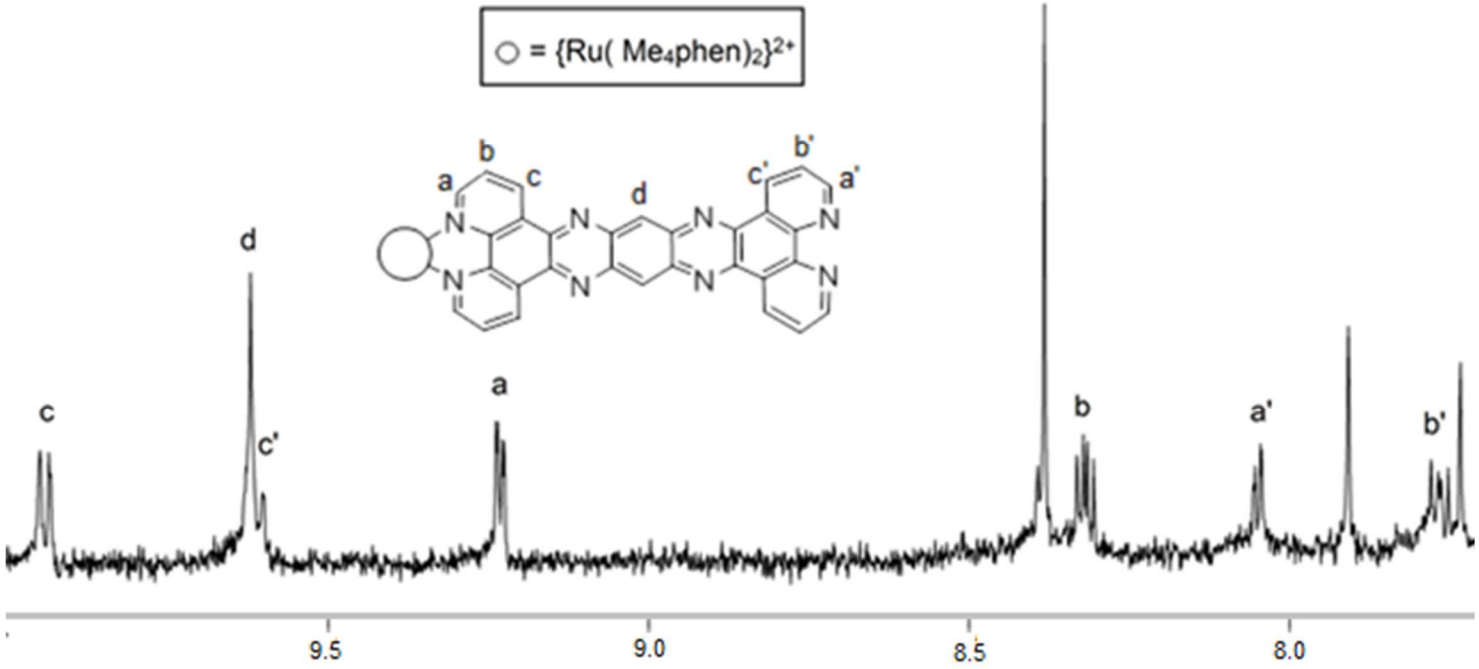

^{1}H NMR Spectrum of $[(Me_4phen)_2Ru(tatpp)]^{2+}$ with excess $Zn(BF_4)_2$

(expended down field region)

Appendix B

IC_{50} of Ruthenium Polypyridyl Complexes

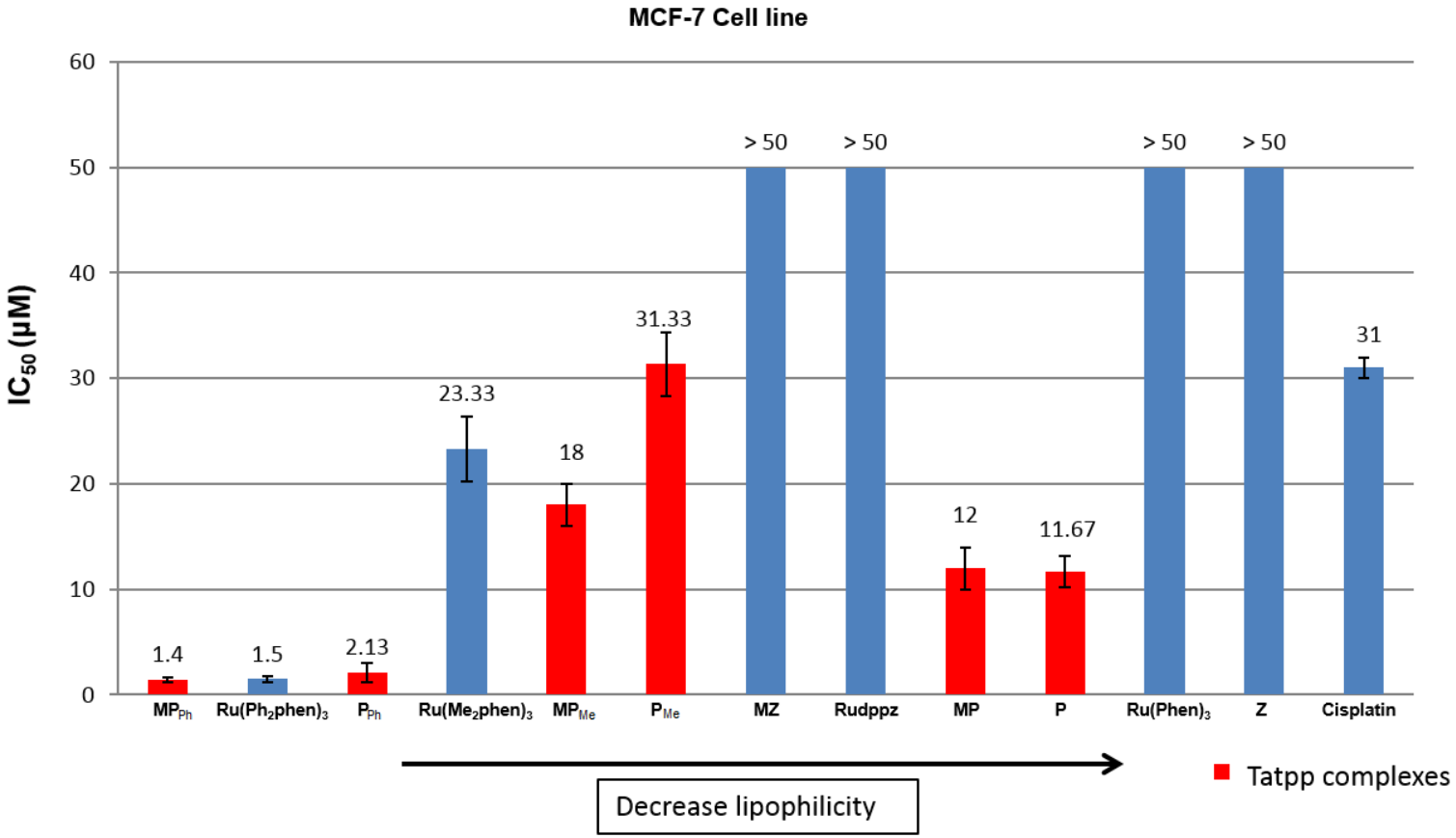

IC_{50} of Ru(II) polypyridyl complexes against breast cancer cell line MCF-7

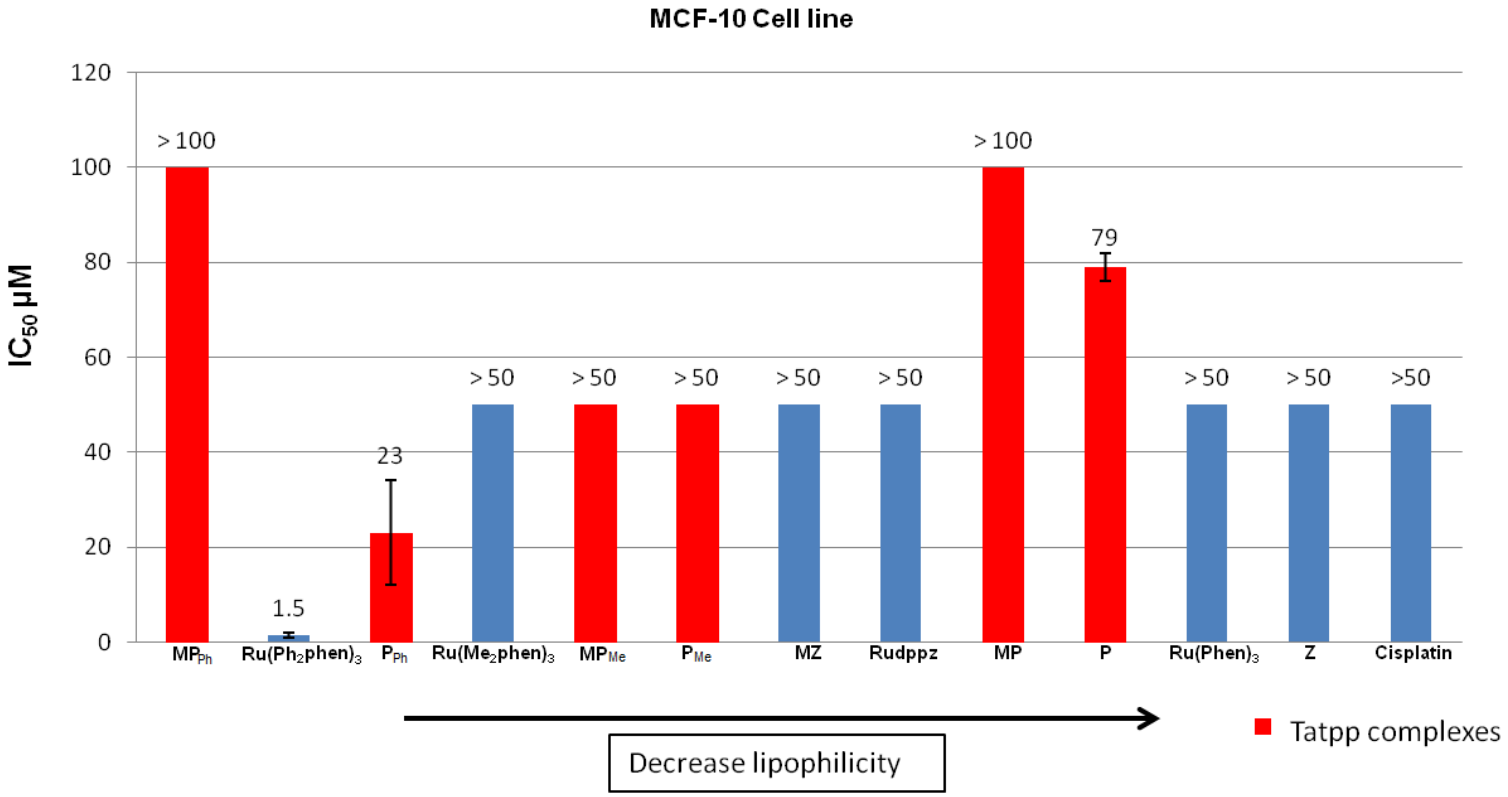

IC_{50} of Ru(II) polypyridyl complexes against breast epithelial cell line MCF-10

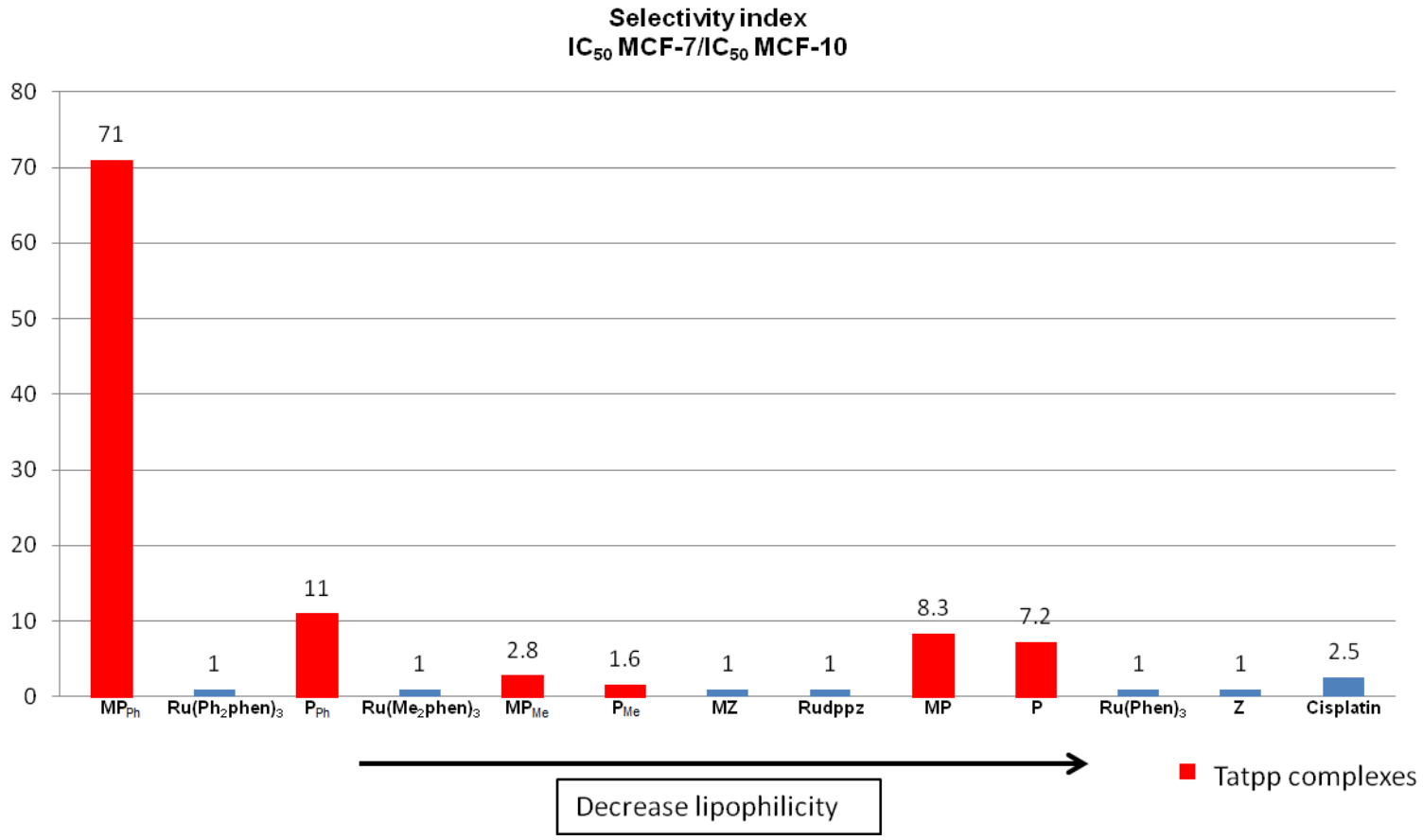

Selectivity Index (SI): IC_{50} MCF-10/ IC_{50} MCF-7

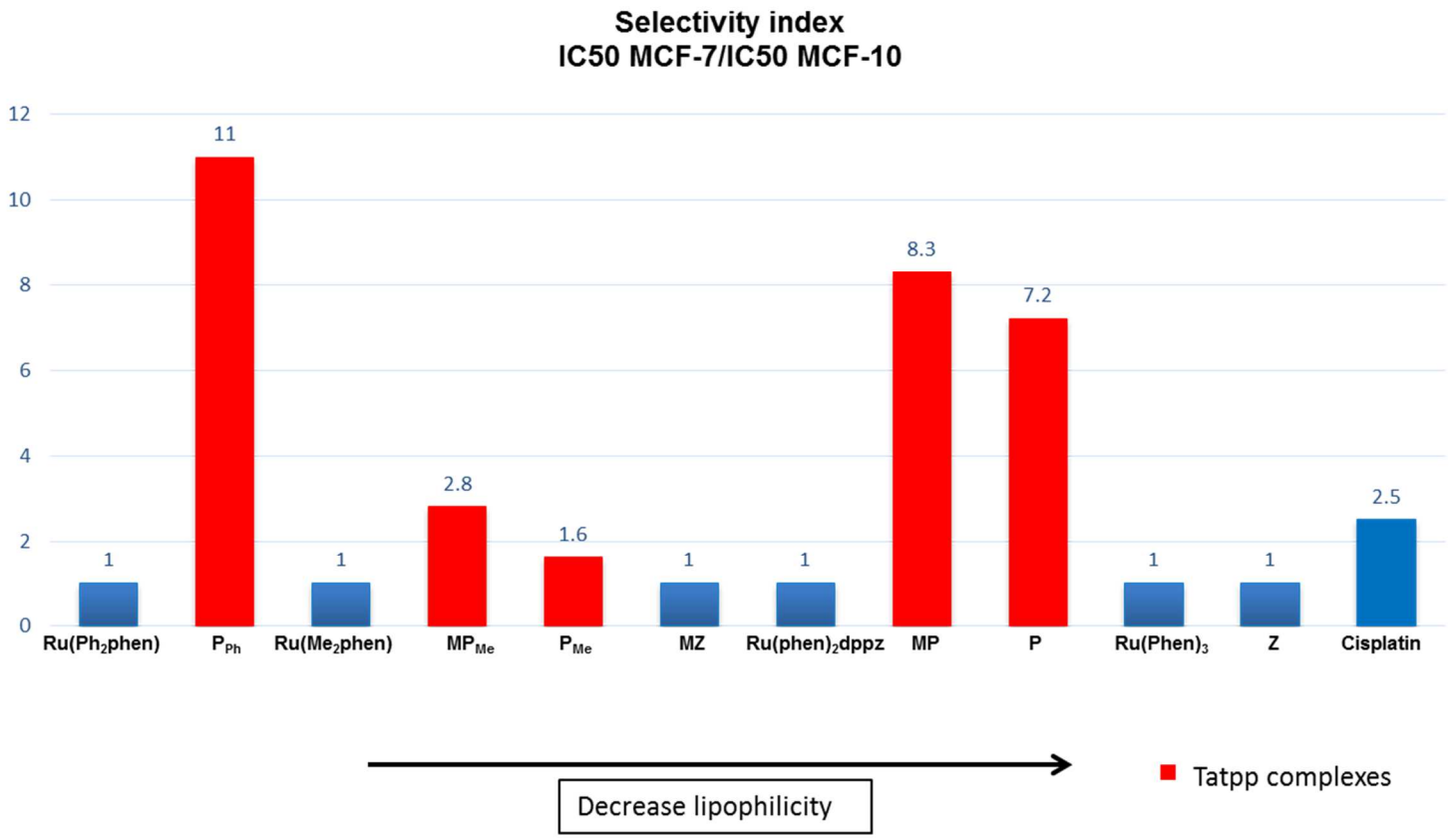

Selectivity Index (SI): IC_{50} MCF-10/ IC_{50} MCF-7 (**MP_{Ph}** excluded)

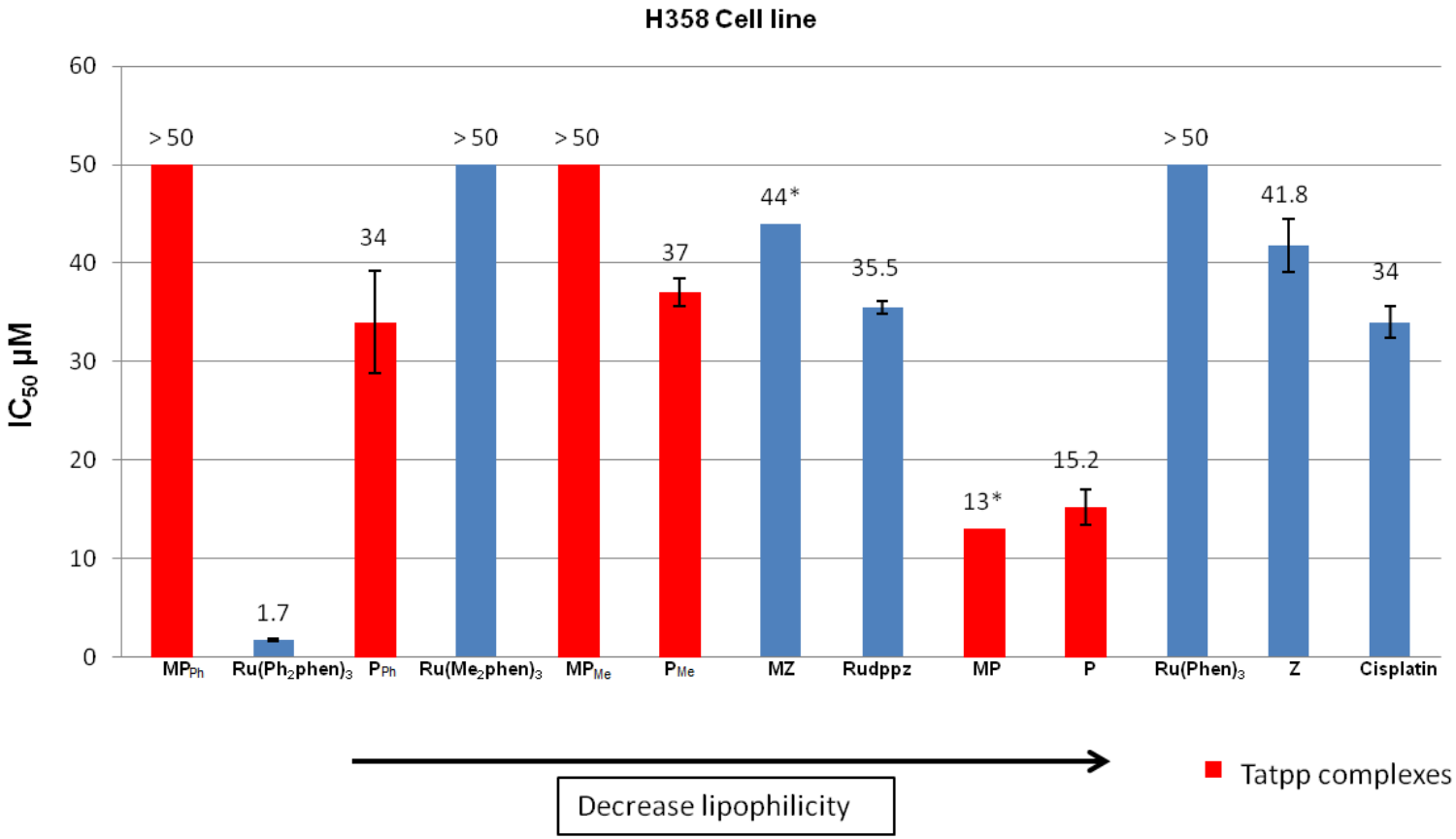

IC_{50} of Ru(II) polypyridyl complexes against non-small cell lung cancer (NSCLC) cell line H358 (Bronchioalveolar), * Yadav *et al*. results

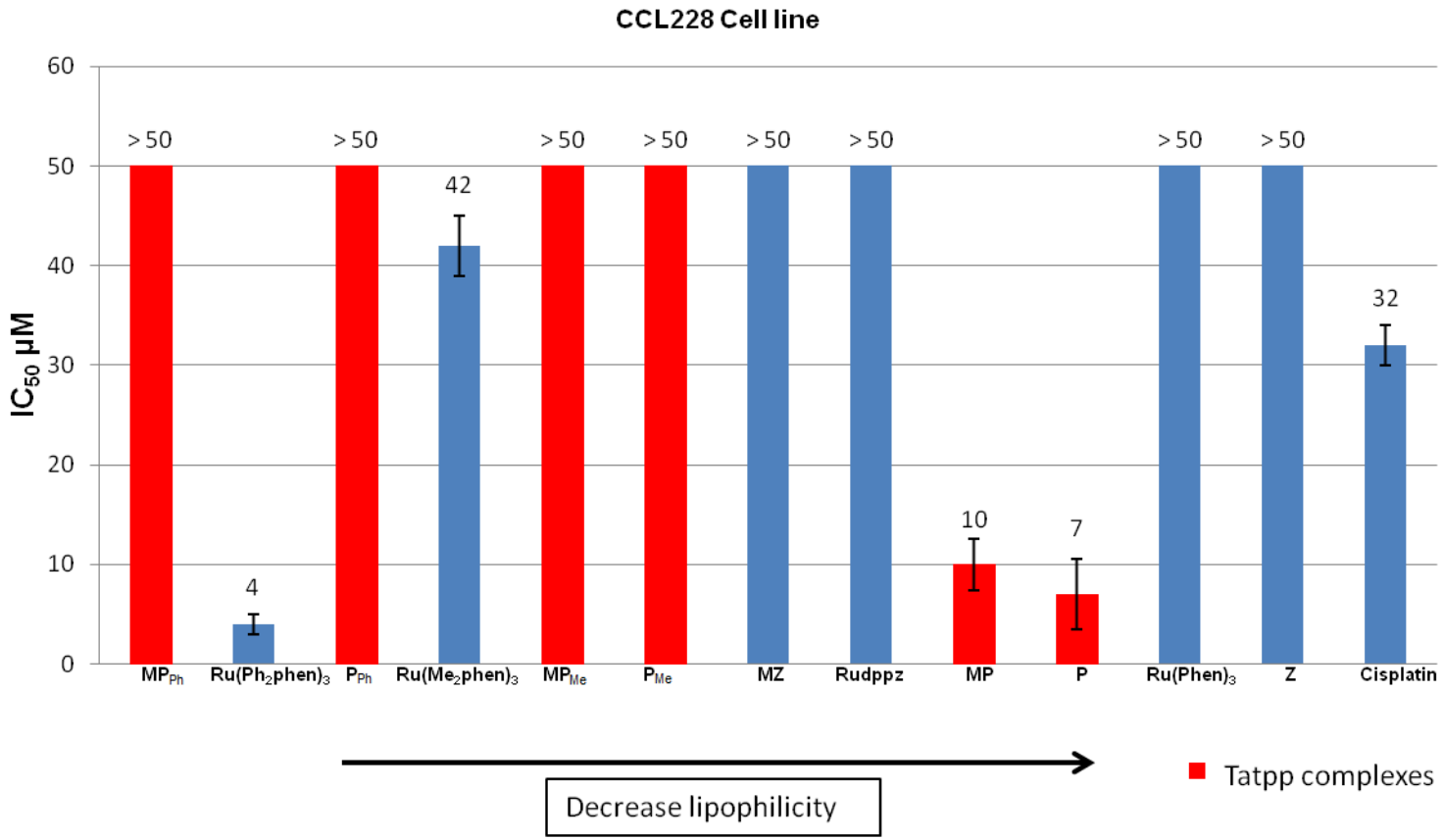

IC_{50} of Ru(II) polypyridyl complexes against colon cancer cell line CCL228

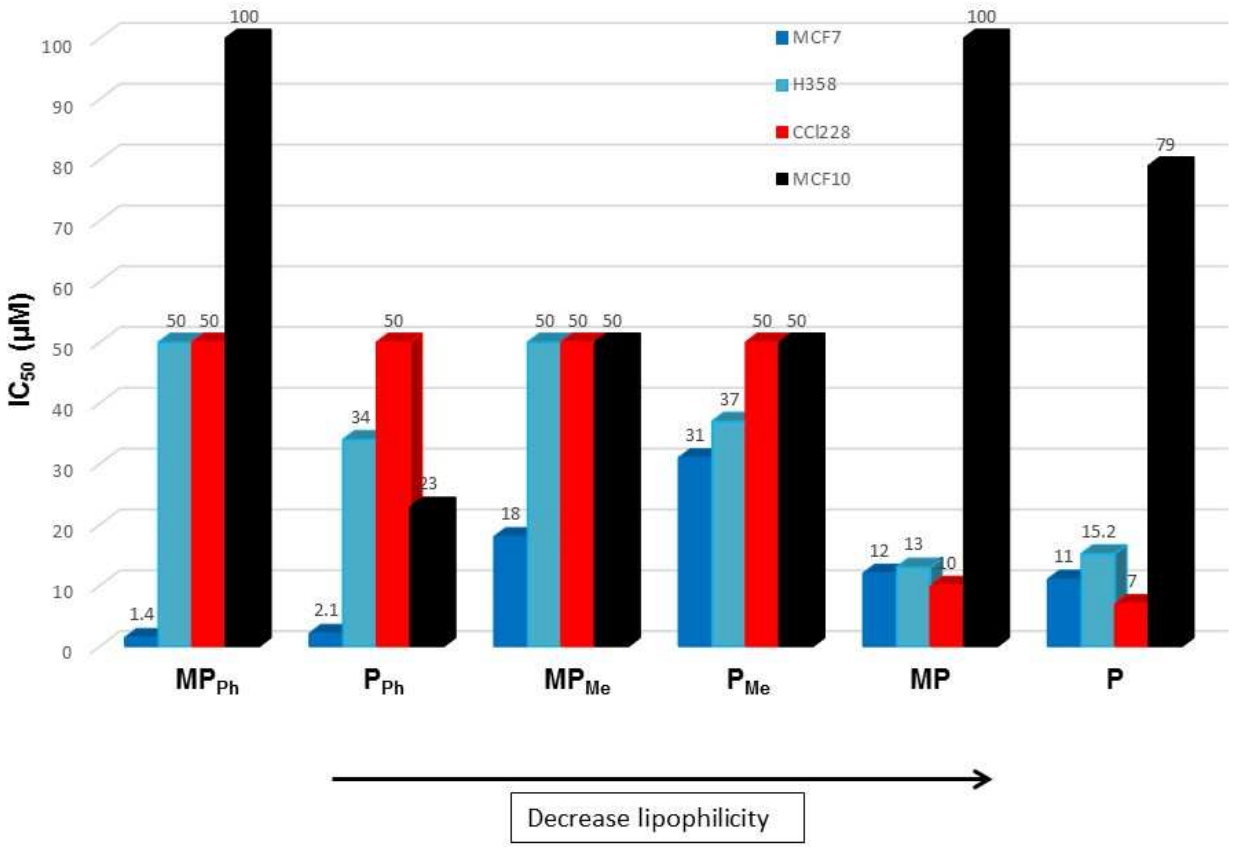

IC_{50} of Ru(II) polypyridyl complexes against cancerous cell line (MCF-7, H358, CCL228) and non-cancerous cell line (MCF-10) for tatpp-based Ru(II) complexes

References

1. Kostova, I., Platinum Complexes as Anticancer Agents. *Recent. Pat. Anti-Cancer.* **2006,** *1* (1), 1-22.

2. Lippert, B., *Cisplatin: Chemistry and Biochemistryof a Leading Anticancer Drug*. Wiley-VCH: Weinhiem, 1999.

3. Kostova, I., Ruthenium Complexes as Anticancer Agents. *Curr. Med. Chem.* **2006,** *13* (9), 1085-1107.

4. Allardyce, C. S.; Dyson, P. J., Ruthenium in Medicine: Current Clinical Uses and Future Prospects. *Platinum Met. Rev.* **2001,** *45* (2), 62-69.

5. Hartmann, J. T.; Lipp, H.-P., Toxicity of Platinum Compounds. *Expert. Opin. Pharmacother.* **2003,** *4* (6), 889-901.

6. Desoize, B.; Madoulet, C., Particular Aspects of Platinum Compounds Used at Present in Cancer Treatment. *Crit. Rev. Oncol. Hematol.* **2002,** *42* (3), 317-325.

7. Gaynor, D.; Griffith, D. M., The Prevalence of Metal-Based Drugs as Therapeutic or Diagnostic Agents: Beyond Platinum. *Dalton. Trans.* **2012,** *41* (43), 13239-13257.

8. Clarke, M. J., Ruthenium Metallopharmaceuticals. *Coord. Chem. Rev.* **2003,** *236* (1–2), 209-233.

9. Allardyce, C. S.; Dyson, P. J., Ruthenium in Medicine: Current Clinical Uses and Future Prospects. *Platin. Met. Rev.* **2001,** *45* (2), 62-69.

10. Gallori, E.; Vettori, C.; Alessio, E.; Vilchez, F. G.; Vilaplana, R.; Orioli, P.; Casini, A.; Messori, L., DNA as a Possible Target for Antitumor Ruthenium(III) Complexes: A Spectroscopic and Molecular Biology Study of the Interactions of Two Representative Antineoplastic Ruthenium(III) Complexes with DNA. *Arch. Biochem. Biophys.* **2000,** *376* (1), 156-162.

11. Sava, G.; Zorzet, S.; Turrin, C.; Vita, F.; Soranzo, M.; Zabucchi, G.; Cocchietto, M.; Bergamo, A.; DiGiovine, S.; Pezzoni, G.; Sartor, L.; Garbisa, S., Dual Action of NAMI-A in Inhibition of Solid Tumor Metastasis: Selective Targeting of Metastatic Cells and Binding to Collagen. *Clin. Cancer Res.* **2003,** *9* (5), 1898-1905.

12. Scolaro, C.; Bergamo, A.; Brescacin, L.; Delfino, R.; Cocchietto, M.; Laurenczy, G.; Geldbach, T. J.; Sava, G.; Dyson, P. J., In Vitro and in Vivo Evaluation of Ruthenium(II)−Arene PTA Complexes. *J. Med. Chem.* **2005,** *48* (12), 4161-4171.

13. Trondl, R.; Heffeter, P.; Jakupec, M. A.; Berger, W.; Keppler, B. K., NKP-1339, AFirst-in-Class Anticancer Drug Showing Mild Side Effects and Activity in Patients Suffering from Advanced Refractory Cancer. *BMC Pharmacol. Toxicol.* **2012,** *13* (1), 1-1.

14. Ott, I.; Gust, R., Non Platinum Metal Complexes as Anti-cancer Drugs. *Arch. Pharm.* **2007,** *340* (3), 117-126.

15. Dyson, P. J.; Sava, G., Metal-Based Antitumour Drugs in the Post Genomic Era. *Dalton. Trans.* **2006,** (16), 1929-1933.

16. Clarke, M. J., Oncological Implications of the Chemistry of Ruthenium", Metal Ions in Biological Systems. **1980,** *11*, 231–283.

17. Monti-Bragadin, C.; Ramani, L.; Samer, L.; Mestroni, G.; Zassinovich, G., Effects of cis-Dichlorodiammineplatinum (II) and Related Transition Metal Complexes on Escherichia coli. *Antimicrob. Agents Chemother.* **1975,** *7* (6), 825-827.

18. Dwyer, F. P.; Gyarfas, E. C.; Rogers, W. P.; Koch, J. H., Biological Activity of Complex Ions. *Nature* **1952,** *170* (4318), 190-191.

19. Shulman, A.; Dwyer, F. P., Metal Chelates in Biological Systems. In *Chelating Agents and Metal Chelates*, Dwyer, F. P.; Mellor, D. P., Eds. Academic Press: New York, 1964; pp 383-439.

20. Puckett, C. A. The Cellular Uptake of Luminescent Ruthenium Complexes. California Institute of Technology Pasadena, California, 2010.

21. Koch, J. H.; Rogers, W. P.; Dwyer, F. P.; Gyarfas, E. C., The Metabolic Fate of Tris-1,10-Phenanthroline Ruthenium-106 (II) Perchlorate, a Compound with Anticholinesterase and Curare-Like Activity. *Australian J. Biol. Sci.* **1957,** *10*, 342-350.

22. Dwyer, F. P.; Gyarfas, E. C.; Wright, R. D.; Shulman, A., Effect of Inorganic Complex Ions on Transmission at a Neuromuscular Junction. *Nature* **1957,** *179* (4556), 425-426.

23. Dwyer, F. P. M., E.; Roe, E. M. F.; Shulman, A., Inhibition of Land-schutz Ascites Tumour Growth by Metal Chelates Derived from 3,4,7,8-Tetramethyl-1,10-Phenanthroline. *Br. J. Cancer* **1965,** *19*, 195-199.

24. Meggers, E., Targeting Proteins With Metal Complexes. *Chem. Commun.* **2009,** (9), 1001-1010.

25. Mulcahy, S. P.; Li, S.; Korn, R.; Xie, X.; Meggers, E., Solid-Phase Synthesis of Tris-heteroleptic Ruthenium(II) Complexes and Application to Acetylcholinesterase Inhibition. *Inorg. Chem.* **2008,** *47* (12), 5030-5032.

26. Yadav, A.; Janaratne, T.; Krishnan, A.; Singhal, S. S.; Yadav, S.; Dayoub, A. S.; Hawkins, D. L.; Awasthi, S.; MacDonnell, F. M., Regression of Lung Cancer by Hypoxia-Sensitizing Ruthenium Polypyridyl Complexes. *Mol. Cancer Ther.* **2013,** *12* (5), 643-653.

27. Yadav, A. Investigation of Redox-active Ruthenium(ii) Polypyridyl Complexes as Potential Anti-cancer Drugs. The University of Texas at Arlington, Arlington, TX, 2008.

28. Janaratne, T. K. Investigation of Ruthenium (II) Polypyridyl Dimers as Potential Chemotherapeutic Agents. The University of Texas at Arlington, Arlington, TX, 2006.

29. Janaratne, T. K.; Yadav, A.; Ongeri, F.; MacDonnell, F. M., Preferential DNA Cleavage under Anaerobic Conditions by a DNA-Binding Ruthenium Dimer. *Inorg. Chem.* **2007,** *46* (9), 3420-3422.

30. Wang, T.-H.; Popp, D. M.; Wang, H.-S.; Saitoh, M.; Mural, J. G.; Henley, D. C.; Ichijo, H.; Wimalasena, J., Microtubule Dysfunction Induced by Paclitaxel Initiates Apoptosis through Both c-Jun N-terminal Kinase (JNK)-dependent and -Independent Pathways in Ovarian Cancer Cells. *J. Biol. Chem.* **1999,** *274* (12), 8208-8216.

31. Notte, A.; Ninane, N.; Arnould, T.; Michiels, C., Hypoxia Counteracts Taxol-Induced Apoptosis in MDA-MB-231 Breast Cancer Cells: Role of Autophagy and JNK Activation. *Cell Death Dis.* **2013,** *4*, e638.

32. Barton, J. K.; Danishefsky, A.; Goldberg, J., Tris(phenanthroline)Ruthenium(II): Sereoselectivity in Bnding to DNA. *J. Am. Chem. Soc.* **1984,** *106* (7), 2172-2176.

33. Lincoln, P.; Broo, A.; Nordén, B., Diastereomeric DNA-Binding Geometries of Intercalated Ruthenium(II) Trischelates Probed by Linear Dichroism: $[Ru(phen)_2DPPZ]^{2+}$ and $[Ru(phen)_2BDPPZ]^{2+}$. *J. Am. Chem. Soc.* **1996,** *118* (11), 2644-2653.

34. Haq, I.; Lincoln, P.; Suh, D.; Norden, B.; Chowdhry, B. Z.; Chaires, J. B., Interaction of Δ- and Λ-$[Ru(phen)_2DPPZ]^{2+}$ with DNA: A Calorimetric and Equilibrium Binding Study. *J. Am. Chem. Soc.* **1995,** *117* (17), 4788-4796.

35. Novakova, O.; Kasparkova, J.; Vrana, O.; van Vliet, P. M.; Reedijk, J.; Brabec, V., Correlation between Cytotoxicity and DNA Binding of Polypyridyl Ruthenium Complexes. *Biochem.* **1995,** *34* (38), 12369-12378.

36. Velders, A. H.; Kooijman, H.; Spek, A. L.; Haasnoot, J. G.; de Vos, D.; Reedijk, J., Strong Differences in the in Vitro Cytotoxicity of Three Isomeric Dichlorobis(2-phenylazopyridine)ruthenium(II) Complexes. *Inorg. Chem.* **2000,** *39* (14), 2966-2967.

37. Gill, M. R.; Garcia-Lara, J.; Foster, S. J.; Smythe, C.; Battaglia, G.; Thomas, J. A., A Ruthenium(II) Polypyridyl Complex for Direct Imaging of DNA Structure in Living Cells. *Nat. Chem.* **2009,** *1* (8), 662-667.

38. Puckett, C. A.; Barton, J. K., Methods to Explore Cellular Uptake of Ruthenium Complexes. *J. Am. Chem. Soc.* **2006,** *129* (1), 46-47.

39. Puckett, C. A.; Barton, J. K., Targeting a Ruthenium Complex to the Nucleus with Short peptides. *Bioorg. Med. Chem.* **2010,** *18* (10), 3564-3569.

40. Jonas, S. K.; Riley, P. A., The Effect of Ligands on the Uptake of Iron by Cells in Culture. *Cell Biochem. Funct.* **1991,** *9* (4), 245-253.

41. Kalayda, G. V.; Fakih, S.; Bertram, H.; Ludwig, T.; Oberleithner, H.; Krebs, B.; Reedijk, J., Structure-Toxicity Relationships for Different Types of Dinuclear Platinum Complexes. *J. Inorg. Biochem.* **2006,** *100* (8), 1332-1338.

42. Ghezzi, A.; Aceto, M.; Cassino, C.; Gabano, E.; Osella, D., Uptake of Antitumor Platinum(II)-Complexes by Cancer Cells, Assayed by Inductively Coupled Plasma Mass Spectrometry (ICP-MS). *J. Inorg. Biochem.* **2004,** *98* (1), 73-78.

43. Zeglis, B. M.; Pierre, V. C.; Barton, J. K., Metallo-Intercalators and Metallo-Insertors. *Chem. Commun.* **2007,** (44), 4565-4579.

44. Zava, O.; Zakeeruddin, S. M.; Danelon, C.; Vogel, H.; Grätzel, M.; Dyson, P. J., A Cytotoxic Ruthenium Tris(Bipyridyl) Complex that Accumulates at Plasma Membranes. *Chem. Bio. Chem.* **2009,** *10* (11), 1796-1800.

45. Lin, J. H.; Lu, A. Y. H., Role of Pharmacokinetics and Metabolism in Drug Discovery and Development. *Pharmacol. Rev.* **1997,** *49* (4), 403-449.

46. Toon, S.; Rowland, M., Structure-Pharmacokinetic Relationships among the Barbiturates in the Rat. *J. Pharmacol. Exp. Ther.* **1983,** *225* (3), 752-763.

47. Ishizaki, J.; Yokogawa, K.; Nakashima, E. M. I.; Ichimura, F., Relationships between the Hepatic Intrinsic Clearance or Blood Cell-Plasma Partition Coefficient in the Rabbit and the Lipophilicity of Basic Drugs. *J. Pharm. Pharmacol.* **1997,** *49* (8), 768-772.

48. Pisani, M. J.; Fromm, P. D.; Mulyana, Y.; Clarke, R. J.; Körner, H.; Heimann, K.; Collins, J. G.; Keene, F. R., Mechanism of Cytotoxicity and Cellular Uptake of Lipophilic Inert Dinuclear Polypyridylruthenium(II) Complexes. *Chem. Med. Chem.* **2011,** *6* (5), 848-858.

49. Camenisch, G.; Alsenz, J.; van de Waterbeemd, H.; Folkers, G., Estimation of Permeability by Passive Diffusion Through Caco-2 Cell Monolayers Using the Drugs' Lipophilicity and Molecular Weight. *Eur. J. Pharm. Sci.* **1998,** *6* (4), 313-319.

50. Dwyer, F. P., Chemistry of ruthenium. III. Reduction-oxidation potentials of the ruthenium(II)complexes with substituted derivatives of 2,2'-bipyridyl and 1,10-phenanthroline. *J. Proc. R. Soc. N. S. W.* **1950,** *83*, 134-7.

51. Yadav, A.; MacDonnell, F. M. In *Synthesis, Characterization and Biological Activity of the Stereoisomers of a Redox Active Ruthenium Polypyridyl Complex*, J. Am. Chem. Soc.: 2007; pp INOR-082.

52. Bolger, J.; Gourdon, A.; Ishow, E.; Launay, J.-P., Mononuclear and Binuclear Tetrapyrido[3,2-a:2‘,3‘-c:3‘‘,2‘‘-h:2‘‘‘,3‘‘‘-j]phenazine (tpphz) Ruthenium and Osmium Complexes. *Inorg. Chem.* **1996,** *35* (10), 2937-2944.

53. Bird, C. W.; Cheeseman, G. W. H.; Sarsfield, A. A., 912. 2,1,3-Benzoselenadiazoles as Intermediates in o-Phenylenediamine Synthesis. *J. Chem. Soc.* **1963**, 4767-4770.

54. Kim, M.-J.; Konduri, R.; Ye, H.; MacDonnell, F. M.; Puntoriero, F.; Serroni, S.; Campagna, S.; Holder, T.; Kinsel, G.; Rajeshwar, K., Dinuclear Ruthenium(II) Polypyridyl Complexes Containing Large, Redox-Active, Aromatic Bridging Ligands: Synthesis,

Characterization, and Intramolecular Quenching of MLCT Excited States. *Inorg. Chem.* **2002,** *41* (9), 2471-2476.

55. Chitakunye, R. Investigation of the Photochemistry of Ruthenium Complexes Containing Unusual Acceptor Ligands. The University of Texas at Arlington, Arlington, TX, 2006.

56. Sullivan, B. P.; Salmon, D. J.; Meyer, T. J., Mixed Phosphine 2,2'-Bipyridine Complexes of Ruthenium. *Inorg. Chem.* **1978,** *17* (12), 3334-3341.

57. Hartshorn, R. M.; Barton, J. K., Novel Dipyridophenazine Complexes of Ruthenium(II): Exploring Luminescent Reporters of DNA. *J. Am. Chem. Soc.* **1992,** *114* (15), 5919-5925.

58. Mabrouk, P. A.; Wrighton, M. S., Resonance Raman Spectroscopy of the Lowest Excited State of Derivatives of Tris(2,2'-bipyridine)Ruthenium(II): Substituent Effects on Electron Localization in Mixed-Ligand Complexes. *Inorg. Chem.* **1986,** *25* (4), 526-531.

59. Griffith, C. A.; Yadav, A.; Abayan, K.; MacDonnell, F. M., Mechanism of DNA Cleavage By Hypoxia Sensitive Ruthenium Polypyridyl Complexes.

60. Warnmark, K.; Thomas, J. A.; Heyke, O.; Lehn, J.-M., Stereoisomerically Controlled Inorganic Architectures: Synthesis of Enantio- and Diastereo-merically Pure Ruthenium-Palladium Molecular Rods from Enantiopure Building Blocks. *Chem. Commun.* **1996,** (6), 701-702.

61. Kleineweischede, A.; Mattay, J., Synthesis of Amino- and Bis(bromomethyl)-Substituted bi- and Tetradentate N-Heteroaromatic Ligands: Building Blocks for Pyrazino-Functionalized Fullerene Dyads. *Eur. J. Org. Chem.* **2006,** (4), 947-957.

62. Kleineweischede, A.; Mattay, J., Synthesis, Spectroscopic and Electrochemical Studies of a Series of Transition Metal Complexes with Amino- or Bis(bromomethyl)-

Substituted dppz Ligands: Building Blocks for Fullerene-Based Donor-Bridge-Acceptor Dyads. *J. Organomet. Chem.* **2006,** *691* (9), 1834-1844.

63. de Tacconi, N. R.; Chitakunye, R.; MacDonnell, F. M.; Lezna, R. O., The Role of Monomers and Dimers in the Reduction of Ruthenium(II) Complexes of Redox-Active Tetraazatetrapyridopentacene Ligand. *J. Phys. Chem. A* **2008,** *112* (3), 497-507.

64. Campagna, S.; Giannetto; Serroni, S.; Denti, G.; Trusso, S.; Mallamace, F.; Micali, N., Aggregation in Fluid Solution of Dendritic Supermolecules made of Ruthenium(II) and Osmium(II)-Polypyridine Building Blocks. *J. Am. Chem. Soc.* **1995,** *117*, 1754-1758.

65. Gut, D.; Rudi, A.; Kopilov, J.; Goldberg, I.; Kol, M., Pairing of Propellers: Dimerization of Octahedral Ruthenium(II) and Osmium(II) Complexes of Eilatin via π−π Stacking Featuring Heterochiral Recognition. *J. Am. Chem. Soc.* **2002,** *124* (19), 5449-5456.

66. Bolger, J.; Gourdon, A.; Ishow, E.; Launay, J.-P., Stepwise Syntheses of Mono- and Dinuclear Ruthenium tpphz Complexes $[(bpy)_2Ru(tpphz)]^{2+}$ and $[(bpy)_2Ru(tpphz)Ru(bpy)_2]^{4+}$. *J. Chem. Soc., Chem. Comm.* **1995,** *17*, 1799-1800.

67. Bergman, S. D.; Kol, M., Pi-Stacking Induced NMR Spectrum Splitting in Enantiomerically Enriched Ru(II) Complexes: Evaluation of Enantiomeric Excess. *Inorg. Chem.* **2005,** *44*, 1647-1654.

68. Bergman, S. D.; Golberg, I.; Barbieri, A.; Barigelleti, F.; Kol, M., Mononuclear and Dinuclear Complexes of Dibenzoeilatin: Synthesis, Structure, and Electrochemical and Photophysical Properties. *Inorg. Chem.* **2004,** *43*, 2355-2367.

69. Bilakhiya, A. K.; Tyagi, B.; Paul, P.; Natarajan, P., Di- and Tetranuclear Ruthenium(II) and/or Osmium(II) Complexes of Polypyridyl Ligands Bridged by a Fully

Conjugated Aromatic Spacer: Synthesis, Characterization, and Electrochemical and Photophysical Studies. *Inorg. Chem.* **2002,** *41*, 3830-3842.

70. Ishow, E.; Gourdon, A.; Launay, J.-P.; Lecante, P.; Verelst, M.; Chiorboli, C.; Scandola, F.; Bignozzi, C.-A., Tetranuclear Tetrapyrido[3,2-a:2',3'-c:3'',2''-h:2''',3'''-j]phenazine Ruthenium Complex: Synthesis, Wide Angle Scattering, and Photophysical Studies. *Inorg. Chem.* **1998,** *37*, 3603-3609.

71. Rajput, C.; Rutkaite, R.; Swanson, L.; Haq, I.; Thomas, J. A., Dinuclear Monointercalating RuII Complexes that Display High Affinity Binding to Duplex and Quadruplex DNA. *Chem. Eur. J.* **2006,** *12* (17), 4611-4619.

72. Le, V. H.; McGuire, M. R.; Ahuja, P.; MacDonnell, F. M.; Lewis, E. A., Thermodynamic Investigations of $[(phen)_2Ru(tatpp)Ru(phen)_2]^{4+}$ Interactions with B-DNA. *J. Phys. Chem. B.* **2015,** *119* (1), 65-71.

73. Meyer, G. J., Molecular Approaches to Solar Energy Conversion with Coordination Compounds Anchored to Semiconductor Surfaces. *Inorg. Chem.* **2005,** *44* (20), 6852 - 6864.

74. Campagna, S.; Puntoriero, F.; Nastasi, F.; Bergamini, G.; Balzani, V., Photochemistry and Photophysics of Coordination Compounds: Ruthenium. *Top. Curr. Chem.* **2007,** *280*, 117-214.

75. Vos, J. G.; Kelly, J. M., Ruthenium Polypyridyl Chemistry; from Basic Research to Applications and Back Again. *Dalton Trans.* **2006**, 4869-4883.

76. Elvington, M.; Brown, J.; Arachchige, S. M.; Brewer, K. J., Photocatalytic Hydrogen Production from Water Employing A Ru, Rh, Ru Molecular Device for Photoinitiated Electron Collection. *J. Am. Chem. Soc.* **2007,** *129* (35), 10644-10645.

77. Elvington, M.; Brewer, K. J., Photoinitiated Electron Collection at a Metal in a Rhodium-Centered Mixed-Metal Supramolecular Complex. *Inorg. Chem.* **2006,** *45* (14), 5242-5244.

78. Alstrum-Acevedo, J. H.; Brennaman, M. K.; Meyer, T. J., Chemical Approaches to Artificial Photosynthesis. 2. *Inorg. Chem.* **2005,** *44* (20), 6802-6827.

79. Lomoth, R.; Magnuson, A.; Sjodin, M.; Huang, P.; Styring, S.; Hammarstrom, L., Mimicking the electron donor side of Photosystem II in artificial photosynthesis. *Photosynth. Res.* **2006,** *87* (1), 25-40.

80. MacDonnell, F. M., Photochemical Splitting of Water. In *Solar Hydrogen Generation: Toward a Renewable Energy Future Ch. 6*, Rajeshwar, K.; Licht, S., Eds. Springer Publishers: New York, 2008.

81. Berger, S.; Fiedler, J.; Reinhardt, R.; Kaim, W., Metal vs. Ligand Reduction in Complexes of Dipyrido[3,2-a:2',3'-c]phenazine and Related Ligands with $[(C_5Me_5)ClM]^+$ (M = Rh or Ir): Evidence for Potential Rather Than Orbital Control in the Reductive Cleavage of the Metal-Chloride Bond. *Inorg. Chem.* **2004,** *43* (4), 1530-1538.

82. Brennaman, M. K.; Alstrum-Acevedo, J. H.; Fleming, C. N.; Jang, P.; Meyer, T. J.; Papanikolas, J. M., Turning the $[Ru(bpy)2dppz]^{2+}$ light-switch on and off with temperature. *J. Am. Chem. Soc.* **2002,** *124* (50), 15094-8.

83. Chambron, J.-C.; Suavage, J.-P.; Amouyal, E.; Kiffi, P., $Ru(bipy)_2(Dipyridophenazine)^{2+}$: A Complex with a Long Range Directed Charge Transfer Excited State. *Nouv. J. Chem.* **1985,** *9*, 527-529.

84. Chiorboli, C.; Bignozzi, C.-A.; Scandola, F.; Ishow, E.; Gourdon, A.; Launay, J.-P., Photophysics of Dinuclear Ru(II) and Os(II) Complexes Based on the Tpphz Bridging Ligand. *Inorg. Chem.* **1999,** *38*, 2402-2410.

85. Chiorboli, C.; Fracasso, S.; Scandola, F.; Campagna, S.; Serroni, S.; Konduri, R.; MacDonnell, F. M., Primary Processes in Photoinduced Pultielectron Storage Systems. A dinuclear Ruthenium(II) Species Featuring a Charge-Separated State with a Lifetime of 1.3 μs. *Chem. Comm.* **2003**, 1658-1659.

86. Fees, J.; Ketterle, M.; Klein, A.; Fiedler, J.; Kaim, W., Electrochemical, Spectroscopic and EPR Study of Transition Metal Complexes of Dipyrido[3,2-a:2',3'-c]Phenazine. *J. Chem. Soc., Dlat. Trans.* **1999,** *15*, 2595-2600.

87. Wouters, K. L.; Tacconi, N. R.; Konduri, R.; Lezna, R. O.; MacDonnell, F. M., Driving Multi-Electron Reactions with Photons: Dinuclear Ruthenium Complexes Capable of Stepwise and Concerted Multi-Electron Reduction. *Photosyth. Res. J.* **2006,** *87* (1), 41-55.

88. Friedman, A. E.; Chambron, J. C.; Sauvage, J. P.; Turro, N. J.; Barton, J. K., A molecular Light Switch for DNA: $Ru(bpy)_2(dppz)^{2+}$. *J. Am. Chem. Soc.* **1990,** *112* (12), 4960-2.

89. Hiort, C.; Lincoln, P.; Nordén, B., DNA Binding of Δ- and Λ-$[Ru(phen)_2DPPZ]^{2+}$. *J. Am. Chem. Soc.* **1993,** *115*, 3448-3454.

90. Tysoe, S. A.; Kopelman, R.; Schelzig, D., Flipping the Molecular Light Switch Off: Formation of DNA-Bound Heterobimetallic Complexes Using $Ru(bpy)_2tpphz^{2+}$ and Transition Metal Ions. *Inorg. Chem.* **1999,** *38*, 5196 - 5197.

91. Lutterman, D. A.; Chouai, A.; Liu, Y.; Sun, Y.; Stewart, C. D.; Dunbar, K. R.; Turro, C., Intercalation Is Not Required for DNA Light-Switch Behavior. *J. Am. Chem. Soc.* **2008,** *130* (4), 1163-1170.

92. Haas, K. L.; Franz, K. J., Application of Metal Coordination Chemistry to Explore and Manipulate Cell Biology. *Chem. Rev.* **2009,** *109* (10), 4921-60.

93. Macdonald, I.; Dougherty, T. J., Basic Principles of Photodynamic Therapy. *J. Porphyrins Phthalocyanines.* **2001,** *05* (02), 105-129.

94. Schumacker, P. T., Reactive Oxygen Species in Cancer Cells: Live by The Sword, Die by The Sword. *Cancer Cell* **2006,** *10* (3), 175-176.

95. Gill, M. R.; Thomas, J. A., Ruthenium(ii) polypyridyl Complexes and DNA-from Structural Probes to Cellular Imaging and Therapeutics. *Chem. Soc. Rev* **2012,** *41* (8), 3179-3192.

96. Lin, G. J.; Jiang, G. B.; Xie, Y. Y.; Huang, H. L.; Liang, Z. H.; Liu, Y. J., Cytotoxicity, Apoptosis, Cell Cycle Arrest, Reactive Oxygen Species, Mitochondrial Membrane Potential, and Western Blotting Analysis of Ruthenium(II) Complexes. *J. Biol. Inor.g Chem.* **2013,** *18* (8), 873-82.

97. Sun, D.; Liu, Y.; Liu, D.; Zhang, R.; Yang, X.; Liu, J., Stabilization of G-Quadruplex DNA, Inhibition of Ttelomerase Activity and Live Cell Imaging Studies of Chiral Ruthenium(II) complexes. *Chem.* **2012,** *18* (14), 4285-95.

98. Tan, C.; Lai, S.; Wu, S.; Hu, S.; Zhou, L.; Chen, Y.; Wang, M.; Zhu, Y.; Lian, W.; Peng, W.; Ji, L.; Xu, A., Nuclear Permeable Ruthenium(II) Beta-Carboline Complexes Induce Autophagy to Antagonize Mitochondrial-Mediated Apoptosis. *J. Med. Chem* **2010,** *53* (21), 7613-24.

99. Pisani, M. J.; Weber, D. K.; Heimann, K.; Collins, J. G.; Keene, F. R., Selective Mitochondrial Accumulation of Cytotoxic Dinuclear Polypyridyl Ruthenium(II) Complexes. *Metallomics.* **2010,** *2* (6), 393-396.

100. Chen, T.; Liu, Y.; Zheng, W. J.; Liu, J.; Wong, Y. S., Ruthenium Polypyridyl Complexes that Induce Mitochondria-Mediated Apoptosis in Cancer Cells. *Inorg. Chem.* **2010,** *49* (14), 6366-8.

101. Puckett, C. A.; Barton, J. K., Mechanism of Cellular Uptake of a Ruthenium Polypyridyl Complex. *Biochem.* **2008,** *47* (45), 11711-11716.

102. Schatzschneider, U.; Niesel, J.; Ott, I.; Gust, R.; Alborzinia, H.; Wölfl, S., Cellular Uptake, Cytotoxicity, and Metabolic Profiling of Human Cancer Cells Treated with Ruthenium(II) Polypyridyl Complexes $[Ru(bpy)_2(N\text{--}N)]Cl_2$ with N--N=bpy, phen, dpq, dppz, and dppn. *Chem. Med. Chem* **2008,** *3* (7), 1104-1109.

103. Koch, J. H.; Gyarfas, E. C.; Dwyer, F. P., Biological Activity of Complex Ions. Mechanism of Inhibition in Acetylcholinesterase. *Aust. J. Biol. Sci.* **1956,** *9*, 371-381.

104. Mulcahy, S. P.; Li, S.; Korn, R.; Xie, X.; Meggers, E., Solid-Phase Synthesis of Tris-heteroleptic Ruthenium(II) Complexes and Application to Acetylcholinesterase Inhibition. *Inorg. Chem.* **2008,** *47*, 5030 - 5032.

105. Wenlock, M. C.; Potter, T.; Barton, P.; Austin, R. P., A Method for Measuring The Lipophilicity of Compounds in Mixtures of 10. *J. Biomol. Screen.* **2011,** *16* (3), 348-55.

106. Hansch, C.; Anderson, S. M., The Effect of Intramolecular Bydrophobic Bonding on Partition Coefficients. *J. Org. Chem.* **1967,** *32* (8), 2583-2586.

107. Minna, J., 2015.

108. Franken, N. A.; Rodermond, H. M.; Stap, J.; Haveman, J.; van Bree, C., Clonogenic assay of cells in vitro. *Nat Protoc.* **2006,** *1* (5), 2315-9.

109. Rockwell, S., Effects of Clumps and Clusters on Survival Measurements with Clonogenic Assays. *Cancer Res.* **1985,** *45* (4), 1601-7.

110. Jenner, G. A.; Longerich, H. P.; Jackson, S. E.; Fryer, B. J., ICP-MS — A powerful Tool for High-Precision Trace-Element Analysis in Earth Sciences: Evidence from Analysis of Selected U.S.G.S. Reference Samples. *Chem. Geol.* **1990,** *83* (1–2), 133-148.

111. Liu, J.; Brown, A. K.; Meng, X.; Cropek, D. M.; Istok, J. D.; Watson, D. B.; Lu, Y., A Catalytic Beacon Sensor for Uranium with Parts-Per-Trillion Sensitivity and Millionfold Selectivity. *Proc. Natl. Acad. Sci.* **2007,** *104* (7), 2056-2061.

Biographical Information

Nagham Alatrash was born and grew up in Syria. After finishing high school in Syria, she moved to the United States and attended the University of Texas Pan American majoring in Chemistry with a minor in Biology. She was a 2008 LSAMP scholar and was involved in undergraduate research under the supervision of Dr. Hassan Ahmad. With Dr. Ahmad, she investigated the effect of green tea polyphenols in cancer prevention. She continued her research in the spring of 2009 as a Biochemistry Research Assistant and served as a lab manager in Dr. Ahmad's research laboratory.

Nagham received her B.S. degree from the University of Texas Pan American in May 2009. In the summer of 2010, she worked as a Cardiothoracic Research Assistant at Rhode Island Hospital. Nagham started her graduate studies in fall 2010 in the Department of Chemistry and Biochemistry at the University of Texas at Arlington after she had LSAMP fellowship from the National Science Foundation where she worked under Prof. Frederick MacDonnell. She worked on the development of novel lipophilic anticancer drugs. She synthesized and characterized new ruthenium-polypyridyl complexes containing unusual redox-active ligands. She also studied their biological activity including DNA cleavage activity, cytotoxicity and animal toxicity.

Nagham Alatrash graduated from the University of Texas at Arlington with a Master in Chemistry in 2012 and with PhD in chemistry in 2015.